



Lawrence Berkeley Laboratory

UNIVERSITY OF CALIFORNIA

EARTH SCIENCES DIVISION

Seasonal Thermal Energy Storage in Unsaturated Soils: Model Development and Field Validation

C. Doughty, A. Nir, and C.-F. Tsang

March 1993



DISCLAIMER

This document was prepared as an account of work sponsored by the United States Government. While this document is believed to contain correct information, neither the United States Government nor any agency thereof, nor the Regents of the University of California, nor any of their employees, makes any warranty, express or implied, or assumes any legal responsibility for the accuracy, completeness, or usefulness of any information, apparatus, product, or process disclosed, or represents that its use would not infringe privately owned rights. Reference herein to any specific commercial product, process, or service by its trade name, trademark, manufacturer, or otherwise, does not necessarily constitute or imply its endorsement, recommendation, or favoring by the United States Government or any agency thereof, or the Regents of the University of California. The views and opinions of authors expressed herein do not necessarily state or reflect those of the United States Government or any agency thereof or the Regents of the University of California.

**Seasonal Thermal Energy Storage in Unsaturated Soils:
Model Development and Field Validation**

Christine Doughty, Aharon Nir, and Chin-Fu Tsang*

Earth Sciences Division
Lawrence Berkeley Laboratory
University of California
Berkeley, California 94720

*Visiting Scientist

March 1993

ABSTRACT

This report summarizes ten years of activity carried out at the Earth Sciences Division of the Lawrence Berkeley Laboratory (LBL) in the subject of seasonal storage of thermal energy in unsaturated soils. The objectives of the work were to make a conceptual study of this type of storage, to offer guidelines for planning and evaluation of the method, to produce models and simulation for an actual field experiment, to participate in an on-line data analysis of experimental results, and to evaluate the results in terms of the validation of the concept, models and the experimental techniques. The actual field experiments were performed in Beer-Sheva, Israel, jointly with E. Korin and coworkers of the Ben-Gurion University of the Negev. Details of engineering and field operations are not included in this report.

Most investigations on seasonal storage of thermal energy have concentrated mainly on cold and moderate climatic regions, and have emphasized aquifer storage. In warm and semi-arid climatic zones, where the use of groundwater aquifers is not feasible, unsaturated soil has been identified as one of the most suitable media for seasonal energy storage. We first investigated general concepts and theoretical models for the design of a heat storage facility in unsaturated soil. Subsequently, more detailed modeling was done to aid in the design of a field experiment, the object of which was to a) validate the theoretical models of the proposed storage design and relevant heat transfer processes in unsaturated soils; b) test the proposed technologies for the construction of the storage facility, including heat-exchanger emplacement and operational control; and c) provide cost estimates of the implementation of this method. The field experiment consisted of two successive storage cycles, in which heat transfer to the soil was effected through a heat exchanger constructed of flexible polybutylene pipe in a helical configuration of 1 m diameter and 6 m length, which was inserted into a 10-m-deep well. In the first cycle, the storage was charged with heat by circulating water at 65-70°C through the exchanger for 9 months, and discharged for 1 month by reversing the flow direction and circulating 20°C water. In the second cycle, the charge cycle lasted 35 days, at higher flow rates and temperatures. The results were found to be consistent with model predictions and confirmed the technological solution, and indicated several possibilities for improvement. A theoretical study of coupled fluid and heat flow in unsaturated soils was carried out, which indicated that the use of a linear and uncoupled heat-flow model was appropriate for the conditions of the field experiment.

TABLE OF CONTENTS

Abstract	ii
Table of Contents	iii
List of Tables	v
List of Figures	vi
Notation	viii
Scope of Report	1
Part I. Design, modeling, and simulation of a UZTES system	2
I.1 Introduction	2
I.1.1 Motivation	2
I.1.2 Method of approach	3
I.1.3 Scope of investigation	3
I.2 Methods of seasonal heat storage	4
I.2.1 Factors affecting design	4
I.2.2 Storage media	4
I.2.3 Environmental considerations	5
I.2.4 Comparison with other storage media	5
I.3 Design approach	6
I.3.1 Consideration of soil properties	6
I.3.2 Spatial variability of soil properties	8
I.3.3 Siting considerations	8
I.3.4 Technological considerations	9
I.4 Mathematical modeling of a UZTES system	10
I.4.1 Conceptual and numerical model description	10
I.4.2 Verification of the numerical model with an analytical solution	13
I.4.3 Multiyear simulation	14
I.4.4 Sensitivity analysis	17
I.4.5 Future model development	18
I.5 Potential applications	18
I.5.1 Residential and industrial space heat supply	18
I.5.2 Agricultural uses	19
I.5.3 Effects on alternate-energy resource development	19
Part II. Design and construction of an experimental field facility for UZTES	20
II.1 Introduction	20
II.1.1 Scope of investigation	20
II.1.2 Objectives of the field experiment	20
II.2 Modeling and simulation as a design tool for the field experiment	20
II.2.1 Simulation of the planned field experiment	20
II.2.2 Verification of the cylindrical representation of the helical heat exchanger	21

II.3 Establishment of an environmental database	23
II.3.1 Data requirements	23
II.3.2 Estimate of soil thermal parameters by an inverse method	23
II.3.3 Environmental effects	24
II.4 Site preparation	25
II.4.1 Description of the storage well	25
II.4.2 Summary	25
Part III. Description and evaluation of two heat storage cycles	27
III.1 1989 charge/discharge cycle	27
III.1.1 Base-case model	27
III.1.2 Sensitivity studies	27
III.1.3 Model improvements	29
III.2 1990 charge/discharge cycle	30
III.3 Summary of experimental operation	30
III.4 Multiyear full-scale modeling	31
Part IV. Studies of heat and mass transfer in unsaturated soils	33
IV.1 Introduction	33
IV.2 Theoretical investigation	33
IV.2.1 Mathematical model	34
IV.2.2 Sample results	34
IV.2.3 Conclusions	35
IV.3 Laboratory experimental program	35
Conclusions and Recommendations	37
1. Project status	37
2. Recommendations for continued activities	37
2.1 Experimental studies	37
2.2 Theoretical studies	37
2.3 System studies	37
3. Projected applications of the seasonal storage of thermal energy	38
Acknowledgements	38
References	39
Appendix A: Issues involved in establishment of an environmental database	42
A.1 Hydrogeological background	42
A.2 Temperature and moisture data	42
Appendix B: Algorithmic search for soil thermal properties	44
B.1 Introduction	44
B.2 Inversion of synthetic temperature data	44
B.2.1 Uniqueness test – Synthetic data without noise	45
B.2.2 Stability test – Synthetic data with noise	46
B.3 Inversion of real temperature data	47
B.4 Alternate approach to inversion	50

LIST OF TABLES

I.1 Comparison between UZTES, ATEs, and Rock TES	6
I.2 Calculations made using the insulated-boundary model to represent an interior duct	15
III.1 Sensitivity studies for the 1989 test	28
III.2 Model improvements	29
III.3 New Model	30
B.1 Inversion of synthetic temperature data with noise	47
B.2 Inversion of real temperature data from different depth ranges	48
B.3 Inversion of real temperature data from different time periods	49
B.4 Inversion of real temperature data with random noise added	49

LIST OF FIGURES

Figure I.1	Schematic diagram showing a vertical cross-section of one duct of the storage system. The optimal dimensions of the system have been found to be a 12 m long heat exchanger located at a depth of 4-16 m, with adjacent ducts separated by 6 m (see Section I.4.4). For the reduced-scale field experiment (Parts II and III), the heat exchanger is 6 m long at a depth of 4-10 m and the shallow storage zone is absent.	51
Figure I.2	Top view of an array of heat-exchanger ducts.	52
Figure I.3	Analytical and numerically calculated temperature distributions for a simplified problem involving radial heat flow from a cylinder; the curves labeled 1, 2, and 3 represent different boundary conditions for the numerical model, as explained in the text.	53
Figure I.4	Boundary conditions (A and B) and calculated results (C, D, E, and F) for Case 2.	54
Figure I.5	Temperature distributions (in °C) for several times for Case 2.	55
Figure I.6	Outlet temperature (T_{out}) calculated with averaged and discontinuous pumping schedules for the final 10 days of the 1S-1L-2S sequence.	56
Figure I.7	Computed average daily flow rate (\bar{Q}) and outlet temperature (T_{out}) for Case 2 and an infinite-radius model.	57
Figure II.1	Computed average daily flow rate (\bar{Q}) and outlet temperature (T_{out}) for full-scale and reduced-scale infinite-radius models.	58
Figure II.2	Temperature distributions (in °C) after 2 months of charge assuming thermal conductivity of 0.8 W/m K (A), 1.8 W/m K (B), and their difference, the delta model (C).	59
Figure II.3	Schematic diagram showing the square-cross-section helix and cylindrical conduit models for the heat exchanger.	60
Figure II.4	Energy flux ratio of the square-cross-section helix to the cylindrical conduit, for coil separation distance from 4 to 12 cm.	61
Figure II.5	Ratio of energy density deposited for various helix spacings to energy density deposited for 5 cm spacing.	62
Figure II.6	Temperature distributions (in °C) after 1 hour of 'charge' for the helical and cylindrical heat-exchanger models.	63
Figure II.7	Soil granulometric structure profile for observation well A.	64
Figure II.8	Soil moisture content profile for three wells.	65
Figure II.9	Observed and calculated soil temperature profiles.	66

Figure II.10	Construction of the heat exchanger.	67
Figure II.11	Emplacement of the heat exchanger. The heat exchanger on the left has not yet been lowered into place. The heat exchanger on the right (labeled EW2) is in place and the hole has been backfilled with soil. The stakes labeled OW1 and OW2 identify observation well locations.	68
Figure II.12	Location of sensors in the storage volume.	69
Figure II.13	Heat supply system.	70
Figure III.1	Inlet temperature and flow rate for the 1989 run (gray lines), along with averaged values used in the numerical model (heavy black lines).	71
Figure III.2	Sensor locations (A) and observed and calculated temperatures (B, C, and D) for the 1989 run. The curve labeled Ch0 is the heat-exchanger outlet temperature, while the other curves show temperatures at sensor locations. Frame B shows temperatures at depths near 3 m, C at a 4 m depth, D at 7 and 9 m depths.	72
Figure III.3	Calculated temperature distribution (in °C) at the end of the 1989 charge period (lines), and the observed temperatures at sensor locations (points).	73
Figure III.4	Detailed view of calculated and observed temperatures at selected sensor locations for the discharge portion of the 1989 run.	74
Figure III.5	Fractional discrepancy between observed and calculated temperatures, for the outlet temperature (Ch0) and at selected sensor locations, for the 1989 run.	75
Figure III.6	Results of the five-year simulation for an operational well with a heat-exchanger inlet temperature of 65°C. A: Heat-exchanger outlet temperature (T_{out}) during charge and discharge (bold) periods, and water circulation rate (\bar{Q}). B: Stored energy in the soil; note the three-year transient.	76
Figure III.7	Results of the five-year simulation for an operational well with a heat-exchanger inlet temperature of 80°C. See Figure III.6 for description of variables.	77
Figure IV.1	Simulated moisture-content and temperature (°C) profiles after 4 hours.	78
Figure IV.2	Simulated moisture-content and temperature (°C) profiles after 24 hours.	79
Figure IV.3	Simulated moisture-content and temperature (°C) profiles after 48 hours.	80
Figure IV.4	Simulated moisture-content and temperature (°C) profiles at quasi-steady state.	81

NOTATION

C	volumetric heat capacity ($J/m^3 K$)
c	specific heat ($J/kg K$)
D	decay constant (m; $=\sqrt{2\alpha/\omega}$; Eq. 6)
F	objective function for temperature inversion (Eq. B.2)
f	magnitude of noise added to temperature inversion (Eq. B.3)
\mathbf{P}	vector of parameters for temperature inversion (Eq. B.2)
Q	volumetric flow rate (m^3/s)
\bar{Q}	average daily mass flow rate (kg/s ; Eq. 4)
r	radial coordinate (m)
r_i	inner radius of cylindrical conduit heat exchanger (m)
r_o	outer radius of cylindrical conduit heat exchanger (m)
T	temperature ($^{\circ}C$)
T_{in}	heat exchanger inlet temperature ($^{\circ}C$)
T_{out}	heat exchanger outlet temperature ($^{\circ}C$)
T_0	initial temperature; annual average surface temperature ($^{\circ}C$; Eq. 6)
T_1	constant boundary temperature ($^{\circ}C$)
T_a	amplitude of annual surface temperature variation ($^{\circ}C$; Eq. 6)
ΔT_{frac}	fractional temperature difference between observed and calculated temperatures (Eq. 7)
$\langle \Delta T_{frac} \rangle$	time-averaged value of ΔT_{frac}
t	time (s)
t_0	time of maximum surface temperature (s; Eq. 6)
z	vertical coordinate (m; zero at ground surface, increasing downward)
z_{min}	shallowest data depth used in temperature inversion (m)

Greek Letters

α	thermal diffusivity (m^2/s ; $=\lambda/C$)
θ	volumetric moisture content
λ	effective thermal conductivity ($W/m K$)
ρ	random number to represent noise in temperature inversion (Eq. B.3)
τ	period of annual surface temperature variation (s; Eq. 6)
ω	frequency of annual surface temperature variation (s^{-1} ; $=2\pi/\tau$; Eq. 6)

Subscripts and Superscripts

$calc$	calculated
$init$	initial
obs	observed
s	soil
w	water

SCOPE OF REPORT

This report is comprised of four parts which follow the chronological order of activities during the period 1981-1991.

Part I describes the first stages of conceptual development and adaptation of the seasonal-storage design criteria to the warm climatic zone (WCZ), followed by modeling and simulation related to local climatic conditions. This stage lasted from 1981 to 1985. This work was first reported in Doughty et al. [1983] and Nir et al. [1986].

Part II describes specific modeling and simulation tasks related to a field experiment, a survey of field data, hardware development and acquisition, and the construction of the field experimental facilities. This stage lasted from 1986 to 1989. This work is described in Bensabat et al. [1988b] and Doughty et al. [1990].

Part III describes the actual execution of the field experiment, and compares field observations to numerical simulation results. This stage lasted from 1989 to 1990. This work is described in Doughty et al. [1991], and is analyzed in terms of validation concepts by Nir et al., [1992].

Part IV describes a theoretical study of the detailed behavior of heat and mass transfer at a hot boundary, which was conducted to analyze the effect of assumptions made in the previous modeling studies, in which moisture flow was not considered. It includes also a review of the validation approach that was adopted in this study. This stage lasted from 1989 to 1991. This work is described in Bensabat et al. [1988a], Bear et al. [1991], and Bensabat et al. [1992].

We conclude the report with recommendations for further improvements in the theoretical and experimental procedures and for potential applications of seasonal thermal energy storage.

The experimental and field work of Parts II and III was performed at the Institute of Desert Research and the Institutes of Applied Research of the Ben-Gurion University of the Negev (BGU), while one of the authors (AN) was associated with them. The field experiments were performed jointly with the participation of E. Korin (BGU) and B. Bar-On [Bar-On et al., 1991]. Part IV was conducted in cooperation with J. Bensabat (MIT).

PART I. DESIGN, MODELING, AND SIMULATION OF A UZTES SYSTEM

I.1 INTRODUCTION

I.1.1 MOTIVATION

Seasonal heat storage is an important element in the utilization of alternative energies with low-temperature heat supplies, as it addresses the inherent problems of out-of-phase energy supply and demand, and the stochastic nature of the supply-demand variation. The main energy sources considered here are solar energy, natural thermal waters, and industrial waste heat. A prospective future source of heat is associated with the use of large-scale electrical energy storage in batteries, fuel cells, and compressed air.

Seasonal heat storage concepts and designs have undergone numerous tests and accumulated many years of operational experience in a variety of geologic storage media, including aquifers, caverns, and dry rock, as well as shallow partially saturated soils [International Energy Storage Conferences, 1981, 1983, 1985, 1988, 1990, 1991]. These geological storage media are inexpensive and widely available. However, applications refer mainly to colder or moderate climatic zones, while only limited progress on the application of this concept is reported for warm climatic zones (WCZ). While seasonal heat storage in WCZ may be expected to benefit from lower heat losses to the environment and higher solar inputs, the lower specific demand for domestic heat and shorter heating periods make the need for heat storage seem less urgent and the investment less attractive. Preliminary analysis indicates that this may not be the right conclusion [Nir and Benson, 1982]. These zones, which include the southwest United States, parts of Australia, and the Mediterranean countries, are subject to intensive growth in population and in industrial and agricultural development. They should be expected to develop and benefit from suitable methods of heat storage.

While experience from other storage media and other climatic zones can serve as a useful base of knowledge for designing storage facilities in unsaturated soil, specific features of WCZ give rise to new physical processes in soils, which introduce additional heat transfer mechanisms, and thus require new technological approaches for the design of seasonal heat storage systems. An experimental feasibility study to test these new elements of design and to validate the mathematical models is described in Parts II and III.

1.1.2 METHOD OF APPROACH

Sections I.2 and I.3 analyze the characteristic features of WCZ which determine the preferred methods of seasonal heat (or cold) storage, including climatic factors, sources and demand of heat (or cold), hydrogeological factors, technological developments, and accumulated experience from other climatic zones. Unsaturated soils are indicated as the most suitable medium for seasonal heat storage under these conditions. A preliminary description and mathematical model of a seasonal Unsaturated Zone Thermal Energy Storage (UZTES) system for a specific configuration are presented in Section I.4 and studied through several stages of optimization and sensitivity analysis.

1.1.3 SCOPE OF INVESTIGATION

For the numerical modeling studies in Part I, a solar heat-supply pattern typical of WCZ and a heat demand with inter-year variability are imposed, and the UZTES system is modeled for several years of transient response. In one specific case a greenhouse heat demand including root zone heating is treated. This should not be considered as a limitation of the applicability of UZTES, as these conditions present rather severe design demands, which can be readily relaxed for alternative types of supply and demand. The model is based on an axial 2-D configuration, deemed to provide an efficient heat transfer area and storage volume. System dimensions are improved in several stages of sensitivity analysis. Analytical models of simpler configurations are investigated, and used for verification of the computations.

The model calculates conductive heat transfer with both constant and temperature-dependent values of thermal conductivity, but does not consider coupled heat and fluid flows in the unsaturated-soil storage medium. In Part IV theoretical calculations are outlined, which indicate that the assumption of negligible moisture transport is adequate under the planned storage conditions, in which the moisture content in the unsaturated silty-clay soil is relatively high. The processes that occur when this assumption fails to hold are also described. A preliminary laboratory experiment has been conducted, and further work is planned, to validate this theoretical study.

There is no attempt to include details of engineering design in Part I, but the available new technological options are indicated. This information may allow a preliminary economic estimate of the proposed storage system.

I.2 METHODS OF SEASONAL HEAT STORAGE

I.2.1 FACTORS AFFECTING DESIGN

A number of approaches to the design of seasonal heat storage have been extensively described in the literature of the last decade [International Energy Storage Conferences, 1981, 1983, 1985, 1988, 1990, 1991; Hadorn, 1988] Several reports deal with guidelines and principles of design [Hausz, 1981; Marshall, 1984; Claesson et al., 1985]. Generally, the storage method adopted depends on the local availability of storage media, on environmental conditions, on operational temperatures of sources and demand, and on the type of back-up system required. For example, the storage temperature, which can be above, below, or comparable to the mean ambient temperature, is determined by environmental conditions, source temperatures, and the mode of utilization (direct use or heat pump coupling). Storage temperature in turn influences the physical design of the storage system and the operational procedure of heat injection and extraction. Another classification is made with regard to the mode of storing energy: active replacement, passive replacement, or recharge from a semi-infinite reservoir (earth). Again, each option requires a different technical approach in order to optimize its potential.

Not all design requirements can be satisfactorily fulfilled at present, which is not surprising for a recently developed technology. The research and development needs in this area are mainly on topics of heat transfer, heat losses to the surroundings, entropy losses, drilling, and installation methods. Every adopted design has to account for these (possibly temporary) deficiencies by a certain amount of over-design.

I.2.2 STORAGE MEDIA

There are a number of proposed storage media. Several have been analyzed theoretically or tested experimentally [Boysen, 1985; Bankston, 1985; Hadorn, 1988; Hellstrom, 1991]. Choice of a storage medium is guided by the principles of design discussed above. These guidelines, when applied to WCZ, indicate that unsaturated soil is likely to be the only widely available storage medium. Artificial or excavated storage is excluded for seasonal storage on technological and economic grounds. Rock formations are rare and likely to be too expensive for storage installation. Aquifers are likely to be used or destined for use as sources of water supply, which makes them incompatible with heat storage use. Aquifers with poor water quality, unusable for water supply, are available in more arid zones, but tend to be found at greater depth and at remote locations, thus increasing installation and operation costs. The analysis of the capabilities of unsaturated soils to act as seasonal storage media is therefore seen as a primary goal in the

introduction of this technology into WCZ.

1.2.3 ENVIRONMENTAL CONSIDERATIONS

The effects of environmental conditions in WCZ may be considered under the following headings.

Climate: Climate determines the length of the charge and demand periods, typically 8 months (for solar input) and 4 months, respectively. If cold storage is planned, the cooling demand may last 5-7 months. The insolation intensity and high ambient temperatures allow high collection temperatures with simple solar collector design and cost. In some cases, solar input is available during the demand period, typically 20-25% of the yearly total. There are low heat losses from storage and transport between storage and users, due to high ambient soil and air temperatures and high thermal resistance of dry surface soil. Average ambient temperatures for ground surface, deep soil, and groundwaters are 17-22°C, compared to 4-8°C for cold zones and 10-13°C for intermediate climatic zones. In the more arid areas, rainfall tends to be limited to winter months, with little ground infiltration and direct recharge to aquifers, eliminating a common cause of convective heat loss in rainy areas.

Types of Soil: Soil properties (heat capacity, thermal conductivity, granular structure—which determines permeability and porosity, and chemical composition) determine drying out of soils induced by high temperature gradients, and physicochemical changes at the heat transfer surfaces. These processes, which are studied theoretically in Part IV, have to be accounted for in the design or modified, as discussed in Section I.3.

Hydrogeological Conditions: The relevant condition is the distance to areas of saturated water transport, often found below the storage area. The proximity of aquifers or of seasonal interflow and infiltration paths increases the heat losses of the storage system to the environment.

1.2.4 COMPARISON WITH OTHER STORAGE MEDIA

This comparison is limited to natural storage media. A more general comparison was made by Blahnik [1981], while several points of comparison with aquifer thermal energy storage (ATES) were discussed by Nir [1981]. This discussion is again directed mainly to comparison with ATES, which is, except for dry rock thermal energy storage (TES), closest in design to UZTES and for which there exists a large amount of data. The points of comparison are (a) Availability – UZTES is more widely available at middle latitudes than other options; siting limitations are due to nearby underlying aquifers and interflow zones; (b) Control of heat deposition – better than in aquifers, which are influenced by natural and induced flow regimes of groundwater

and exhibit high thermal dispersion; (c) Heat transfer rates – low, limited by the heat diffusion mechanism; (d) Geochemical problems – minimal, due to closed water system; (e) Heat recovery – high if positioned under user area; (f) Access for geophysical survey – easy due to proximity to the surface; (g) Modeling – more complex than for alternatives but simplifications may be possible; (h) Minimum size – small, with possibility of modular expansion due to factors mentioned in (b); (i) Construction cost – relatively low, as system is positioned close to the surface and has no insulation; (j) surface area can be utilized after installation, with retrofit possibilities under certain conditions. Table I.1 summarizes these considerations.

Table I.1 Comparison between UZTES, ATES, and rock TES for common warm climatic zone conditions.

Characteristic	UZTES	ATES	Rock TES
Availability	+	-	-
Control of heat deposition	+	-	-
Heat transfer rate	-	+	-
Geochemical interactions	+	-	+
Accessibility for survey	+	-	-
Modeling and simulation	-	+/-	+
Minimum module size	+	-	-
Construction cost	?	+	+

Note: A plus indicates favorable conditions, a minus indicates unfavorable conditions, and a question mark indicates unknown conditions.

1.3 DESIGN APPROACH

This section applies the guidelines and principles of Section I.2 to more specific and quantitative design details of a seasonal heat storage system in the unsaturated zone of the soil. Alternative solutions may be suitable under given local conditions, and no generalization of the applicability of this approach is implied.

1.3.1 CONSIDERATION OF SOIL PROPERTIES

An estimate of thermal, hydraulic, and geochemical properties of the soil in the storage area and its environment is required for the planning stage of the storage system. This estimate can be deduced from published data, accumulated experience with local soils, or from *in situ* tests. However, detailed local tests are expensive and time consuming, and may still leave many unexplored features within the storage area. The proposed approach is to estimate not only the expected values of soil properties, but also their variability; the design should then be robust enough to allow effective operation for this range of soil property values.

The information on thermal properties required for designing a UZTES system is outlined below, and is further discussed in Nir [1983]. The thermal processes are coupled to hydraulic processes, which in turn depend on the physicochemical structure of the soil. The theory of these processes is presented in a multitude of references [e.g., Luikov, 1950; Philip and de Vries, 1957]. However, there are still discrepancies between theory and experimentally determined values of effective thermal conductivity, which is composed of a pure conductive component, for transport in solid matrix and liquid water, and a component representing latent heat transport by vapor diffusion.

Temperature- and moisture-dependent values of thermal conductivity for common soil types have been measured [Sepaskah and Boersma, 1979]. An extensive summary of experimental data [Sundberg, 1985] shows a high correlation between thermal conductivity and both quartz content and dry density. A comprehensive summary of thermal and hydraulic properties of soils is given in Childs and Malstaff [1982]. Up to 70°C, the conductivity is a monotonic function of temperature, with a broad plateau above 20% water content. Unfortunately, the common classification of soil types by grain size does not lead to consistent values of thermal conductivity; the results of Sepaskah and Boersma [1979] are lower by 30% than those of Walker et al. [1981] for similar soil designation, water content, and temperature.

Heat capacity, being an extensive property of the medium, can be readily evaluated from known basic data. It is strongly dependent on the variable water content, but weakly dependent on temperature, within the range of conditions found in the storage system. Matric potential has been widely studied for various soil types, primarily in the agricultural domain [Childs and Malstaff, 1982], however its temperature dependence is still controversial [Herkeleth, 1981].

Soils with high clay content are subject to chemical and structural changes at high temperatures and high temperature gradients. Drying and chemical modification are expected at the heat exchanger surface. Effects of drying at the bottom boundary of solar ponds have been analyzed [Lebeouf, 1985]. A field scale experimental model has been used to measure all the above mentioned phenomena in an unsaturated zone above a saturated heat storage area [Benet et al., 1984, 1985]. The kinetics of the drying process under high thermal gradients has been investigated as a function of initial moisture content [Hartley and Black, 1981].

The cumulative experience and theoretical analysis seem to indicate that in clayey and silty soils at a volumetric water content of more than 20% and temperatures below 70°C, there is a high probability of stable heat transfer, and only limited moisture transfer (see Part IV). The heat

transfer process can then be described by a heat transfer equation which is not coupled to the moisture transfer equation, although it is still nonlinear and depends on local moisture content. This uncoupling allows the application of numerical methods with reasonable effort, while the application of the fully coupled equations in two or three dimensions over the whole storage area and storage period is beyond the capabilities of the presently available computational methods.

The initial parameter values adopted for this model are in the intermediate range of the published values, and the calculations include sensitivity tests to parameter variations. An experimental approach to determine these values using an inverse formalism is described in Part II.

1.3.2 SPATIAL VARIABILITY OF SOIL PROPERTIES

Thermal and hydraulic properties of soils may vary significantly over the storage area. Vertical variability is relatively easy to determine from existing well logs. In addition, temperature logs, which are not commonly available but are easily performed, may be used to infer the thermal properties of stratified soils through the attenuation and phase shift of surface temperature variations [de Vries, 1963; Rybakova et al., 1982]. The storage area may also have large horizontal variability, even in areas of generally horizontal stratification. Variations can be studied with geophysical tools such as ray tomography using seismic [e.g., Peterson, 1986] or electromagnetic [e.g., Dines and Lytle, 1979] sources, and ground penetrating radar [e.g., Benson, 1985] to map natural soil and rock conditions in the unsaturated zone. Commonly found variability of soil composition is not expected to have significant effects on heat storage and heat transfer. However, hard rock formations may increase drilling expenses. A simple method to determine heterogeneity employs several test logs of small diameter in the planned storage area equipped with temperature sensors. Similarity of the natural temperature-depth profiles indicates horizontal homogeneity of thermal properties.

1.3.3 SITING CONSIDERATIONS

The main factors affecting site selection are a) soil properties, b) hydrogeological conditions, c) distance to source and users of heat (or cold), and d) economics of excavation, installation, and operation of the storage site. Factors a) and b) are discussed in Sections 1.2 and 1.3.1 above. Distances to source and users may be minimized in order to reduce heat losses in transit, pumping costs, and investment in piping. The WCZ benefit by having lower heat losses in transit. Heat pipes buried in dry surface soil during the summer charge period have lower conductive losses, due to higher thermal resistance of the soil and higher ambient temperatures, than those in cold or moderate zones. Anti-freeze protection is unnecessary in most cases.

Vertical siting has two opposing constraints: shallow sites have high conductive heat losses to the surface, while deeper sites are more expensive to construct and are closer to the saturated zone, which acts as a virtual sink for conductive heat flow. The dimensions selected for this model place the top of the heat exchanger 4 m below the ground surface. The heat exchange process is of the regenerative type, with the thermal front advancing upwards from 16 m below the ground surface. The heat flux to the surface is therefore delayed with respect to the charging period. A specific siting option that offers several operational and economic advantages considers a greenhouse overlying the storage area, thus offering both protection from direct infiltration and lower heat losses [Nir et al., 1981]. An added feature of this design is direct root zone heating, which benefits certain plants more than conventional air space heating [Zeroni et al., 1983]. This siting option is readily available for agricultural applications, but is not suitable for retrofit of existing structures; it is best installed in advance of greenhouse construction as underfloor heating. However, new drilling techniques and exchanger placement methods may allow retrofit to existing structures.

1.3.4 TECHNOLOGICAL CONSIDERATIONS

Part I does not include detailed engineering designs and cost estimates. However, the feasibility of the proposed concepts, storage configurations, and operational procedures depends on the availability of proven technologies and materials, both at reasonable cost; these include the indirect sensing equipment discussed above, techniques of large diameter drilling, and durable components for underground heat exchangers. The configuration of the storage medium and heat exchangers considered here requires the capability of drilling 1-m-diameter wells. This has been reported to be available at moderate expense, following the developments and experience of the Scarborough Project [Mizra et al., 1985]. Buried heat exchange pipes are now used routinely for a multitude of heat transport applications, and polybutylene pipes have a record of over 20 years of continuous use in underground irrigation systems.

The design proposed here is a 1-m-diameter helical coil constructed from 3.2-cm-diameter polybutylene tubing. Thus the small diameter tubing is made 'to look' like a large diameter heat exchange surface with interior and exterior storage volumes. The effects of helically coiled pipes on heat transfer has been investigated [Patankar et al., 1974]. Using that derivation and the parameters assumed here shows that there is no need to consider modifications from linear-pipe heat transfer calculations.

Heat transfer benefits from high water content at the heat exchange surfaces. A circular drip irrigation pipe positioned at the top of the heat exchanger is included in our design. There is considerable experience to date with subsurface irrigation for agricultural purposes.

The storage volume interior to the heat exchanger provides the option for placing Phase Change Material (PCM) in an effective location without additional excavation. This is expected to enhance the operational capabilities of the storage system in terms of heat transfer and amount of stored heat. There is no known PCM material which would justify at present the economics of this arrangement, therefore its inclusion is not planned in the first stage of the proposed experiments, but it certainly is an interesting future option.

I.4 MATHEMATICAL MODELING OF A UZTES SYSTEM

I.4.1 CONCEPTUAL AND NUMERICAL MODEL DESCRIPTION

The heat storage system modeled in Part I consists of a square array of vertical helical storage ducts placed in unsaturated soil initially at 24°C. The top of each helix is 4 m below the ground surface and its height is 12 m. The helix has a diameter of 1 m and the spacing between adjacent ducts is 6 m. Between 0.5 and 1 m below the ground surface there is a shallow charge zone consisting of horizontal ducts. This feature is useful for greenhouse heating [Zeroni et al., 1983] but was not included in our subsequent designs (Parts II and III). Figure I.1 shows a schematic diagram of the storage system.

During summer (deep charge period), water warmed by solar collectors (or other alternative energy sources) to 65°C is pumped into the bottom of the vertical helix and is cooled as it flows to the top, depositing heat in the surrounding soil. During winter (deep discharge period), cool water at 20°C is pumped into the top of the helix and is warmed as it flows to the bottom, extracting heat from the soil. The shallow heat storage zone is used during winter to provide short-term storage between daily peak periods of energy supply (daytime) and demand (night-time) and for variability with periods of a few days to a week (cold or warm spells). Heat is transferred by diffusion from the soil to the ground surface, then into the overlying air.

As described in Section I.3.1, no fluid flow is considered in the unsaturated soil, so heat transfer there is purely by conduction. Uniform temperature- and saturation-independent thermal properties for a medium consisting of 60% soil, 20% water, and 20% air are used. In the heat exchanger, the fluid flow is prescribed and heat transfer by convection and conduction is

calculated.

From symmetry considerations, a duct in the interior of the array can be represented by an isolated duct enclosed in a square insulated boundary (Figure I.2). For modeling purposes, the square boundary is approximated by a circular no-flux boundary. The helical heat exchanger is approximated as an annular cylindrical conduit with inner radius $r_i = 0.4923$ m and outer radius $r_o = 0.5$ m. Fluid flow through the conduit is modeled as vertical incompressible flow that does not vary across the annulus, known as "piston-like displacement." Using these approximations to consider the soil storage volume around a single borehole, an axisymmetric geometry is obtained. The governing equations then become

$$C_s \frac{\partial T_s}{\partial t} - \frac{1}{r} \frac{\partial}{\partial r} \left[\lambda_s r \frac{\partial T_s}{\partial r} \right] - \frac{\partial}{\partial z} \left[\lambda_s \frac{\partial T_s}{\partial z} \right] = 0 \quad (1)$$

in the soil, and

$$C_w \pi (r_o^2 - r_i^2) \frac{\partial T_w}{\partial t} - 2\pi \lambda_s \left[r_o \frac{\partial T_s}{\partial r} \Big|_{r=r_o} + r_i \frac{\partial T_s}{\partial r} \Big|_{r=r_i} \right] + C_w q_w \frac{\partial T_w}{\partial z} = 0 \quad (2)$$

in the heat exchanger, where r is the radial coordinate, z is the vertical coordinate, t is time, T_s and T_w are temperatures in soil and heat exchanger fluid (water), respectively, C_s and C_w are volumetric heat capacities in soil and water, respectively, λ_s is apparent soil thermal conductivity [Childs and Malstaff, 1982], and q_w is volumetric flow rate of water through the heat exchanger. The inlet temperature of the heat exchanger is held fixed at T_{in} . The boundary condition at the heat-exchanger/soil interface, continuity of heat flux, has been invoked to write the second term of Equation (2) in terms of T_s . Initial conditions are specified by a uniform temperature T_0 in the soil and heat exchanger (i.e., the geothermal gradient is not included).

The computer code PT [Bodvarsson, 1982], which calculates fully coupled liquid and heat flows in a water-saturated porous or fractured medium, was developed at LBL as a general-purpose simulator to study hot-water geothermal reservoirs. The governing equations for PT consist of the conservation equations for mass and energy, and Darcy's law for fluid flow. Pressure and temperature are the dependent variables, and the rock matrix and fluid are considered to be in local thermal equilibrium at all times. For the present project, the fluid flow field is considered known, leaving only the energy equation, given above, to be solved.

PT uses the integral-finite-difference method [Narasimhan and Witherspoon, 1976] for space discretization. This method, which is a generalization of the finite-difference method,

treats one-, two-, or three-dimensional problems equivalently, without reference to a global coordinate system, enabling the use of regular or irregular geometries and heterogeneous, anisotropic material properties. Time-stepping is fully implicit, with direct matrix solution [Duff, 1977] of the coupled linear equations arising at each time step. PT has been verified against many analytical solutions and validated against several field experiments [Bodvarsson, 1982; Tsang and Doughty, 1985] as well as being applied to many energy-storage and geothermal-reservoir simulation problems.

A two-dimensional axisymmetric grid composed of 500 nodes is used for the present calculations. The mesh extends vertically from the ground surface to a depth of 50 m, and radially from 0 to 3 m. The mesh spacing is finest close to the duct ($-16 \text{ m} < z < -4 \text{ m}$, $r = 0.5 \text{ m}$). To represent one borehole in the midst of multiple boreholes, the outer radial boundary ($r = 3 \text{ m}$) becomes a no-flux boundary. To represent a single isolated borehole, the radial extent of the model is very large, to represent an infinite medium.

During initial simulations, the heat-exchanger inlet temperature T_m was prescribed at the bottom of the cylindrical conduit. In order to more accurately model the heat-exchanger geometry, the center pipe that carries fluid from the ground surface to the bottom of the heat exchanger was subsequently added to the model; its inclusion has only a small effect on modeled behavior.

The ground surface temperature is modeled as an annual sinusoidal variation with a mean value of 24°C and an amplitude of $\pm 4^\circ\text{C}$. In addition, unusually warm or cold winters are considered in which short-term (5-10 days) changes of $\pm 5^\circ\text{C}$ are added to the sinusoidal pattern.

To determine the average daily fluid flow rate through the heat exchanger, the seasonally variable supply and demand of energy is averaged to a series of constant segments ranging from five days to one month in length. Then, the daily supply or demand of energy for each duct is equated to the energy deposited or extracted for each duct in one day:

$$E = 24c_w(T_{in} - T_{out})\bar{Q} \quad (3)$$

where E is the supply or demand of energy per duct (MJ/day); c_w is the specific heat of water (MJ/kg K); T_{in} is the duct inlet temperature, 65°C during deep charge, 20°C during deep discharge; T_{out} is the variable duct outlet temperature ($^\circ\text{C}$); and \bar{Q} is the average fluid flow rate through the duct (kg/hr). Thus \bar{Q} is given by

$$\bar{Q} = \frac{E}{24c_w(T_{in} - T_{out})} \quad (4)$$

The parameters E , c_w , and T_{in} are given constants, while T_{out} is a variable calculated by PT. To calculate \bar{Q} for the first day of operation, T_{out} is assumed to be 24°C. To calculate \bar{Q} for subsequent days, T_{out} is determined by linear extrapolation from the T_{out} values for the two previous days. Clearly as T_{out} approaches T_{in} , \bar{Q} approaches ∞ . This indicates that heat conduction through the soil cannot keep up with energy supply or demand, or that the storage volume is fully charged or fully depleted.

1.4.2 VERIFICATION OF THE NUMERICAL MODEL WITH AN ANALYTICAL SOLUTION

Analytical solutions for the behavior of the heat exchanger and the storage configuration proposed here are not available. The closest analytical models known to us include several further simplifying assumptions: neglect of vertical conduction in the soil and the interior storage volume. The earliest models originate from the literature on solute transport in porous media with axial convection and radial dispersion [Ogata, 1964; Barker, 1982; van Genuchten et al., 1984; Chen, 1985]. A similar model applied to heat storage [Leroy, 1985] includes sensitivity analyses to several parameter values. Several results of transient heat transfer from heat exchangers are given [Claesson et al., 1985; Hansen, 1985], including some theoretical estimates of heat losses from storage for a variety of subsurface configurations and dimensions. An analytical solution based on Laplace transforms was recently proposed and investigated by E. Merzlyakov [private communication, 1991].

An analytical solution [Carslaw and Jaeger, 1959] for a simplified heat-transfer problem that includes some of the features of the present model is compared to PT-calculated results to verify we are using the code properly (e.g., fine enough spatial discretization, appropriate boundary conditions). The problem considered is radial heat flow from a constant-temperature cylinder. An infinitely long cylinder with radius a is surrounded by an infinite medium with thermal diffusivity $\alpha = \lambda C$. Both are initially at temperature T_0 . For times $t > t_0$, the temperature of the cylinder is held fixed at T_1 . The temperature distribution in the medium for $t > t_0$ is given by

$$T(r,t) = T_0 + (T_1 - T_0) \left\{ 1 - \frac{2}{\pi} \int_0^{\infty} \frac{e^{-\tau u^2} C_0(u, Ru) du}{u [J_0^2(u) + Y_0^2(u)]} \right\} \quad (5)$$

where

$$\tau = \frac{\alpha t}{a^2} \quad R = \frac{r}{a}$$

$$C_0(u, Ru) = J_0(u)Y_0(Ru) - Y_0(u)J_0(Ru)$$

and J_0 and Y_0 are first-order Bessel functions of the first and second kind, respectively.

Three cases are calculated with the numerical model, using the following boundary conditions:

- 1) Constant temperature $T_1=70^\circ\text{C}$ at $r=a=0.5$ m
- 2) Very high fluid flow rate through the duct, with $T_{in}=70^\circ\text{C}$
- 3) Typical summer flow rate ($\bar{Q}=25$ kg/hr), with $T_{in}=70^\circ\text{C}$

In each case there is a uniform initial temperature of $T_0=20^\circ\text{C}$.

The calculated temperature variation with radial distance at mid-duct depth is given in Figure I.3, for a series of times, along with the analytical solution. Cases 1) and 2) give identical results, and match the analytical solution very well. Case 3), which better represents the actual UZTES system, shows a rather different behavior, confirming that use of a numerical model is in fact necessary for analyzing the current UZTES problem.

1.4.3 MULTIYEAR SIMULATION

A number of multi-year energy supply-demand sequences have been modeled using an insulated-boundary model to represent an interior duct. (Edge effects are discussed at the end of the section.) The objective of these simulations was to find the transient period of the storage system, that is, the time beyond which a semi-steady periodic operation exists, and to indicate the sensitivity of the system's ability to respond to large variations in demand and supply.

Table I.2 shows the sequence of seasons considered. In general, summers (energy charge), labeled S, are all similar, while winters (energy discharge) vary. Some winter segments are a response to climatic variations; these segments are labeled C (cold), A (average), or W (warm). Other winter segments are special operational procedures, designed to optimize system performance; these segments are labeled L (low-demand), H (high-demand), or B (bleed, an especially high demand designed to exhaust the stored heat supply). The key measurement of the system's response to varying energy demands is \bar{Q} , the average daily flow rate. If \bar{Q} is greater than 180 kg/hr (a practical limit arising from pump technology), then the system cannot meet the imposed demands. Preliminary simulations gave $\bar{Q}>180$ during the first winter discharge, leading to the inclusion of the low-demand winter to provide a gradual start-up period for the system.

Cases 1, 2, and 3 consider three alternative second winters: warm, average, and cool. The energy demand is met in all cases, with successively higher values of \bar{Q} required in each case.

Table I.2 Calculations Made Using the Insulated-Boundary Model to Represent an Interior Duct.

Case	Sequence of Seasons	Comments
1	1S--1L--2S--2W	7-m-duct also meets demand
2	1S--1L--2S--2A	7-m-duct cannot meet demand
3	1S--1L--2S--2C	
4	1S--1L--2S--2H	
5	1S--1L--2S--2A--3S	$\bar{Q} > 180$ kg/hr during 3S
6	1S--1L--2S--2C--3S	$\bar{Q} > 180$ during 3S
7	1S--1L--2S--2B	$\bar{Q} > 180$ during 2B
8	1S--1L--2S--2Bp--3S--3B' --4S--4B'	

	Season	Heat Transfer Mode	Total Deep Charge (+) or Discharge (-)
S	Average Summer	Deep charge	+18,650 MJ
W	Warm Winter	Deep charge, deep discharge, and shallow charge	-2,000
A	Average Winter	Deep discharge and shallow charge	-6,600
C	Cold Winter	Deep discharge and shallow charge	-8,050
L	Low-demand Winter	Deep discharge and shallow charge	-2,400
H	High-demand Winter	Deep discharge, no shallow charge	-12,000
B	Bleed Winter	Deep discharge and shallow charge	-15,375
B'	Moderate-bleed Winter	Deep discharge and shallow charge	-12,075

Figure I.4 shows the time variation of ground-surface temperature, energy supply and demand, average daily flow rate \bar{Q} , outlet temperature T_{out} , heat flux through the ground surface, and cumulative stored energy for Case 2, and Figure I.5 shows a time sequence of the temperature distributions in the storage volume.

To further explore system capacity, Case 4 considers an especially high-demand situation with no shallow charge. Again the demand is met with an increase in \bar{Q} . Case 5 continues Case 2 for a third summer. Near the end of the charge period, $\bar{Q} > 180$, indicating that $T_{out} \approx T_{in}$, i.e., the heat storage volume is 'full.' Case 6 continues Case 3 for a third summer. Again $\bar{Q} > 180$

near the end of the charge period, despite the lower level of energy in the system at the start of the third year due to the higher demand during the second winter for Case 3 (cold winter) relative to Case 2 (average winter). Case 7 considers a 'bleed' second winter, designed to exhaust the system in preparation for the third year. Too much heat is required, however, and $\bar{Q} > 180$ as $T_{out} \approx T_{in}$, indicating that the heat storage volume is 'empty.' Case 8 considers a more moderate bleed winter, and the system can meet the demand. The third summer's charge can be accepted as well. The moderate bleed winter is repeated for the third and fourth years, successfully. By the end of the fourth year transient effects have greatly diminished. This indicates that there is an operational range of 65% energy recovery (12075 MJ/18650 MJ) after an initial transient period of 3 years. However, the recovery is associated with considerable exergy loss (i.e., T_{out} during discharge is much lower than T_{in} during charge). It is interesting to note that a 7 m long duct can meet the smaller demand of Case 1, but not that of the other cases.

Averaged Pumping Schedule: As described in Section I.4.1, the UZTES system responds to seasonal variations in energy supply and demand by varying the average daily pumping rate \bar{Q} , with \bar{Q} assumed to be constant over the whole day. In reality, each day consists of a pumping period and a resting period. Summer charge occurs during the daytime at a variable rate with a maximum at about 1 PM. Winter discharge occurs during the night-time at a constant rate. Modeling this discontinuous pumping schedule is rather inefficient, as PT takes very small time steps during the transient periods that occur whenever pumping begins or ceases. Because sequences of several years must be calculated, such small time steps are quite impractical. To allow larger time steps, instead of the real system pumping part of the day at a flow rate Q , we model a system pumping continuously at an average flow rate \bar{Q} . Because the change in \bar{Q} from day to day is gradual, PT can take much larger time steps (up to 1 day long) than when the discontinuous pumping schedule is used. Selected short time intervals (one to two weeks) from various portions of the yearly charge-discharge cycle have been calculated with both the discontinuous and averaged pumping schedules, confirming that the averaged schedule gives proper results. Figure I.6 compares averaged and discontinuous T_{out} values for Case 2 for part of the second year. All the calculations listed in Table I.2 are made using the averaged pumping schedule.

Edge Effects: The axisymmetric single-duct model with an insulated outer boundary approximates the behavior of inner ducts of the storage array well. It is also somewhat applicable to outer (edge or corner) ducts at late times, after lateral heat losses from early cycles have

created a warm buffer zone around the storage array. For early-time edge effects, the infinite-radius model is used to provide a lower limit for system behavior. For Case 2 temperature distributions in the storage volume and variations in T_{out} and \bar{Q} (Figure I.7) are very different than the corresponding insulated-boundary results (Figure I.4 C and D). In fact, the 2A (average winter) demand cannot be met by the infinite-radius model. When both interior and edge ducts are considered together, the problem of not accepting summer charge (Cases 5 and 6) will be eliminated; even if interior storage volumes are full, outer ones will not be and \bar{Q} can be varied between ducts to achieve as constant a T_{out} as possible.

1.4.4 SENSITIVITY ANALYSIS

A number of parameter-variation calculations were made during the development of the model described in Section I.4.1.

Storage Volume Geometry: A preliminary version of the model included a 5-m-long duct located at a depth of 3 m, a 6.8-m horizontal spacing between ducts, and an inlet temperature of 60°C during deep charge. Initial calculations indicated that the volume of soil around each duct was not big enough to store the duct's energy supply for a typical summer, so the soil storage volume was enlarged by lengthening the duct from 5 to 7 m, and increasing the distance between ducts from 6.8 to 8 m. The larger volume was big enough to accommodate an entire summer heat supply, however the winter demand could not be met because the thermal conductivity of the unsaturated soil was too low for stored heat to travel from the edge of the storage volume to the duct within the short winter period. To remedy this, the dimensions of the storage volume were varied to allow more effective heat transfer to the duct, by lengthening the duct from 7 to 12 m, while decreasing the spacing between ducts from 8 to 6 m. Heat losses to the ground surface during summer were lessened by increasing the depth of the top of the duct from 3 to 4 m below the ground surface.

Inlet Temperature: Initial information on solar collectors indicated the maximum input temperature for charge periods to be 60°C. More recent developments suggest that 65°C is possible. For otherwise identical conditions, the increase from $T_{in}=60$ to $T_{in}=65$ °C causes a small decrease in outlet temperature T_{out} during the charge period, which is accompanied by a substantial decrease in the flow rate \bar{Q} .

Duct Geometry: In an attempt to improve heat transfer between the duct and the soil, the annular thickness of the duct was doubled, and the velocity of water flowing through the duct correspondingly halved. Heat transfer into the soil was nearly unchanged, indicating that heat

flow through the soil is the limiting factor determining heat exchange, rather than duct fluid velocity.

Soil Properties: The property controlling heat flow through the soil is its thermal conductivity λ . If λ is decreased from the usual value of 1.6 to 0.65 W/m K, corresponding to a decrease in soil moisture content, then \bar{Q} increases dramatically, from 30 to 150 kg/hr. On the other hand, if λ is increased from 1.6 to 2.4 W/m K, \bar{Q} remains nearly unchanged, indicating that the system is less sensitive to thermal conductivity above a value of 1.6 W/m K. Moisture content decreases as high temperatures increase the evaporation rate in the soil. If the dry region is limited to a thin layer adjacent to the duct, then \bar{Q} does not increase appreciably.

1.4.5 FUTURE MODEL DEVELOPMENT

The large difference in behavior between the finite (insulated) and infinite storage volume cases indicates that a multi-duct model may be necessary to properly model the early years of the system operation. Because of the detail necessary for each duct, a fully three-dimensional model would be quite expensive and cumbersome to use. Instead, an alternative approach is being considered, calling for a superposition of local (single well) and global (multi-well) models, and an iteration between models.

In order for the PT calculations of Part I, which assume constant λ , to be valid the moisture content in the field experiment must be constant, because of the strong dependence of thermal conductivity on moisture content. For situations in which moisture content cannot be held fixed, or when fluid flow through the unsaturated soil is important in its own right, a computer code incorporating the coupled flows of water (liquid and vapor phases), air, and heat must be used (see Part IV).

1.5 POTENTIAL APPLICATIONS

1.5.1 RESIDENTIAL AND INDUSTRIAL SPACE HEAT SUPPLY

The application of seasonal heat storage for residential and industrial space heating has been widely studied, experimentally tested, and proven to be technologically sound and even economically competitive in several locations in the colder climatic zones [International Energy Storage Conferences, 1981, 1983, 1985, 1988, 1990, 1991] Our discussion should therefore center on the evaluation of the specific characteristics of its application in the warm climatic zones (WCZ). Most factors specific to the WCZ (Section I.2) seem to favor such applications:

lower heat losses in storage and transport, readily available storage areas, shorter heating periods, higher inputs (for solar source), possibility of direct use, and higher coefficient of performance with heat pump use. The present design favors application to housing areas or industrial structures requiring a storage system with over 2000 m² surface area (30,000 m³ volume), with 1000 GJ energy stored per cycle. However, application for single homes is not efficient.

1.5.2 AGRICULTURAL USES

Agricultural uses were considered initially to be the preferred candidates for seasonal heat storage applications in WCZ. Several designs were offered for greenhouse space heating with an associated or independent root zone heating [Nir, 1983; Zeroni et al., 1983; Nir et al., 1981]. In many WCZ, intensive winter crop cultivation is a major component of the overall agricultural production. Winter productivity is shown to be significantly enhanced by additional heat in protected and semi-protected environments. Therefore the availability of the inexpensive, widely distributed, and reliable heat supply at relatively low temperatures offered by the seasonal storage of thermal energy is of great interest.

1.5.3 EFFECTS ON ALTERNATIVE-ENERGY RESOURCE DEVELOPMENT

The feasibility of seasonal heat storage may have significant influence on investment in the development of alternative energy resources. Due to the relatively short heating season, the mismatch between heat supply and demand is greater in WCZ than in the colder zones, therefore many potential resources, such as solar, low-temperature geothermal, and industrial waste heat, may not justify development. The seasonal storage allows year round operation of the facilities, reduction in peak heat transport demand and the associated investment in transport facilities. Detailed discussion of these factors is given in Nir and Benson [1982].

PART II. DESIGN AND CONSTRUCTION OF AN EXPERIMENTAL FIELD FACILITY FOR UZTES

II.1 INTRODUCTION

II.1.1 SCOPE OF INVESTIGATION

In Part II we describe the modeling, simulation, and construction of a field validation experiment, designed on the basis of the theoretical studies presented in Part I. The field experiment was conducted at the Beer-Sheva campus of the Ben-Gurion University of the Negev, in Israel, jointly with E. Korin, B. Bar-On, and coworkers. The modeling and simulation studies tailor the generic model described in Part I to the conditions of the field-experiment site and thereby guide the experimental design. As in Part I, heat transfer is assumed to be purely conductive, with moisture migration negligible. The experimental work includes the investigation of soil hydrologic and thermal properties, acquisition and development of suitable equipment for heat transfer and data collection, and construction of a scaled-down storage well. Operation of the two experimental storage cycles is described in Part III.

II.1.2 OBJECTIVES OF THE FIELD EXPERIMENT

The objectives of the field experiment are: (a) verification and validation of the theoretical model described in Part I; (b) use of the model for storage-facility design, construction, and operational control on a reduced field scale; (c) test of proposed technologies for excavation, emplacement, operation, and control of the storage facility, especially those associated with the heat-exchange and water-transport pipes; (d) evaluation of total system operation; (e) collection and evaluation of input data for cost estimates; and (f) indication of possible environmental effects.

II.2 MODELING AND SIMULATION AS A DESIGN TOOL FOR THE FIELD EXPERIMENTS

II.2.1 SIMULATION OF THE PLANNED FIELD EXPERIMENT

The modeling study is similar to that described in Part I, but it takes into consideration the smaller size of the experimental storage well, a limited time scale, and utilizes local soil parameters. The shallow heating zone included in Part I is eliminated, and the helical heat exchanger is located between 4 and 10 m depths. A schematic but realistic heat supply and demand pattern is

assumed, thus defining energy input and withdrawn during thermal charging and discharging periods of the storage facility.

Figure II.1 shows the heat-exchanger outlet temperature and flow rate as a function of time for reduced-scale (6-m-long heat exchanger) and full-scale (12-m-long heat exchanger) calculations. The same energy supply and demand pattern and soil properties are used for both calculations. Heat exchanger inlet temperature is 65°C during charge and 20°C during discharge. In the case of the reduced-scale field experiment, the storage volume is more quickly filled or depleted, causing less difference between inlet and outlet temperatures, thus requiring greater flow rates to meet the imposed energy charge or discharge requirement. The time at which the maximum practical flow rate is reached determines the appropriate duration for the field experiment.

The determination of soil properties, described in Section II.3.2, only provides information on thermal conductivity at temperatures below 25°C, thus some uncertainty remains as to what value to use in the simulations, where temperatures will be much higher. Figure II.2 shows the temperature distributions calculated assuming two values of thermal conductivity that differ by more than a factor of two. The difference between the two temperatures, known as the delta model, is also plotted. The delta model identifies locations where the temperature field is very sensitive to the value of thermal conductivity; these are locations where temperature sensors should be placed.

II.2.2 VERIFICATION OF THE CYLINDRICAL REPRESENTATION OF THE HELICAL HEAT EXCHANGER

One of the basic assumptions made for the numerical modeling of the UZTES field experiment is that the vertical helical heat exchanger can be modeled as a cylindrical conduit. This assumption allows the use of a two-dimensional axisymmetric calculational mesh, rather than the three-dimensional mesh which would be required by an exact model of the helical structure, resulting in a great savings in computational effort. The objective of this section is to verify this assumption. An additional objective is to optimize the proposed helical spacing.

A series of calculations have been made with the computer code PT on a simplified conduction problem that models one turn of the helix, and the equivalent length of cylindrical conduit as a vertical cross-section of an axially symmetric system (Figure II.3). The tubing that makes up the helix is modeled as having a square cross-section, to enable use of a calculational mesh with rectangular elements. Due to symmetry, the vertical boundaries of the modeled section are no heat-flow boundaries. The mesh extends radially far beyond the region where temperature

changes are expected. The soil surrounding the heat exchanger is initially at a constant temperature of 22°C, and the heat exchanger is held at a constant temperature of 65°C to model the first 30 days of the injection period. Extraction is modeled by starting with the temperature distribution after 30 days of injection, and holding the heat exchanger at a constant temperature of 20°C.

Various spacings between turns of the helix are examined: 4, 5, 6, 8, 10, and 12 cm. Results are presented as ratios of energy flux between the helical and cylindrical cases as a function of time (Figure II.4), and ratios of deposited energy density between the various helical spacings as a function of time (Figure II.5). For all cases, after about 5 hours the ratios are at least 0.9, indicating that for time scales of interest (days rather than hours), modeling using the cylindrical conduit approximation is verified. The temperature distributions after one hour of 'charge' for the helical and cylindrical cases, shown in Figure II.6 indicate that beyond the immediate vicinity of the heat exchanger the temperature distributions are insensitive to duct geometry. Figure II.6 also helps explain Figures II.4 and II.5. At early times, before the soil temperature has increased much from its initial value, heat is conducted at the same rate from all the surfaces of both the helical and cylindrical ducts. For helical spacings greater than 6 cm the cylinder has greater surface area, thus a greater energy flux. At later times, the temperature of the inner volume ($0 < r < 0.5$ m) nears the duct temperature, excluding the inner surface of the cylinder or helix from contributing to the heat transfer, and the effective heat transfer surface areas for the two configurations tend to become equal. Figures II.4 and II.5 indicate the feasibility of using larger spacing between coils of the helix despite the initial low values of heat transfer rate and deposited energy density. Increased spacing between coils results in a proportional decrease in the cost of tubing, a decrease in heat-exchanger weight, and easier construction. Based on these studies, it was decided to construct the heat exchanger for the reduced-scale field experiment with a helix spacing of 10 cm.

These simulations were performed with two configurations. One involving a center pipe, which will be used in the experiment as the inflow conduit, and one without. The results are not very different, with the central pipe having the expected effects: a slight decrease in T_{in} at the bottom of the helix, accompanied by a small temperature increase in the soil surrounding the center pipe (there is no effect visible in Figure II.6).

II.3 ESTABLISHMENT OF AN ENVIRONMENTAL DATABASE

II.3.1 DATA REQUIREMENTS

The database required for the modeling and simulation, and the scientific evaluation of the results of this project covers a wide range of interdisciplinary subjects. Meteorological measurements including ground surface temperatures are required to determine soil thermal parameters and to simulate local climate-dominated heat demand. Some data were made available to this project by the local meteorological service, others were obtained from soil temperature logs performed on site. Soil properties are required to estimate soil thermal parameters under varying moisture and temperature conditions, and to study boundary effects under thermal gradients in unsaturated soils, as discussed in Part IV. Two 5-cm-diameter observation wells were drilled in the storage area. Soil samples and temperature profiles were obtained down to 7 m depth. Soil granulometry, moisture content, and bulk density were measured at the Water Resources Center at the Jacob Blaustein Institute of Desert Research, Sede Boker. Moisture gauges with electronic response were calibrated on the soils of the experimental area, but yielded only qualitative results. Hydraulic conductivity and matric potential curves for silty-clay and sand were obtained from local data measured by other researchers [A. Hadas, personal communication, 1967; M. Silberbush, personal communication, 1987]. These values were subsequently used in the model calculations of Part IV. General soil characteristics at the storage location were deduced from local geological maps and from the analysis of soil sample logs of the 7-m-deep observation well OW1 and two storage wells, EW1 and EW2. The granulometric structure of the 7 m profile is shown in Figure II.7. Figure II.8 shows the moisture content (in weight %) for three profiles. Comments on the extent and evaluation of the database are given in Bar-On et al. [1991].

II.3.2 ESTIMATE OF SOIL THERMAL PARAMETERS BY AN INVERSE METHOD

As a part of the efforts to establish an environmental database, two observation wells, one 7 m deep (OW1) one 1 m deep (OW2) were drilled and equipped with temperature sensors. Several typical temperature logs are shown in Figure II.9. These experimentally measured temperature profiles may be used to determine the value of soil thermal diffusivity ($\alpha = \lambda / C$), by matching them against an analytical solution for the temperature profile in a homogeneous semi-infinite medium with a sinusoidal surface temperature. The equation for the temperature distribution is

$$T(z,t) = T_0 + T_a e^{(-z/d)} \cos[\omega(t - t_0) - z/D] \quad (6)$$

where T is temperature; z is depth below the ground surface; t is time; T_0 is the annual average

surface temperature; T_a is the amplitude of the temperature variation; $\omega = 2\pi/\tau$, where τ is the period of the variation; D is the decay constant, given by $D = \sqrt{2\alpha/\omega}$; and t_0 is the time of the maximum surface temperature. Because short-term temperature variations are not considered, the upper 1.5 m of the temperature profile, which is most sensitive to these variations, is not used in the matching procedure. Incomplete temperature records at the experimental site require that T_0 , T_a , and t_0 be determined by the matching procedure, as well as D .

The matching procedure consists of plotting the experimentally measured temperature profiles for a sequence of times, then plotting the corresponding analytical solutions for various values of the parameters T_0 , T_a , t_0 , and D . The experimental and analytically calculated sequence of profiles are compared visually, and the parameters corresponding to the profiles that best match the experimental data are judged to best represent the real system.

The best match to the observed data, shown in Figure II.9, gives $T_0 = 22.7^\circ\text{C}$, $T_a = 8.2^\circ\text{C}$, $t_0 = 192$ days, and $D = 2.94$ m (January 1 is day 1). Assuming a value of $2.1 \times 10^6 \text{ MJ/m}^3\text{K}$ for C , the coefficient of the apparent thermal conductivity, λ , was found to be 1.8 W/mK . These values are consistent with those found in the literature. However, we consider this to be a first approximation, as data from only a limited time period were used. Furthermore, air and shallow soil temperature data could be used to fit higher Fourier components of the surface temperature (daily or weekly variations) within the context of this analysis.

An advantage of using this field-scale method to estimate λ , as opposed to doing laboratory analysis of soil samples, is that it gives a spatially averaged value of λ , which may be difficult to obtain in the laboratory for a heterogeneous soil. Other more general methods for estimating hydrogeological and thermal properties of the storage area are discussed in Part I.

While the above value of the thermal conductivity was used for the initial simulation (the base case), the subsequent application of an algorithmic parameter search to a wider set of data of soil temperature profiles provided a range of estimates with a resulting value of $\lambda = 1.1$ to 1.2 W/mK as the best estimate. Details of the parameter search procedure and the results of its application are discussed in Appendix B. The sensitivity of the validation results to the change in parameter values is presented in Part III.

II.3.3 ENVIRONMENTAL EFFECTS

Environmental effects on the seasonal storage system, and conversely those created by the storage itself, are of major concern in the case of several storage methods, such as those based on aquifers and open water bodies. However in our case, no environmental effects have been

observed up to this date, and further observations are planned to detect possible long-term geo-chemical effects.

These observations are valid under the postulated conditions of a semi-arid climate, with negligible direct fluid recharge and no proximity to aquifers, which can act as heat sinks.

II.4 SITE PREPARATION

II.4.1 DESCRIPTION OF THE STORAGE WELL

The thermal energy storage medium is the unsaturated soil volume, extending downwards from 4 m below ground level. The heat is transferred to the soil through a polybutylene pipe heat exchanger, in a vertical helix configuration of 1 m diameter and 6 m length. It is positioned in a 1.1 m diameter well, 10 m deep, located on the campus of the Institutes of Applied Research of the Ben-Gurion University of the Negev in Beer Sheva. Figures II.10 and II.11 illustrate the heat exchanger construction and emplacement [Nir et al., 1990]. The well volume is refilled with the original silty-clay soil under water saturated condition. Temperature and moisture sensors are placed in the interior of the helix, and in a 7-m deep observation well located at 1.68 m away from the center of the heat exchanger. Wetting coils are placed at four locations on the heat exchanger, in order to compensate for possible drying of the soil at the hot boundary. The location and designation of the sensors are shown in Figure II.12 [Doughty et al., 1990]. Details of heat exchanger construction and emplacement are given in Bar-On et al. [1991]. The heat is supplied by circulating hot water in a closed flow system, shown in Figure II.13. Heat extraction is done by circulating ambient temperature water in a reverse direction.

II.4.2 SUMMARY

The site-preparation work may be summarized as follows:

- a) area layout planning;
- b) construction of two observation wells (OW1 and OW2) to aid in preparation of an environmental database;
- c) purchase and calibration of temperature and moisture sensors and the computerized logging system;
- d) design of a new heat exchanger and construction of component parts;
- e) development of a technique for heat-exchanger emplacement;
- f) drilling of a 1.1-m-diameter, 3-m-deep 'practice' well (EW1);

- g) assembly and placement of a 3-m-deep heat exchanger;
- h) drilling of the 10-m-deep storage well (EW2);
- i) placement of the 6-m-long heat exchanger equipped with sensors and wetting coils;
- j) erection of two housing sheds for the heat supply and data logging equipment; and
- k) connection and test of the heat supply and data logging equipment.

PART III. DESCRIPTION AND EVALUATION OF TWO HEAT STORAGE CYCLES

III.1 1989 CHARGE/DISCHARGE CYCLE

The first storage cycle consisted of a 9 month charge and a 1 month discharge period beginning in February 1989. The heat-exchanger input temperature and flow rate are shown in Figure III.1, along with the time-averaged values used as input for the numerical simulation of the test. During the last month of the charge period the wetting coils were used to add water to the soil close to the heat exchanger.

III.1.1 BASE-CASE MODEL

The 1989 experiment was simulated using the model described in Section II.2.1, the boundary conditions shown in Figure III.1, and uniform constant values of thermal conductivity (1.8 W/m K) and heat capacity (2.35 MJ/m³K). Figure III.2 shows observed and calculated time sequences of temperature for selected sensor locations. The experiment was interrupted several times due to electrical breakdowns. This provided an unintentional test of the high-frequency thermal response of the system. The above figures indicate that in all relevant sensor locations this response was well reproduced by the model. The calculated temperatures are generally within 4°C of the observed values, and in most cases underpredict them.

Figure III.3 shows the observed temperatures superposed on the calculated isotherms at the end of the charge period. Figure III.4 presents a detailed comparison of observed and calculated temperatures during the October-November 1989 discharge period. These figures confirm the generally good agreement between the observed and calculated temperatures.

Several factors can contribute to the discrepancies between observed and calculated temperatures. These can be categorized as a) simplifications in modeling due to the neglect of spatial heterogeneity, nonlinearity of the heat transfer, coupling of heat and mass transfer, and heat flux from the inlet and outlet pipes; b) errors in initial estimates of parameters and soil properties; and c) quality of the collected data. All of these issues are discussed in the next sections.

III.1.2 SENSITIVITY STUDIES

Figure III.5 shows the fractional difference between the calculated and observed temperatures as a function of time, for selected sensor locations for the base-case model (Case A) and a subsequent model (Case G, described below). To enable a convenient comparison between various models, we examine the time-average of the fractional difference between the observed and

calculated temperatures

$$\langle \Delta T_{frac} \rangle = \left\langle \frac{T_{obs} - T_{calc}}{T_{obs} - T_{obs}^{init}} \right\rangle \quad (7)$$

where T_{obs} and T_{calc} are observed and calculated temperatures, respectively, T_{obs}^{init} is the observed temperature at the start of the experiment, and $\langle \rangle$ denotes the time-average over days 160-290 of the 1989 test (see Figure III.1). The quantity $\langle \Delta T_{frac} \rangle$ is calculated for three locations (see Figure III.2):

- Ch0 The heat exchanger outlet temperature
- Ch6 The deepest temperature sensor inside the heat exchanger
- A7 The deepest temperature sensor outside the heat exchanger.

Although the *in situ* value of soil thermal conductivity λ was estimated from the soil temperature profiles (Section II.3.2), the actual value of λ within the heat exchanger may be different due to variations in temperature, moisture content, and soil density resulting from the excavation and refilling procedure. It was therefore considered worthwhile to treat λ as an unknown parameter and model the 1989 storage cycle using a range of values. Results of this study are summarized in Table III.1. In each case, λ is assumed constant in time and space. A comparison of the $\langle \Delta T_{frac} \rangle$ values indicates that the thermal conductivity has a large effect on the system behavior. Increasing λ by 25% compared to Case A results in larger $\langle \Delta T_{frac} \rangle$ values (Case B), while decreasing λ by 20% results in smaller $\langle \Delta T_{frac} \rangle$ values (Case C), indicating that $\lambda < 1.8$ W/m K is probably appropriate to represent the system. This finding is consistent with the soil temperature profile analyses (Section II.2.3 and Appendix B).

Table III.1 Sensitivity studies.

Case	λ (W/mK)	Comments	$\langle \Delta T_{frac} \rangle$ (%)		
			Ch0	Ch6	A7
A	1.8	Base case Most calculated T 's are too low	4.1	5.8	3.6
B	2.25	Worse than A	9.0	9.8	5.4
C	1.44	Better than A	-1.1	2.4	2.2

III.1.3 MODEL IMPROVEMENTS

Three additional mechanisms, described below, can be included in PT to more accurately reflect physical processes occurring during the storage cycles. The results of calculations that include these effects are summarized in Table III.2.

- (1) It is generally accepted in the soil physics literature that soil thermal conductivity increases with temperature. For simplicity we consider a linear variation with a value of λ at $T = 22^\circ\text{C}$ of 1.8 W/m K (Case D). Case D produces larger values of $\langle \Delta T_{frac} \rangle$ than the base case (Case A). This is not surprising in view of Table III.1, which shows that using a larger constant value of λ also increases $\langle \Delta T_{frac} \rangle$. For a case with temperature-dependent λ , to decrease $\langle \Delta T_{frac} \rangle$ the value of λ at 22°C must be smaller.
- (2) Soil heat capacity C varies with soil moisture content, which is larger within the heat exchanger because the backfilled soil was saturated with water during heat exchanger construction. Allowing C to vary in space has a very small affect on $\langle \Delta T_{frac} \rangle$ (compare Cases A and E).
- (3) In the base-case model, the center pipe was assumed to be perfectly insulated between the ground surface and the top of the heat exchanger (0 to 4 m depth). Using realistic thermal properties for the insulation allows a small part of the heat stored to be deposited in the shallow soil overlying the heat exchanger (Case F). Including this effect decreases $\langle \Delta T_{frac} \rangle$ a moderate amount (compare Cases A and F).

Table III.2 Model improvements.

Case	Description	$\langle \Delta T_{frac} \rangle$ (%)		
		Ch0	Ch6	A7
D	$\lambda(T)$: linear variation $d\lambda/dT = 0.009 \text{ W/mK}^2$, $\lambda(22^\circ\text{C}) = 1.8 \text{ W/mK}$	5.7	7.5	3.3
E	$C(r,z)$ duct interior $C = 3.2 \text{ MJ/m}^3\text{K}$ elsewhere $C = 2.35 \text{ MJ/m}^3\text{K}$	4.1	5.8	3.5
F	Shallow heat flow included	3.3	5.1	3.0
F-90	1990 test, same model as F	5.0	3.7	1.8

The results of a new model (Case G), which combines all the improvements shown in Table III.2 and uses a smaller value of $\lambda = 1.35 \text{ W/m K}$ at $T = 22^\circ\text{C}$, are shown in Figure III.5 and Table III.3. The ΔT_{frac} values are much improved relative to the base case (Case A).

Another useful comparison to make is between Cases F and G, which use different representations of the thermal properties λ and C . Case F simply considers uniform, constant values, while Case G considers a temperature dependent λ , and a moisture dependent C . Although Tables III.2 and III.3 show that for all temperature sensors, $\langle \Delta T_{frac} \rangle$ is smaller for Case G than for Case F, the value of the more complex modeling effort required for Case G has to be judged in the context of how the modeling results will be used.

Table III.3 New model.

Case	Description	$\langle \Delta T_{frac} \rangle$ (%)		
		Ch0	Ch6	A7
G	Combine all three improvements (see text)	-1.0	2.5	0.4
G-90	1990 test, same model as G	2.6	4.2	2.3

Note: Cases A, B, C, D, E, F, and G show $\langle \Delta T_{frac} \rangle$ for the 1989 test. Cases F-90 and G-90 show $\langle \Delta T_{frac} \rangle$ for the 1990 test.

III.2 1990 CHARGE/DISCHARGE CYCLE

The second test, performed in February 1990, consisted of a charge period of 35 days, and used higher temperatures and flow rates and better control capability than the first test. Comparing Case F (constant λ and C) and Case G (temperature-dependent λ , moisture-dependent C) for the 1990 cycle (Cases F-90 and G-90 in Tables III.2 and III.3), shows a substantial decrease in $\langle \Delta T_{frac} \rangle$ for the outlet temperature Ch0, and a small increase in $\langle \Delta T_{frac} \rangle$ for the temperature sensor locations Ch6 and A7. The most important indicator is the heat-exchanger outlet temperature (Ch0) which provides an integrated value of the temperatures throughout the storage volume. Hence, we consider Case G the optimal representation of the system.

III.3 SUMMARY OF EXPERIMENTAL OPERATION

The problems which were of major concern at the outset of the experimental program related to the availability and reliability of large-diameter well drilling, heat exchanger construction and emplacement techniques, and the stability of the heat transfer process in unsaturated soils.

Recent advances in drilling techniques allowed fast, reliable and relatively inexpensive construction of storage wells. A novel method of heat exchanger construction and emplacement was developed, but was found to be cumbersome and expensive. However the experience gained in its use led to a modified design which promises a significant improvement over the previous one [Bar-On et al., 1991].

The heat transfer process did not indicate any significant deterioration during the 9 month charging period. On the other hand, there was no indication of improvement of heat transfer due to the wetting application during the last month of the charge period. Together, these observations indicate that the soil near the heat exchanger does not dry out during the charge period. This may be ascribed to the type of soil (silty clay) and to its initial high saturation. However, the possibility of dry out remains for multiyear operation, and therefore the wetting coil arrangement should not be discarded on the basis of this experience. Furthermore, based on the insight obtained through these studies (and those of Section IV), we are concerned with the possibility of an accumulation of solutes at the hot boundary, a potential problem which justifies further theoretical and experimental investigation.

III.4 MULTIYEAR FULL-SCALE MODELING

Following the modeling of the reduced-scale field experiment, a multi-year simulation for a full-scale pilot project was carried out using the base-case model (Case A). Based on the results shown in Tables III.1–III.3, we believe the new model (Cases G and G-90) best represents conditions at the field site. However, Cases A and C produce similar results, and are simpler to simulate since none of the additional mechanisms shown in Table III.2 are included. The larger value of λ used in the base-case model is well within the range of values found in the literature for unsaturated soils, so the full-scale simulation, while not optimal for the present field site, does represent typical unsaturated soil conditions.

The simulation considers storage around a borehole located near the center of a multiple borehole storage field (i.e., neglecting edge effects). Five yearly cycles of heat charge and discharge are simulated, with inlet temperatures of 65°C during the charge periods and 20°C during the discharge periods, and a 36°C minimum outlet temperature during discharge. The energy supply and demand is determined iteratively to be the maximum value the storage system can handle: each charge period ends when the outlet temperature nears the inlet temperature, and each

discharge period ends when $T_{out} = 36^{\circ}\text{C}$, a predetermined lower limit for useful outlet temperatures. The simulation indicates a discharge capability of 6 MWh per annual storage cycle, with an energy recovery of 72% and an exergy efficiency of 0.3, for a nominal size heat exchanger of 18 m length and 1.3 m diameter. The key results of the simulation (heat-exchanger outlet temperature, flow rate, and stored energy) are shown in Figure III.6. Increasing inlet temperature from 65°C to 80°C results in an increase in energy recovery from 72% to 75%; the corresponding outlet temperature, flow rate, and stored energy are shown in Figure III.7.

The energy recovery can be further increased by other changes in operating conditions such as a) lower minimum usable outlet temperature (e.g. for agricultural uses or with heat pump coupling); b) longer heat exchanger; and c) siting the heat exchanger at a greater depth. The thermal energy supplied by a 4000 m^2 storage field (110 boreholes) would be between 500 to 1000 MWh per storage season, depending on the above operating conditions, after an initial transient period of three years. This size can be considered to be the basic module, which can be expanded by adding similar units according to local conditions of supply and demand.

The theoretical and experimental evidence indicate the feasibility of cold storage using a similar design procedure.

PART IV. STUDIES OF HEAT AND MASS TRANSFER IN UNSATURATED SOILS

IV.1 INTRODUCTION

Extensive simulations of seasonal heat storage in unsaturated soils have been performed, as described in Parts I, II, and III. All those simulations assumed that under the conditions of the field experiments, i.e., water at temperatures in the range of 65 to 75°C, stored in silty-clay soils with a high initial water content, heat transfer in the soil is a purely conductive process. However, drying of the soil at the thermal front may cause a significant reduction in thermal conductivity, the onset of convective heat transfer, a redistribution of solutes, and chemical and physical changes in soil properties. The present section describes initial studies of the importance of these effects in the context of heat storage in unsaturated soils. Vermeer et al. [1982], Groeneveld et al. [1984], Nassar and Horton [1989], and Tarnawski et al. [1990] have conducted experimental and theoretical studies in this area. Understanding these processes is important not only for this project, but is also of basic interest in a number of related fields, e.g., disposal of heat-generating nuclear and chemical waste.

IV.2 THEORETICAL INVESTIGATION

Theoretical results presented by Bear et al. [1991] indicate that for a certain temperature and moisture-content range the dominant mechanism for heat transfer in unsaturated soils may change from conduction to convection in the vicinity of a hot boundary. Whether or not this transition occurs depends strongly on the initial moisture content of the soil and on the relation between the hydraulic conductivity and the matric potential, which vary among soil types. The transition greatly affects the quantity of heat that can be transferred through the soil,

In order to facilitate validation of this theory through laboratory experiments, additional extensive modeling and simulation studies have been performed. The work includes extending the one-dimensional analytical model used by Bear et al. [1991] to a two-dimensional numerical model which matches the geometric configuration of the planned laboratory experiment and incorporates the actual hydraulic parameters of the sandy and silty-clay soils to be used. The objectives of the simulation were to find the appropriate time and space scales and the precision required for the proposed validation experiments, which will measure temperature and moisture distributions in two dimensions, for given boundary temperatures in the 65-80°C range. At a

subsequent stage solute transport will be included. If the theory is validated, it can be used to optimize heat transfer by determining appropriate initial moisture conditions, thus improving the performance of the heat exchanger in many types of soil.

IV.2.1 MATHEMATICAL MODEL

A detailed description of the mathematical model for heat and moisture transport in unsaturated soils is presented by Bear et al. [1991]. The model follows the approach of Philip and de Vries [1957], but uses matric potential as a primary variable instead of water content. Thermodynamic equilibrium is assumed to exist locally between solid, liquid and gaseous phases. The governing equations consist of a mass balance for water (which includes liquid and vapor phases) and an energy balance. A mass flow factor accounts for the effect of air [Philip and de Vries, 1957]. Liquid, vapor, and heat fluxes are all driven by matric potential and temperature gradients. For heat flux, the coefficient of the temperature gradient is described as an effective thermal conductivity, but it accounts for all heat transfer processes driven by temperature gradients, whether conductive or not.

The computer program UNSATHM [Bensabat et al., 1992] is a transient two-dimensional finite element code that embodies the mathematical formulation outlined above. For the present work, we consider a vertical cross-section of soil, 36 cm wide and 12 cm tall. In the mathematical model, all boundaries are closed to fluid flow. In the planned experiment, the excess pressure due to increased temperature is released at the cold boundary, with a resulting insignificant moisture loss. The upper and lower boundaries are insulated and the lateral boundaries are held at fixed temperatures, T_1 and T_0 , with $T_1 > T_0$.

IV.2.2 SAMPLE RESULTS

Three simulations were performed, two for sand and one for silty-clay. The initial temperature of the soil in each case is a uniform 25°C, and the temperature boundary conditions are either $T_1 = 65^\circ\text{C}$ or 80°C at the hot boundary and $T_0 = 25^\circ\text{C}$ at the cold boundary. Initial moisture content is $\theta = 0.05$ for the sand and $\theta = 0.25$ for the silty-clay. Because the two types of soil have very different relationships between matric potential and water content, these different initial water contents correspond to similar matric potentials. Figures IV.1 – IV.4 show temperature and moisture profiles for four times: 4, 24, and 48 hours and at quasi-steady state.

Silty-clay: Note that the moisture content scales are quite different for the sand and silty-clay soils. In fact, for the silty-clay soil the moisture content changes very little over the entire simulation period. A slight enhancement in moisture content with depth illustrates the small

effect of gravity, but temperature does not vary at all with depth. Steady-state conditions are reached in 5 days, but examination of Figures IV.2 and IV.3 show that near-steady conditions have already been reached after 1 day. The steady-state temperature profile is linear, indicating that the effective heat transfer coefficient is constant.

Sand: For both sand simulations, moisture content varies strongly with position and time, and a dry region forms near the hot boundary. As expected, the results are qualitatively similar for the two hot-boundary temperatures, but drying effects are stronger for the higher temperature. Steady-state conditions are reached in 10 days for the 65°C hot-boundary case and in 17 days for the 80°C case. For both cases, the steady-state temperature profile is nonlinear, implying that in sandy soils the effective heat transfer coefficient varies in space.

IV.2.3 CONCLUSIONS

Although the geometries of the numerical model and the UZTES system are very different, some general conclusions from the simulations can be applied to the field-scale operation. For the UZTES system to work effectively, sufficient heat transfer from the heat exchanger to the soil must be maintained. It is apparent that silty-clay soils minimize moisture transport, tending to make conductive heat transfer stable, so if the system starts out with sufficient heat transfer it will be likely to remain so. On the other hand, moisture redistribution is large in the sandy soils, indicating that extensive dried out regions may develop, with a possible associated loss of heat transfer ability.

We have done other calculations for sand, using higher initial values of moisture content (results not shown). In these cases, a dried out region does not develop for the temperature range considered here. Altogether, we interpret these results to indicate that for effective UZTES we should try to find silty-clay rather than sandy soils, and ensure that the initial moisture content is high, as demonstrated in Section III.

IV.3 LABORATORY EXPERIMENTAL PROGRAM

In order to study heat and mass transfer in unsaturated soils, and to validate the theoretical investigation described above, a laboratory experimental system was planned and its construction initiated at the Institutes of Applied Science, BGU [Bensabat et al., 1988a]. It consists of two identical plexiglass containers, one containing sand and the other silty clay. The soil is emplaced at known bulk density and initial moisture content. Attempts are made to prepare as

homogeneous a sample as possible. The initial distribution of water content is made uniform. A thermostatic controller maintains the same constant-temperature boundary conditions for the two containers. The hot ends are held at either 65 or 80°C, while the cold ends are held at 25°C. Soil homogeneity and moisture content are determined using narrow beam gamma absorption. This method provides two-dimensional scanning with a space resolution of 0.5 cm. Its precision in water-content determination, based on previous calibrations, is 1%, with a high level of significance. Measurement of solute concentration can be achieved by microscale sample extraction.

Further studies have provided the basis and direction for a more precise and general approach that will use recent developments in positron emission tomography (PET) and temperature stabilization using phase change materials (PCM). This would allow simultaneous measurements of solute, temperature, and moisture distributions [Nir, 1990].

CONCLUSIONS AND RECOMMENDATIONS

1. PROJECT STATUS

This investigation has achieved the following objectives: a) progress in validation of the concept, models, and technical solution for seasonal storage of thermal energy in an unsaturated zone under semi-arid climatic conditions; b) development and field test of heat exchanger construction and emplacement techniques, and proposals for an improved heat exchanger design; c) field validation of the concept of seasonal storage of thermal energy in the unsaturated zone; d) theoretical investigations of the stability of heat transfer processes under these storage conditions; and d) initial cost estimates of this storage method [Bar-On et al., 1991].

2. RECOMMENDATIONS FOR CONTINUED ACTIVITIES

The activities described below are beyond the planned scope of this project. They can be advanced by multi-institutional efforts comprising governmental, industrial, and academic initiatives.

2.1 EXPERIMENTAL STUDIES

a) Test of the improved heat exchanger design and modified emplacement method [Bar-On et al., 1991]; b) laboratory studies of solute effects on heat transfer at a hot boundary, using positron emission tomography (PET), [Nir, 1990]; c) pilot field experiment including a full size multi-well configuration; d) cold storage field experiments.

2.2 THEORETICAL STUDIES

a) Adaptation of the existing numerical model (for constant effective thermal conductivity λ) to a PC or work station; b) development of approximate analytical solutions using Laplace transforms for quick estimate of optimal storage configurations; c) review of exergy efficiency approaches relevant to the storage of heat (or cold).

2.3 SYSTEM STUDIES

a) Review the potential sources of heat/cold in selected areas, and their relation to prospective uses; b) investigate environmental aspects of the storage methods; c) assess the effect of the seasonal storage capability on energy conservation and energy policy [Nir and Benson, 1982].

3. PROJECTED APPLICATIONS OF THE SEASONAL STORAGE OF THERMAL ENERGY

While novel applications of seasonal thermal energy storage are expected to appear beyond those seen now, we can summarize the present possibilities as being mainly for space heating or cooling and industrial preheating.

An initial cost/benefit analysis [Bar-On et al., 1991] indicates that the seasonal storage method should not be based on energy sources which have potential for direct application. Rather, the identified candidates are sources of waste heat at temperatures in the 70-90°C range, of industrial, geothermal, or solar origin, which are out of phase with the seasonal demand. Utilization of these sources for other purposes (e.g., irrigation) or disposal to the environment may require additional investment, effectively making their cost to the storage system negative. Sources of cold are primarily produced by low winter temperatures. All these sources are limited by the requirement that they be located a short distance from the user. Their utilization is shown to be greatly extended by coupling with heat pumps [International Energy Storage Conferences, 1981-1991].

ACKNOWLEDGEMENTS

The careful review of this report by Drs. T. Hadgu and M.J. Lippmann is gratefully acknowledged. We also acknowledge Dr. Eli Korin, The Institutes for Applied Research, Ben-Gurion University of the Negev, Israel, for his collaboration in the field experiments; Dr. Jacob Bensabat, Massachusetts Institute of Technology, for the theoretical developments described in Part IV; and Dr. Gudmundur S. Bodvarsson, Lawrence Berkeley Laboratory, for assistance in the use of the numerical model PT. This project was supported in part by the United States-Israel Binational Science Foundation under Grant No. 85-00129, and in part by the Director, Office of Energy Research, Office of Basic Energy Sciences, Engineering and Geosciences Division, of the U.S. Department of Energy under Contract No. DE-AC03-76SF00098.

REFERENCES

- Bankston, C.A., Technical and economic feasibility of central solar heating plants with seasonal storage, in Proc. ENERSTOCK 85, p. 353, 1985.
- Barker, J.A., Laplace transform solutions for solute transport in fissured aquifers, *Adv. Water Resour.*, 5, 98, 1982.
- Bar-On, B., Doughty, C., Korin, E., Nir, A., and Tsang, C.-F., Seasonal storage of thermal energy in unsaturated soils: experimental procedure and technological developments, In Proc. THERMASTOCK 91, p. 4.4, 1991.
- Bear, J., Bensabat, J., and Nir, A., Heat and mass transfer in unsaturated porous media at a hot boundary: I. One-dimensional analytical model, *Transport in Porous Media*, 6, 281-298, 1991.
- Benet, J.C. et al., Physical model for the study of mass and energy transfer in the non-saturated layer of soil located above a solar energy storage zone, in *Solar Energy Applications to Dwellings*, Vol. 4, T.C. Steemers and C. Den Ouden (eds.), Reidel Co., 1984.
- Benet, J.C., Saix, C., and Jouanna, P., Etude experimentale des transferts de masse et d'energie au-dessus d'un stockage de chaleur en sol non sature, in Proc. ENERSTOCK 85, p. 213, 1985.
- Bensabat, J., Bear, J., Korin, E. and Nir, A., On validation attempts of the instability of heat transfer in unsaturated soils at the hot boundary, presented at Conference on Validation of Flow and Transport Models for the Unsaturated Zone, Ruidoso, New Mexico, 1988a.
- Bensabat, J., Doughty, C., Korin, E., Nir, A., and Tsang, C.F., Validation experiments of seasonal thermal energy storage models in unsaturated soils, In Proc. JIGASTOCK 88, p. 121, 1988b.
- Bensabat, J., Bear, J., Doughty, C., and Nir, A., Heat and mass transfer in unsaturated porous media at the hot boundary. Part II. Two dimensional numerical model, in preparation, 1992.
- Benson, R.C., Evaluation of conditions in the unsaturated zone, *EOS, Trans. AGU*, 66, 46, 881, 1985.
- Blahnik, D., Preliminary assessment of promising nonaquifer STES, in Proc. Int. Conf. on STES and CAES, p. 70, 1981.
- Bodvarsson, G.S., Mathematical modeling of the behavior of geothermal systems under exploitation, *Rep. LBL-13937*, Lawrence Berkeley Laboratory, Berkeley, Calif., 1982.
- Boysen, A., Central solar heating plants with seasonal storage: an international feasibility study, in Proc. ENERSTOCK 85, p. 365, 1985.
- Carslaw, H.S. and Jaeger, J.C., *Conduction of heat in solids*, 2nd Edition, Oxford, London, 1959.
- Chen, C.S., Analytical and approximate solutions to radial dispersion from an injection well to a geological unit with simultaneous diffusion into adjacent strata, *Water Resour. Res.*, 21, 1069-1076, 1985.
- Childs, S.W. and Malstaff, G., Final Report: Heat and mass transfer in porous media, *Rep. PNL-4036*, Pacific Northwest Laboratory, Richland, Washington, 1982.
- Claesson, J., Efring, B., Eskilson, P., and Hellstrom, G., Markvarme: En Handbok om Termiska Analyser, *Rep. T16-18:1985*, Swedish council for Building Research, Stockholm, Sweden, 1985.
- de Vries, D.A., Thermal properties of soils, in *Physics of plant environment*, W. R. van Wijk (ed.), North-Holland, Amsterdam, p. 210-236, 1963.
- Dines, K.A. and Lytle, R.J., Computerized geophysical tomography, *Proc. IEEE*, 67, 7, 1065-1073, 1979.
- Doughty, C., Korin, E., Nir, A., and Tsang, C.-F., Seasonal storage of thermal energy in unsaturated soils: simulation and field validation. STES Newsletter, Vol XII, Nos. 1 and 2, International Council for Thermal Energy Storage, 1990.
- Doughty, C., Nir, A., Tsang, C.-F. and Bodvarsson, G. S., Heat storage in unsaturated soils: Initial theoretical analysis of storage design and operational method, In Proc. Int. Conf. on

- Subsurface Heat Storage in Theory and Practice, p. 518-523, 1983.
- Doughty, C., Tsang, C.-F., Korin, E., and Nir, A., Seasonal storage of thermal energy in unsaturated soils: modeling, simulation, and field validation. In Proc. THERMASTOCK 91, p. 4.3-1. 1991.
- Duff, I.S., MA28—A set of Fortran subroutines for sparse unsymmetric linear equations, *Rep. AERE-R 8730*, Harwell/Oxfordshire, Great Britain, 1977.
- Groeneveld, G.J., Snijders, A.L., Koopmans, G., and Vermeer, J., Improved method to calculate the critical conditions for drying out sandy soils around power cables, in IEEE Proceedings, Vol. 131, Pt. C, No. 2, March 1984.
- Hadorn, J.-C., Guide to seasonal heat storage, SIA Documentation D 028, Zurich, Switzerland, 1988. (English translation, E. Morofsky, Public Works Canada, 1990.)
- Hansen, P.N., General theory of heat and cold storage, in Proc. ENERSTOCK 85, p. 567, 1985.
- Hartley, J.G. and Black, W.Z., Transient simultaneous heat and mass transfer in moist unsaturated soils, *Trans. ASME*, 103, 5, 376, 1981.
- Hausz, W., Conceptual design options for a real STES application, in Proc. Int. Conf. on STES and CAES, p. 292, 1981.
- Hellstrom, G., Ground Heat Storage: thermal analyses of duct storage systems, Dept. of Mathematical Physics, University of Lund, Sweden, 1991.
- Herkelrath, W., Comment on 'Analysis of water and heat flow in unsaturated-saturated porous media' by Marios Sophocleous, *Water Resour. Res.*, 17, 255, 1981.
- International Energy Storage Conferences: Int. Conf. on Seasonal Thermal Energy Storage (STES) and Compressed Air Energy Storage (CAES), Pacific Northwest Laboratory CONF-811066, Seattle, October 19-21, 1981; Int. Conf. on Subsurface Heat Storage in Theory and Practice, Swedish Council for Building Res., Stockholm, June 6-8, 1983; ENERSTOCK 85 – Third Int. Conf. on Energy Storage for Building Heating and Cooling, Public Works Canada, Toronto, September 22-26, 1985; JIGASTOCK 88 – Fourth Int. Conf. on Energy Storage, International Council for Thermal Energy Storage, Versailles, October 17-20, 1988; Workshop on STES in Duct Systems, K. Knoblich et al. (eds.), Weihenstephen, Germany, 1990; THERMASTOCK 91 – Fifth Int. Congress on Thermal Energy Storage, Netherlands Agency for Energy and the Environment, Scheveningen, The Netherlands, May 13-16, 1991.
- Lebeouf, C.M., Analysis of simultaneous heat and mass transfer in soils below solar ponds, *Rep. SERI/TP-253-2744*, Solar Energy Research Institute, Golden, Colorado, 1985.
- Leroy, G., Reponse transitoire d'un echangeur cylindrique vertical dans le sol, in Proc. ENERSTOCK 85, p. 249, 1985.
- Lewis, T. and Wang, K., Geothermal research related to past climate, *Eos, Trans. AGU*, 73, 25, 265-269, 1992.
- Luikov, A.V., *Drying theory*, Gosenergoizdat, Moscow, 1950.
- Marshall, R.H., Evaluation of thermal storage systems, in *Solar Energy Applications to Dwellings*, Vol. 4, T.C. Steemers and C. Den Ouden (eds.), Reidel Co., 1984.
- Mirza, C., Lau, K.C., Morofsky, E.L., and Crawford, A.M., ATEs experience with the Scarborough field trial, in Proc. ENERSTOCK 85, p. 110, 1985.
- Narasimhan, T.N. and Witherspoon, P.A., An integrated finite-difference method for analyzing fluid flow in porous media, *Water Resour. Res.*, 12, 1, 57-64, 1976.
- Nassar, I.N. and Horton, R., Water transport in unsaturated nonisothermal salty soil: I. Experimental results, *Soil Sci. Soc. Am. J.*, 53, 1323-1329, 1989.
- Nassar, I.N. and Horton, R., Water transport in unsaturated nonisothermal salty soil: II. Theoretical development, *Soil Sci. Soc. Am. J.*, 53, 1330-1339, 1989.
- Nir, A., Comparison between soil heat storage and ATEs, *STES Newsletter*, IV, 1, 4, Lawrence Berkeley Laboratory, Berkeley, Calif., 1981.
- Nir, A., Heat storage in unsaturated soils: from theory to application, in Proc. Int. Conf. on

- Subsurface Heat Storage in Theory and Practice, p. 572, 1983.
- Nir, A., Proposal for a preliminary investigation of a hydrogeochemical problem in an industrial PET facility, Lawrence Berkeley Laboratory, Earth Sciences Division Internal Report, 1990.
- Nir, A., Amiel, A., and Meir, R., Seasonal heat storage in greenhouse soil, in Proc. Int. Conf. on STES and CAES, p. 95, 1981.
- Nir, A. and Benson, S., The effect of thermal energy storage on the development of alternative energy, low temperature sources, Lawrence Berkeley Laboratory, Earth Sciences Division Internal Report, 1982.
- Nir, A., Doughty, C., and Tsang, C.-F., Seasonal heat storage in unsaturated soils: Example of design study, In Proc. 21 Intersoc. Energy Conversion Engineering Conf., San Diego, California, Vol. 2, p. 669, 1986.
- Nir, A., Korin, E., and Tsang, C.-F., Seasonal heat storage in unsaturated soils: model development and field validation. Final Report Sept. 1986-Dec. 1989, Ben-Gurion University of the Negev, 1990.
- Nir, A., Doughty, C., and Tsang, C.-F., Validation of design procedure and performance modeling of a heat and fluid transport field experiment in the unsaturated zone, *Adv. in Water Resourc.* 15,3,153-166, 1992.
- Ogata, A., Spread of a dye stream in an isotropic granular medium, USGS Professional paper 411-G, 1964.
- Patankar, S.V. et al., Prediction of laminar flow and heat transfer in helically coiled pipes, *J. Fluid Mech.*, 62, 539, 1974.
- Peterson, J.E., Jr., The application of algebraic reconstruction techniques to geophysical problems (Ph.D. Thesis), University of California, Berkeley, 188 p., 1986.
- Philip, J.R. and de Vries, D.A., Moisture movement in porous materials under temperature gradients, *Trans. AGU*, 38, 2, 222-232, 1957.
- Rybakova, L.E. et al., Temperature patterns in soil with variable thermophysical coefficients with given temperature conditions in greenhouses, *J. of Engineering Physics*, 42, 2, 313, 1982.
- Sepaskah, A.R., and Boersma, L.L., Thermal conductivity of soils as a function of temperature and water content, *Soil Sci. Soc. of America J.*, 43, 439-444, 1979.
- Sundberg, J., Thermal conductivity of rock and soil, in Proc. ENERSTOCK 85, p. 284, 1985.
- Tarantola, A., *Inverse problem theory: methods for data fitting and model parameter estimation*, Elsevier, New York, 1987.
- Tarnawski, V.R., Leong, W.H., Wagner, B., Reuss, M., and Schulz, H., Heat and moisture interactions in high temperature ground heat storage, *Z. angew. Geowiss.*, 9, 131-151, 1990.
- Tsang, C.-F. and Doughty, C., Detailed validation of a liquid and heat flow code against field performance, in Proc. Eighth SPE Symposium on Reservoir Simulation, Dallas, Texas, February 10-13, 1985.
- van Genuchten, M.T., Tang, D.H., Guennelon, R., Some exact solutions for solute transport through soils containing large cylindrical macropores, *Water Resour. Res.*, 20, 335-346, 1984.
- Vermeer, J., van de Wiel, G.M.L.M., and Snijders, A.L., The conditions controlling the drying out of soil around power cables, *Electra*, 84, 53-67, 1982.
- Walker, W.R., Sabey, J.D., and Hampton, D.R., Studies of heat transfer and water migration in soils. Dept. of Agricultural and Chemical Engineering, Colorado State Univ., Fort Collins, 1981.
- Zeroni, M., Nir, A., and Kopel, R., Root zone heating as an element in energy conservation in a seasonal heat storage greenhouse, *Acta Hortic.*, II, 859, 1983.

APPENDIX A: ISSUES INVOLVED IN ESTABLISHMENT OF AN ENVIRONMENTAL DATABASE

In this section we discuss the problems and options in the establishment of and evaluation of an environmental information database, required to select a storage site and to monitor its operation.

A.1. HYDROGEOLOGICAL BACKGROUND

There are preferred hydrogeological conditions for the selection of a seasonal storage site for thermal energy:

- 1.1 Soil types – silty clay and silty soils are preferable to sandy soils, due to their higher initial water content and better moisture retention at higher temperatures, thus allowing better heat transfer from the heat exchanger to the soil (see discussion in Part IV).
- 1.2 The selected site should not be in high infiltration areas, which may remove heat below the storage zone. While the design is based on semi-arid, low rainfall regions, low lying sites may be in the path of local runoff.
- 1.3 Hydrogeological maps should be consulted for information on local replenishable aquifers or interflow regions, below or in the close vicinity (20-30 m) of the storage region, as these may act as heat sinks.
- 1.4 The lack of such an information necessitates drilling observation wells to the desired depths for securing such information. Observation wells are required in any case for the characterization of the relevant soil properties discussed in Section II.3. These wells, extending to a depth of 5 m below the heat exchanger bottom, are equipped with temperature sensors. The number of wells depends on the variability of soil characteristics within the storage area, with three being the minimum number for a storage module of 4000 m².

A.2. TEMPERATURE AND MOISTURE DATA

- 2.1 Meteorological information is useful in the estimate of local rainfall distribution and air temperatures. However it does not provide a reliable estimate of local surface temperatures. These are required, together with the thermal profile data, for the inversion method to obtain the soil thermal conductivity, discussed in Section II.3.

- 2.2 Measurement of soil temperature profiles in the observation wells should precede the operation, preferably by several months, allowing the collection of several data sets required for the inversion procedure. The problems with the measurement of surface temperature are discussed in Lewis and Wang [1992].
- 2.3 Moisture sensors, with a precision of 5% relative change and operating in the temperature range of 5-85°C are desirable for a meaningful evaluation of the storage operation. There has been no such equipment available to us up to now, therefore moisture data were not used to validate the drying behavior of the soil. Recent time domain reflectometry developments will possibly offer that performance. Until then, laboratory experiments have to be relied upon to provide moisture distributions.

APPENDIX B: ALGORITHMIC SEARCH FOR SOIL THERMAL PROPERTIES

B.1. INTRODUCTION

Section II.3.2 describes the first step of the procedure that was used to determine soil thermal properties and the local surface temperature variation by visually comparing experimentally measured temperature profiles to profiles calculated using an analytical solution. The analytical solution applied here assumes that the soil is homogenous and semi-infinite; the surface temperature is uniform in space and varies sinusoidally in time with constant parameters; and the heat transfer through the soil is purely conductive. With these assumptions, the temperature T at any depth below the ground surface z and time t is given by [Carslaw and Jaeger, 1957, Section 2.12; de Vries, 1963]

$$T(z,t) = T_0 + T_a e^{(-z/d)} \cos[\omega(t-t_0) - z/D] \quad (\text{B.1})$$

where T_0 is the annual average surface temperature; T_a is the amplitude of the temperature variation; $\omega = 2\pi/\tau$, where $\tau = 365$ days is the period of the variation; D is the decay constant, given by $D = \sqrt{2\alpha/\omega}$, where α is the soil thermal diffusivity; and t_0 is the time of the maximum surface temperature. Note that z is a positive number that increases downward from 0 at the ground surface. The parameters T_0 , T_a , D , and t_0 were varied over ranges considered physically reasonable and the resulting calculated temperature profiles were visually compared to the measured profiles. The values of the parameters for the calculated profiles that best matched the measured profiles were accepted as representative of the physical system.

This parameter-determination procedure is improved through the use of an inversion algorithm [Tarantola, 1987]. Instead of visually comparing the measured and calculated temperature profiles for a trial set of parameters, the square of the difference between measured and calculated temperatures is summed over all observation depths z_m and times t_m . This quantity, known as the objective function F , is a function of the parameters of the analytical solution:

$$F(\mathbf{P}_i) = \frac{1}{N} \sum_{t_m} \sum_{z_m} (T_m - T_c(\mathbf{P}_i))^2 \quad (\text{B.2})$$

where N is the total number of measurements, the subscripts m and c denote measured and calculated, respectively, and the vector \mathbf{P}_i denotes the values of the parameters T_0 , T_a , D , and t_0 for the i th trial. In an inversion algorithm, \mathbf{P}_i is systematically varied until the objective function

reaches a minimum value. If this final value of F is smaller than a specified tolerance and the corresponding value of P_i is physically reasonable, then this value of P_i is deemed to provide an optimal approximation to the true value of the unknown parameters, denoted P_0 , and the inversion is said to have converged. Furthermore, the inversion algorithm should return the same final values of P_i and F for a variety of starting values of P_i .

There are a wide variety of inversion algorithms available, which differ primarily in the manner in which successive trial values of P_i are chosen. We use a routine from the Numerical Algorithms Group (NAG) Library, called E04FDF.

B.2. INVERSION OF SYNTHETIC TEMPERATURE DATA

To verify that E04FDF is appropriate for our problem, and to determine the quantity and quality of data necessary to get reliable parameter values, the inversion algorithm was tested using synthetic temperature measurements, which were created using the analytical solution and known parameter values, and in some instances adding random noise. When no noise is added to the synthetic measured data, a converged inversion will yield $F = 0$ and $P_i = P_0$ for the final value of i . On the other hand, if noise has been added to the synthetic data, $F > 0$ at the end of a converged inversion.

Synthetic temperature data were generated for 14 depths below the ground surface at 0.5 m intervals ($0.5 \leq z \leq 7.0$ m), and for 20 times at 18 day intervals ($0 \leq t \leq 360$ days). The parameter values used (P_0) were $T_0 = 22.7^\circ\text{C}$, $T_a = 10.2^\circ\text{C}$, and $D = 2.94$ m, and $t_0 = 0$ days. These values are assumed to be close to the best experimental values and convergence to these values reinforces our confidence in the inversion methodology.

B.2.1 UNIQUENESS TEST – SYNTHETIC DATA WITHOUT NOISE

We first inverted the entire data set ($0.5 \leq z \leq 7.0$ m, $0 \leq t \leq 360$ days). A variety of initial values were used for P_i , ranging from good (i.e., close to P_0): $T_0 = 20^\circ\text{C}$, $T_a = 8^\circ\text{C}$, $D = 4$ m, $t_0 = 6$ days, to bad: $T_0 = 15^\circ\text{C}$, $T_a = 15^\circ\text{C}$, $D = 10$ m, $t_0 = 180$ days. In all cases, the algorithm converged, with $F < 10^{-9}$ in each case.

We then inverted subsets of the data, considering time periods of $0 \leq t \leq 60$, $0 \leq t \leq 120$, or $0 \leq t \leq 360$ days and depth intervals of $0.5 \leq z \leq 7$, $2 \leq z \leq 7$, $4 \leq z \leq 7$, or $6 \leq z \leq 7$ m. The larger number of each time interval is known as t_{\max} and the smaller number of each depth interval is referred to as z_{\min} . When the good initial value given above ($P_i = (20, 8, 4, 6)$) was used, the algorithm converged for all subsets of the data. When a less good value was used

($P_i = (15.15, 1.6)$), the inversion only converged for $z_{\min} \leq 2$ m. When the bad value given above ($P_i = (15.15, 10, 180)$) was used, the inversion did not converge unless all data depths were used ($z_{\min} = 0.5$).

B.2.2 STABILITY TEST – SYNTHETIC DATA WITH NOISE

Noisy synthetic temperature measurements were created by adding a term

$$f \cdot (\rho - 0.5) \tag{B.3}$$

to the analytically calculated temperature, where ρ is a random number drawn from a uniform distribution between 0 and 1, and f is a measure of the magnitude of the noise.

The behavior of the algorithm is summarized in Table B.1 for different subsets of the data, for values of f ranging from 0.2 to 1.0°C. The expected precision of the thermistors used for temperature measurements is estimated to be about 0.2°C, but soil heterogeneities could also cause temperatures to deviate from the analytical solution given by Equation (B.1), so it is useful to study larger values of f .

For each entry in Table B.1, ten different sequences of random numbers were used to generate noisy temperature data to be inverted. The value of F shows the average for the ten inversions, while P_i shows the range of returned values. An initial value of $P_i = (18, 15, 2, 6)$ was used for all the inversions.

It is apparent from Table B.1 that a number of factors affect the robustness of E04FDF, and that they do not act independently. The range of the returned values of P_i increases not only as f increases, but also as fewer depths and times of data are considered. The results of Table B.1 indicate high stability for the algorithm and model, even for significant data errors, a limited quantity of data, and initial value errors.

Table B.1. Inversion of synthetic temperature data with noise.

z_{\min} (m)	t_{\max} (days)	F ($^{\circ}\text{C}^2$)	T_0 ($^{\circ}\text{C}$)	T_a ($^{\circ}\text{C}$)	D (m)	t_0 (days)
$f = 0.2^{\circ}\text{C}$						
0.5	360	1×10^{-5}	22.70	10.20	2.94	0
	120	4×10^{-5}	22.70	10.20	2.94	0
	60	8×10^{-5}	22.69-22.71	10.19-10.21	2.94-2.95	0
2.0	360	2×10^{-5}	22.7	10.20	2.94	0
	120	6×10^{-5}	22.70	10.18-10.21	2.94	0
	60	7×10^{-5}	22.69-22.71	10.19-10.21	2.94	0
4.0	360	2×10^{-5}	22.70	10.20	2.94	0
	120	3×10^{-5}	22.70	10.14-10.27	2.92-2.95	0
	60	1×10^{-4}	22.69-22.71	10.11-10.29	2.92-2.96	-1 - +1
$f = 0.5^{\circ}\text{C}$						
0.5	360	3×10^{-5}	22.70	10.20	2.94	0
	120	2×10^{-4}	22.70-22.71	10.19-10.20	2.94	0
	60	4×10^{-4}	22.67-22.73	10.18-10.22	2.93-2.95	0
2.0	360	8×10^{-5}	22.70	10.20	2.94	0
	120	1×10^{-4}	22.70	10.16-10.24	2.93-2.95	0
	60	5×10^{-4}	22.68-22.73	10.16-10.23	2.93-2.94	0
4.0	360	1×10^{-4}	22.70	10.20	2.94	0
	120	6×10^{-4}	22.70-22.71	9.99-10.46	2.88-2.99	-1 - +2
	60	6×10^{-4}	22.67-22.73	9.94-10.42	2.90-3.00	-3 - +2
$f = 1.0^{\circ}\text{C}$						
0.5	360	2×10^{-4}	22.70	10.20	2.94	0
	120	1×10^{-3}	22.69-22.71	10.18-10.22	2.94	0
	60	1×10^{-3}	22.65-22.74	10.17-10.25	2.92-2.96	0
2.0	360	2×10^{-4}	22.70	10.2	2.94	0
	120	1×10^{-3}	22.70	10.14-10.28	2.92-2.96	0
	60	2×10^{-3}	22.65-22.75	10.13-10.27	2.93-2.95	-1 - +1
4.0	360	5×10^{-4}	22.70	10.20-10.21	2.94	0
	120	2×10^{-3}	22.69-22.71	9.74-10.71	2.83-3.05	-3 - +4
	60	3×10^{-3}	22.63-22.74	9.93-10.71	2.84-3.00	-3 - +6

B.3. INVERSION OF REAL TEMPERATURE DATA

Temperature profiles were measured weekly for a two-year period. Because Equation (B.1) does not include short-term temperature variations, temperature data from depths above about 2 m, which are strongly affected by these variations, should not be used in the inversion (i.e., we want $z_{\min} \geq 2$ m). Our knowledge of the system is adequate to provide good initial values compared to the range of initial values used in Section B.2. Altogether, the studies of Section B.2 indicate that E04FDF should be robust for the problem at hand.

Tables B.2 and B.3 summarize a series of inversions done using different subsets of the data. A few obviously incorrect measurements (2 from the first year, 5 from the second year) were replaced with reasonable values after initial analyses were made. This had the effect of markedly decreasing F , but did not significantly modify the returned values of P_i .

The decaying exponential form of Equation (B.1) means data from greater depths provides information only on the average temperature T_0 , thus to determine the other parameters shallower data points must be used. This requirement is illustrated in Section B.2, where the inversion of synthetic data was less successful when shallow points were not used (large z_{\min}). However, very shallow data will include the effect of the short-term (e.g., daily) temperature variations, which are not included in Equation (B.1). Hence, care must be taken in determining the value of z_{\min} to use in the inversion. Table B.2 shows the results of a series of inversions using data from different depth ranges. It is clear that as z_{\min} increases from 0.5 to 2 m, F steadily decreases, as the effects not included in Equation (B.1) diminish. As expected, the returned value of T_0 remains fixed as the depth range changes, but the other parameters vary. The variation between $z_{\min} = 2.0$ and $z_{\min} = 2.5$ m is small, so 2.0 is considered an appropriate limit.

Table B.2. Inversion of real temperature data from different depth ranges.

z_{\min} (m)	F ($^{\circ}\text{C}^2$)	T_0 ($^{\circ}\text{C}$)	T_a ($^{\circ}\text{C}$)	D (m)	t_0 (days)	λ^\dagger (W/mK)
0.5	2.11	22.2	11.1	2.46	201	1.42
1.0	1.14	22.2	13.1	2.16	193	1.10
1.5	0.99	22.2	13.2	2.11	190	1.04
2.0	0.46	22.2	12.5	2.20	194	1.13
2.5	0.29	22.2	12.1	2.24	196	1.17

\dagger Soil thermal conductivity $\lambda = D^2\pi C/\tau$, where a value of $C = 2.35 \text{ MJ/m}^3\text{K}$ has been used for soil heat capacity.

Table B.3 show the results of a series of inversions using data from different time periods. The variation between parameters returned for the 1987 and 1989 inversions is relatively small. The largest differences are for the amplitude of the temperature variation T_a , and the time of the maximum temperature t_0 , whereas average temperature T_0 and soil thermal conductivity λ change very little. This finding is physically reasonable, and it provides confidence in the use of this method for the determination of λ .

The time period March through May, 1987 has been singled out to compare to the previous manual determination of parameters discussed in Section II.3.2. The most notable differences from the full-year inversions are a smaller value of T_a and a larger value of D , which is

consistent with results of the previous analysis. The reason for these differences is considered an open question, but a contributing factor could be the relatively short time after insertion of the thermistor chain tube, which prevented the achievement of thermal equilibrium with the surrounding soil.

Table B.3. Inversion of real temperature data from different time periods.

Time Period	F ($^{\circ}\text{C}^2$)	T_0 ($^{\circ}\text{C}$)	T_a ($^{\circ}\text{C}$)	D (m)	t_0 (days)	λ (W/mK)
1987	0.12	22.4	13.6	2.22	191	1.15
1988	0.74	22.1	11.3	2.25	198	1.19
1987 and 1988	0.46	22.2	12.5	2.20	194	1.13
March-May, 1987	0.03	22.5	10.6	2.69	206	1.69

Note: In each case no data for depths shallower than 2 m were used.

As a further check of the robustness of E04FDF, noise was added to the measured temperature data and the inversion repeated. As in Section B.2, noise was added as $f \cdot (\rho - 0.5)$ where ρ is a random number drawn from a uniform distribution from 0 to 1. Table B.4 shows results for a series of inversions with f ranging from 0 to 2. In each case the shallowest data depth is 2 m and data from both 1987 and 1988 were used. For each value of f , ten different sequences of random numbers were used to generate noise. Even for the largest value of f the returned parameter values do not differ appreciably from those found with no added noise. For all values of f , the average value of the objective function is $F = 0.46$.

Table B.4. Inversion of real temperature data with random noise added.

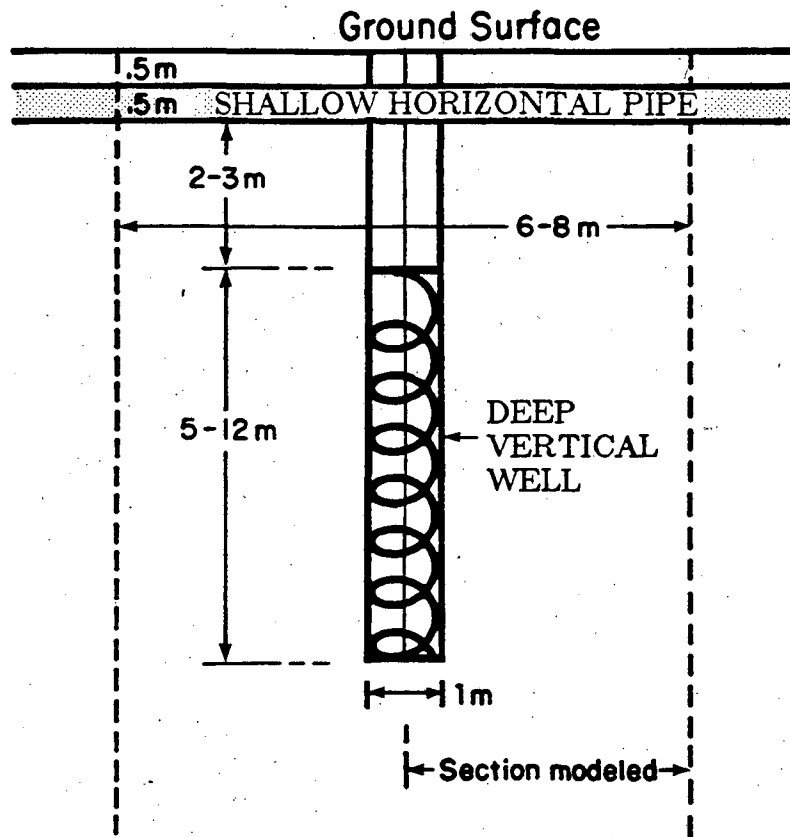
f ($^{\circ}\text{C}$)	T_0 ($^{\circ}\text{C}$)	T_a ($^{\circ}\text{C}$)	D (m)	t_0 (days)	λ (W/mK)
0	22.2	12.5	2.20	194	1.13
0.2	22.2	12.5	2.20	194	1.13
0.5	22.2	12.5	2.20	194	1.13
1.0	22.2	12.4-12.5	2.20	194	1.13
2.0	22.2	12.4-12.6	2.19-2.21	194	1.12-1.14

The value of effective thermal conductivity λ , based on the best fit to the validation experiments and ultimately deemed best for the modeling studies, was 1.35 W/mK rather than the optimal value predicted by the inversion of the data prior to the validation experiment, 1.13 W/mK. The discrepancy reflects anticipated differences in the operating conditions of the heat-storage experiment compared to the temperature-profile measurements, such as increased levels of moisture saturation and temperature, which are both expected to increase λ , as discussed in

Section IV.

B.4 ALTERNATE APPROACH TO INVERSION

As an alternative to the present approach, in which we model the surface temperature as a cosine function with three unknown parameters, we can consider the temperature at a depth of, say, 0.5 m described by an n-component Fourier series, whose coefficients are determined by the measured data at 0.5 m depth. The Fourier coefficients would not be subject to further parameter fit, and the remainder of the temperature data would be inverted to determine the value of just a single parameter, the soil thermal conductivity, λ . The residual variability of λ should be more stable than in the present approach, and reflect local inhomogeneities of the soil. In order to analyze λ variations with depth, a one-dimensional numerical model comprised of zones with different values of λ could be used in place of Equation (B.1) in the inversion. It should be pointed out again, that this procedure determines a constant thermal conductivity as an approximation to the moisture and temperature dependent apparent thermal conductivity, as discussed in Section I.3.1.



XBL 832-1716

Figure I.1

Schematic diagram showing a vertical cross-section of one duct of the storage system. The optimal dimensions of the system have been found to be a 12 m long heat exchanger located at a depth of 4-16 m, with adjacent ducts separated by 6 m (see Section I.4.4). For the reduced-scale field experiment (Parts II and III), the heat exchanger is 6 m long at a depth of 4-10 m and the shallow storage zone is absent.

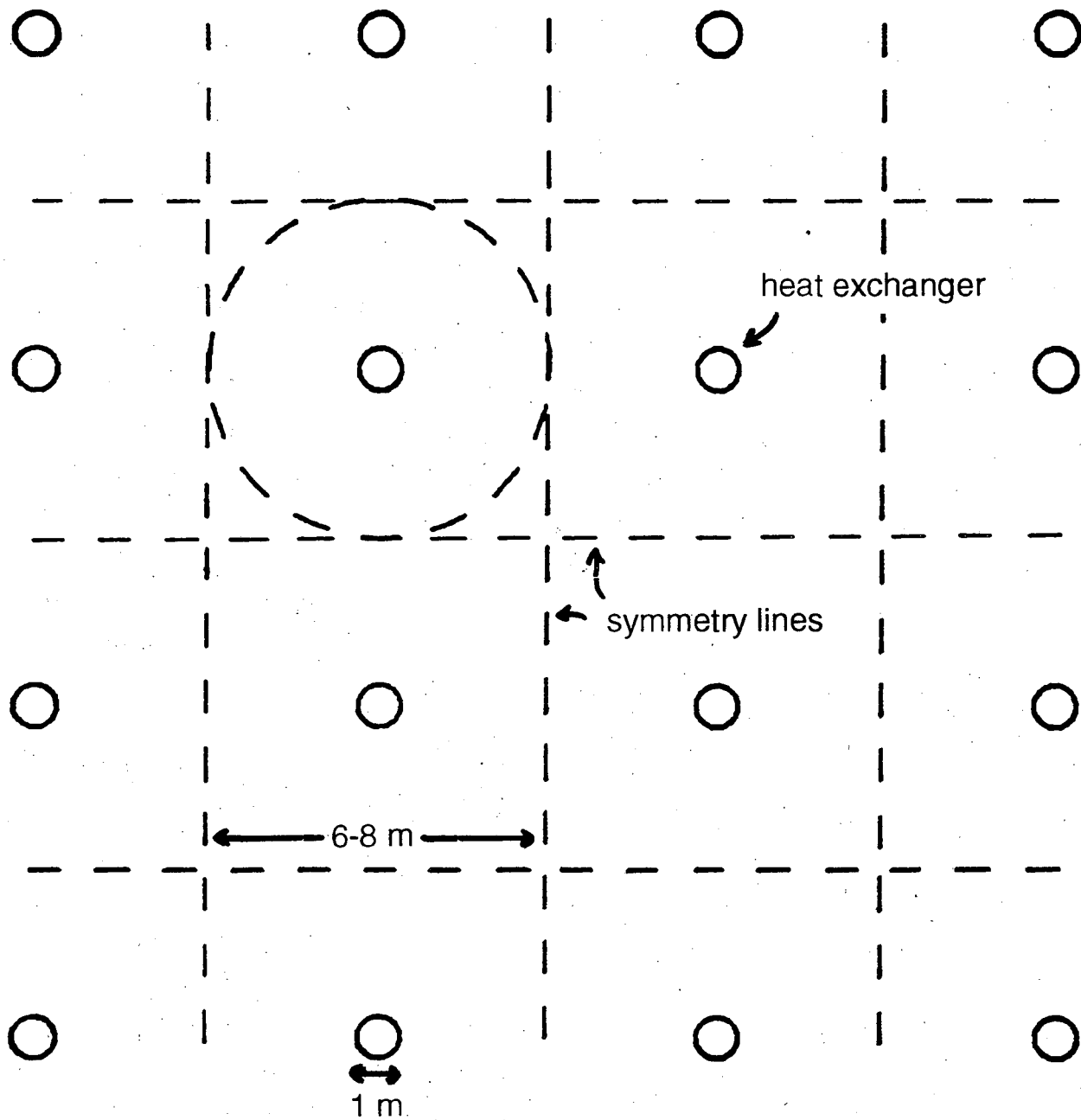
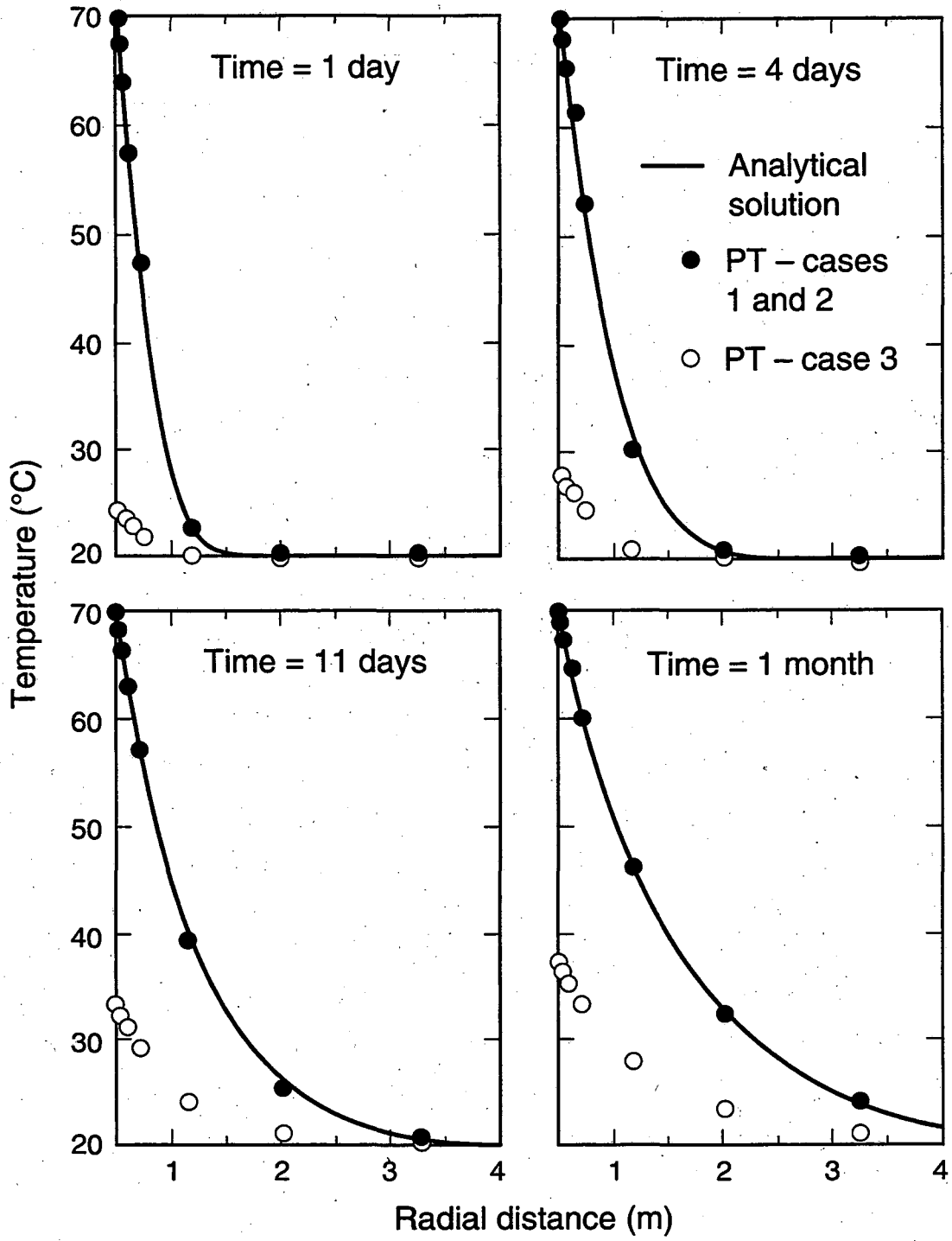
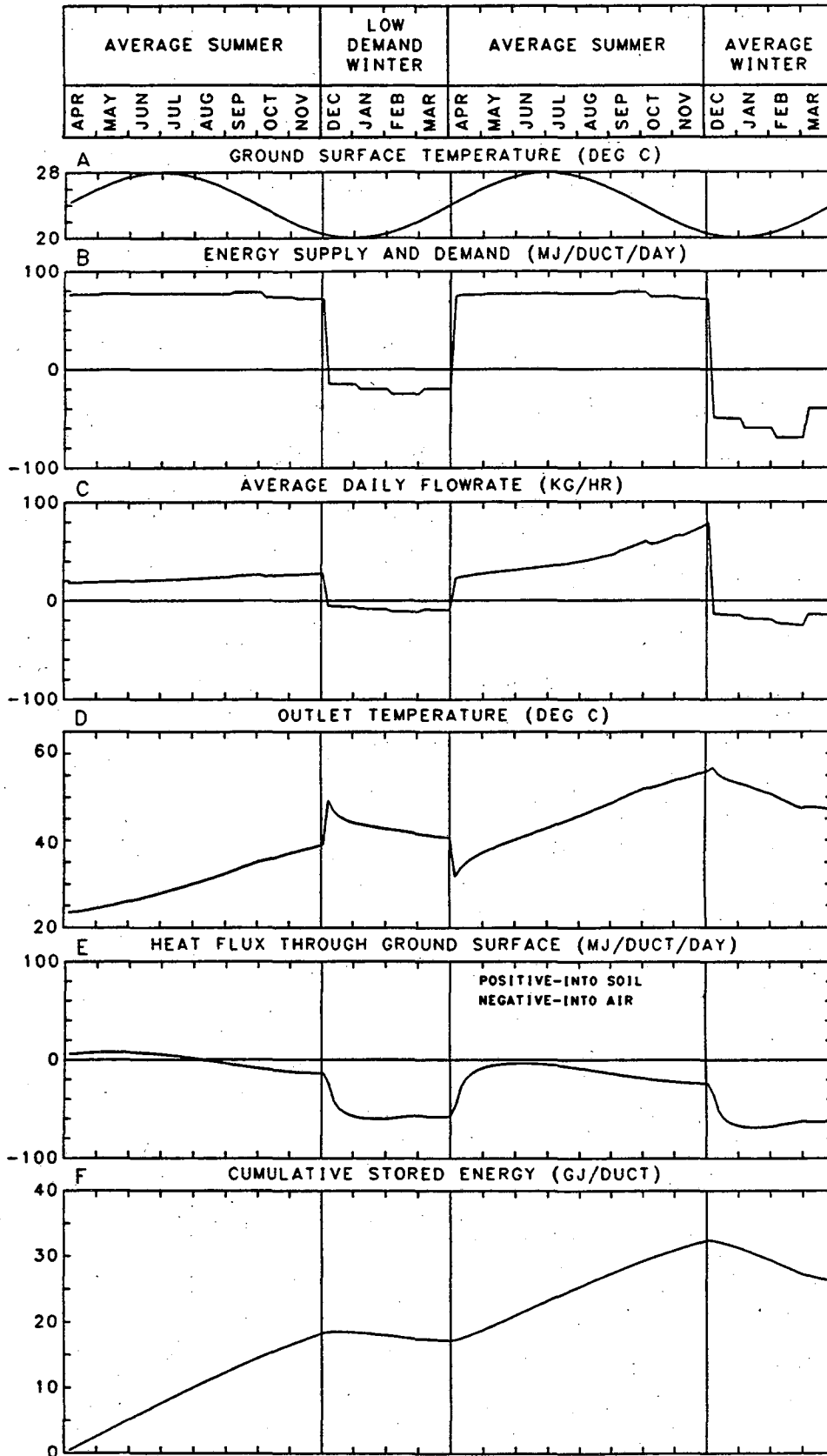


Figure I.2 Top view of an array of heat-exchanger ducts.



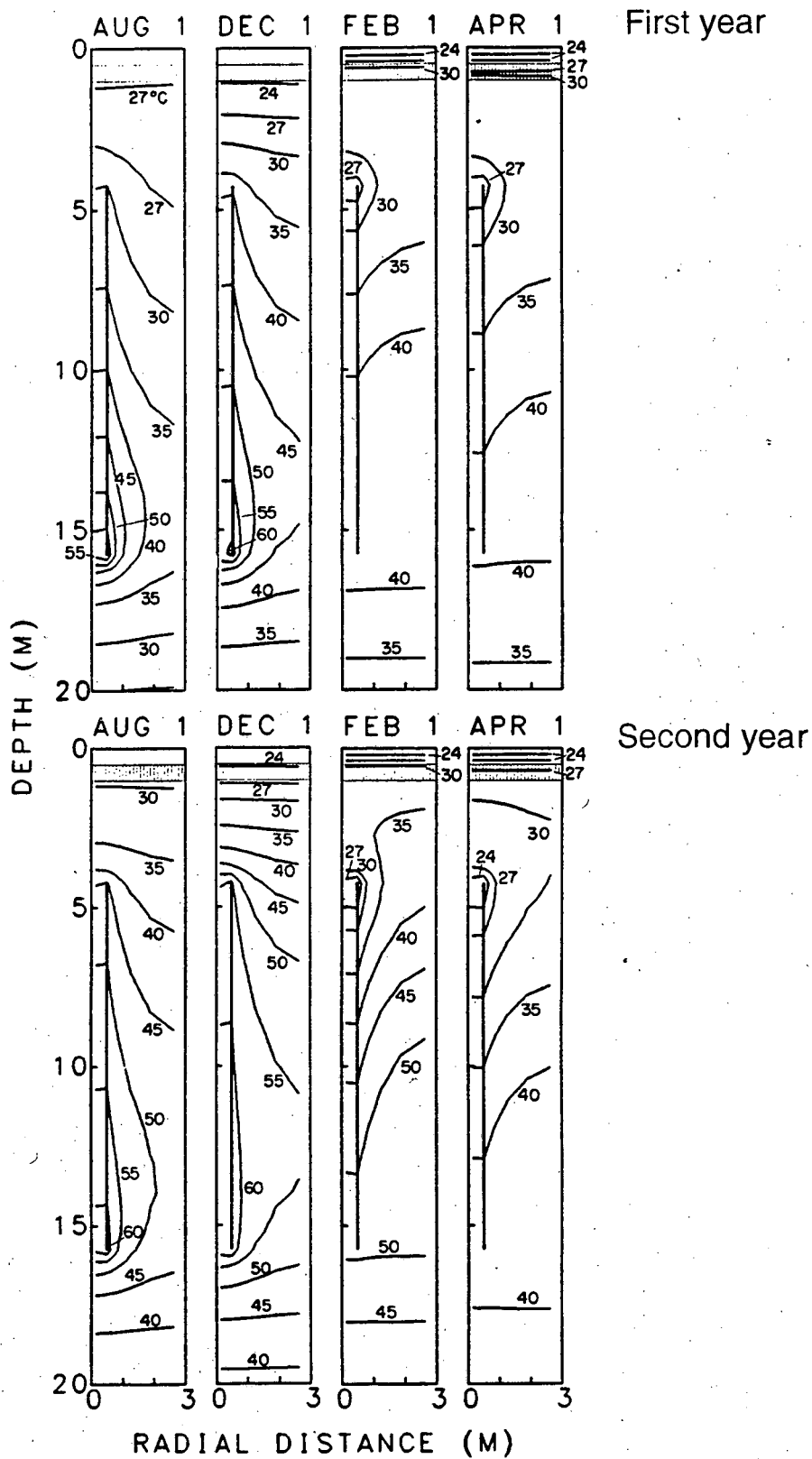
XBL 913-6702

Figure I.3 Analytical and numerically calculated temperature distributions for a simplified problem involving radial heat flow from a cylinder; the curves labeled 1, 2, and 3 represent different boundary conditions for the numerical model, as explained in the text.



XBL 8312-2414

Figure I.4 Boundary conditions (A and B) and calculated results (C, D, E, and F) for Case 2.



XBL 8312-2413

Figure I.5 Temperature distributions (in °C) for several times for Case 2.

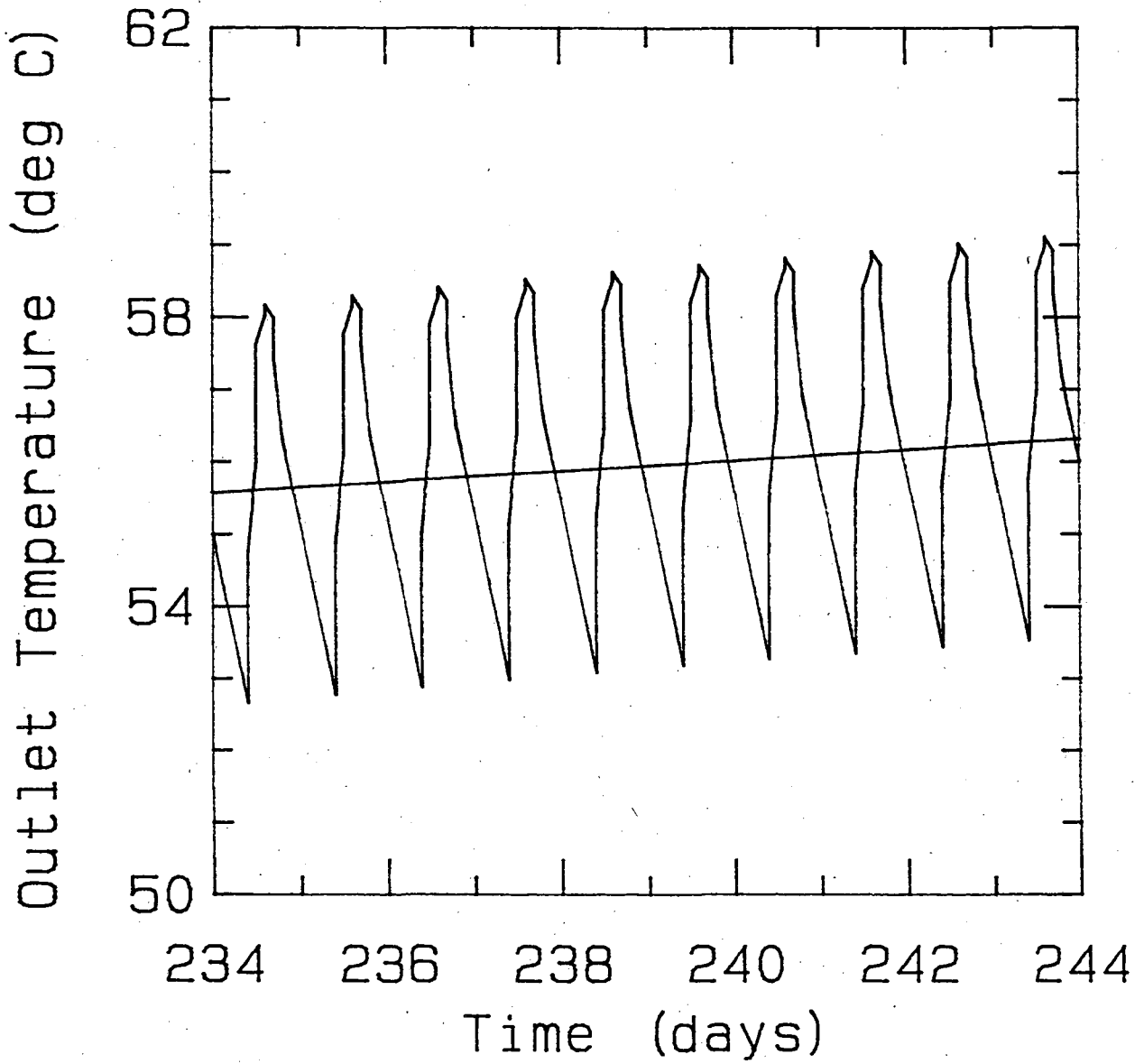


Figure I.6 Outlet temperature (T_{out}) calculated with averaged and discontinuous pumping schedules for the final 10 days of the 1S-1L-2S sequence.

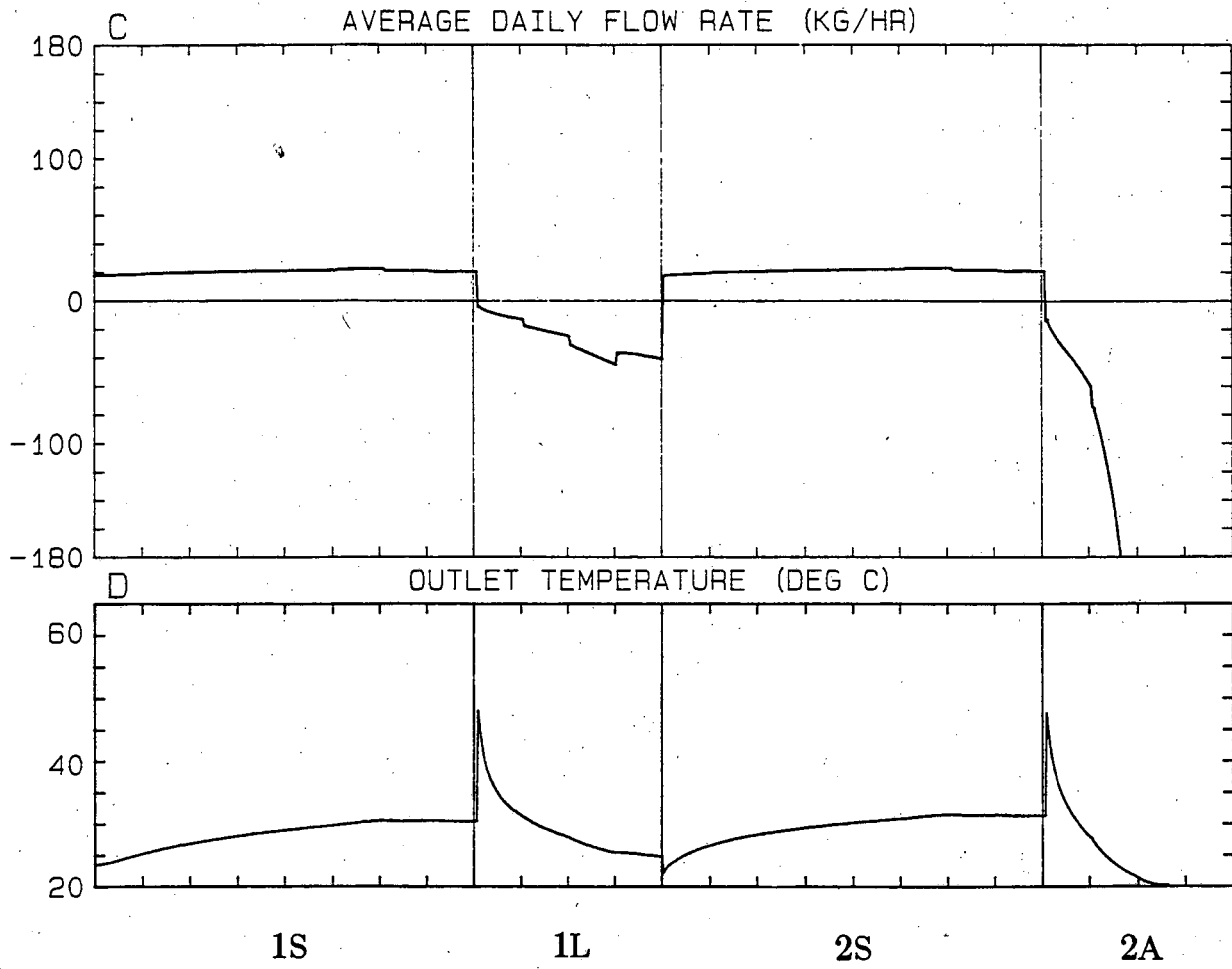
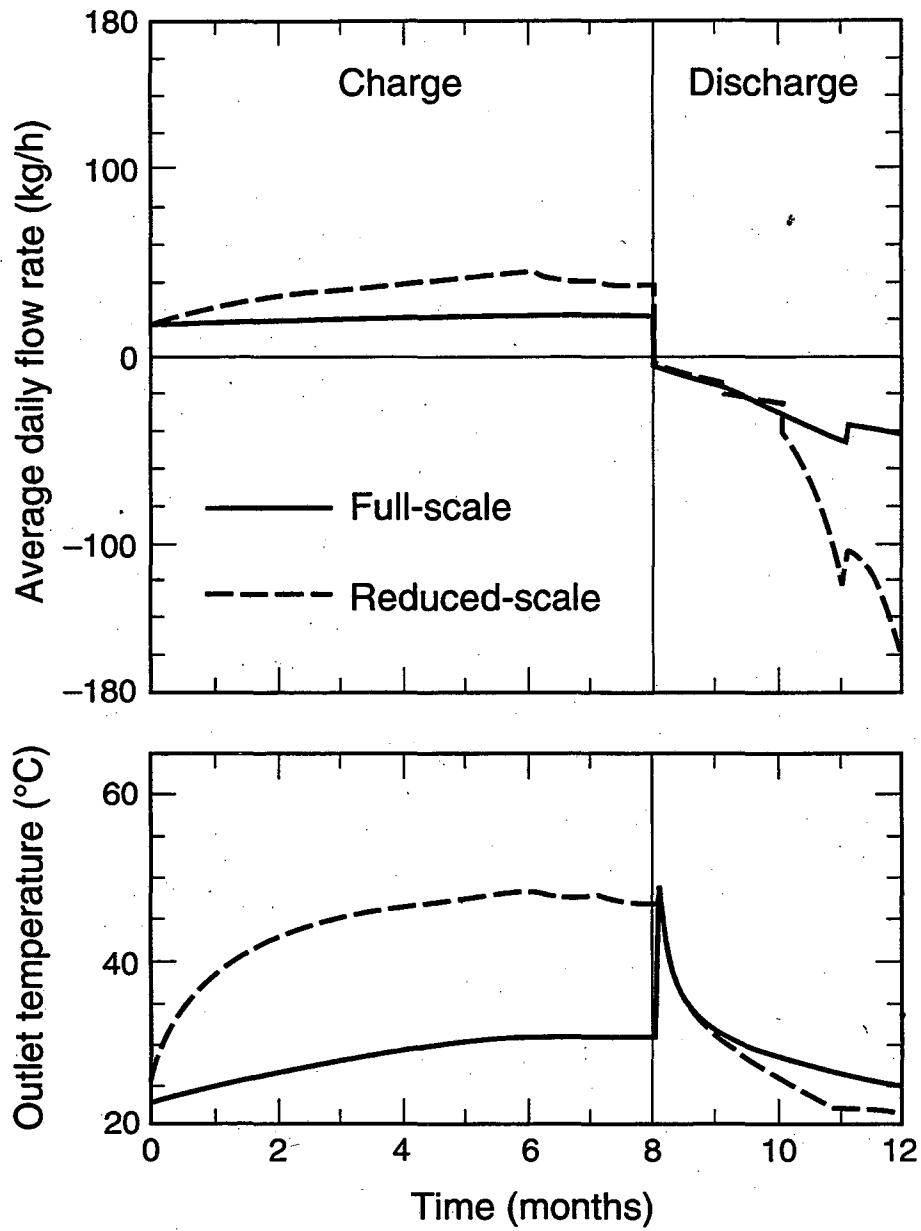
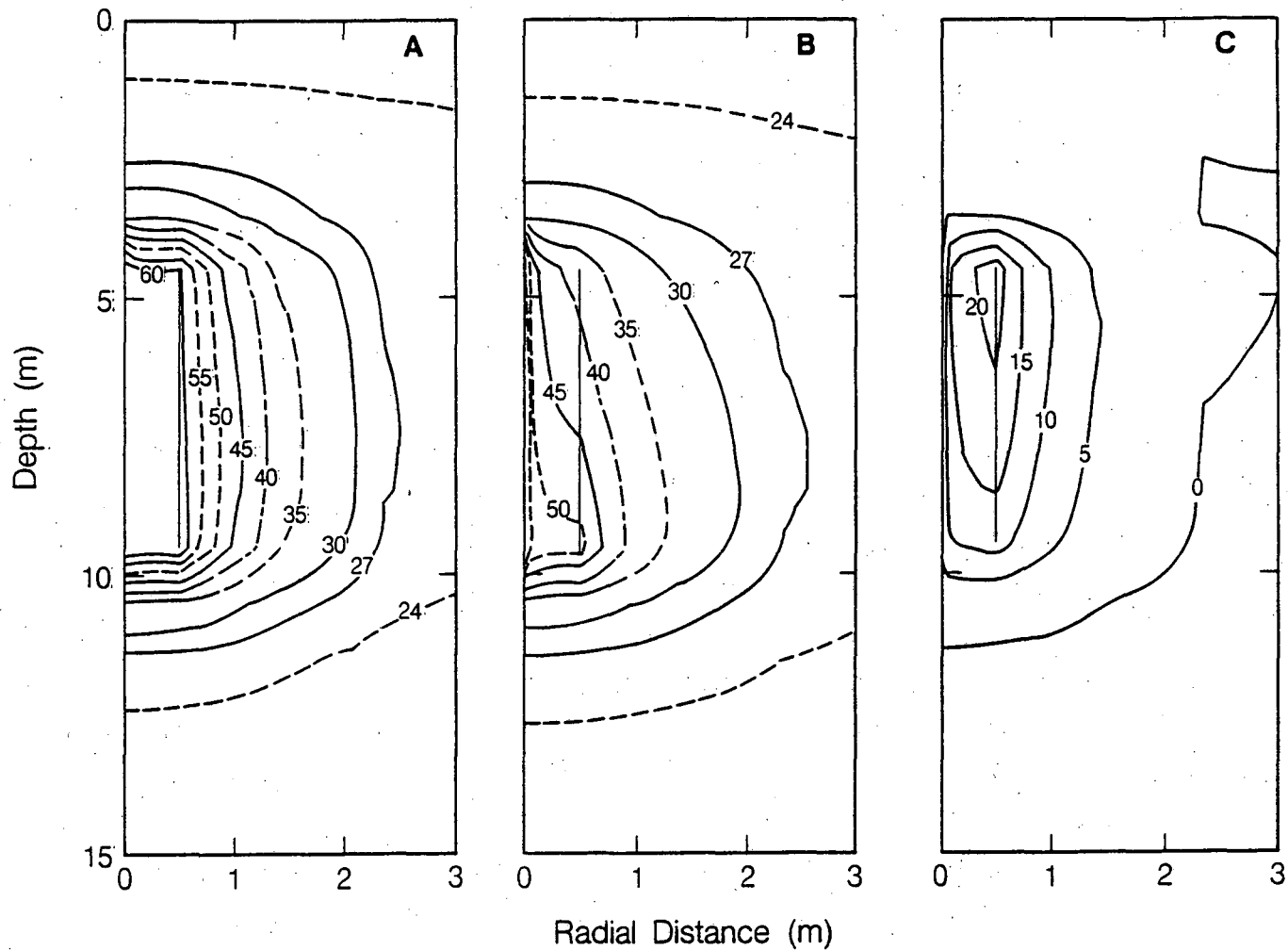


Figure I.7 Computed average daily flow rate (\bar{Q}) and outlet temperature (T_{out}) for Case 2 and an infinite-radius model.



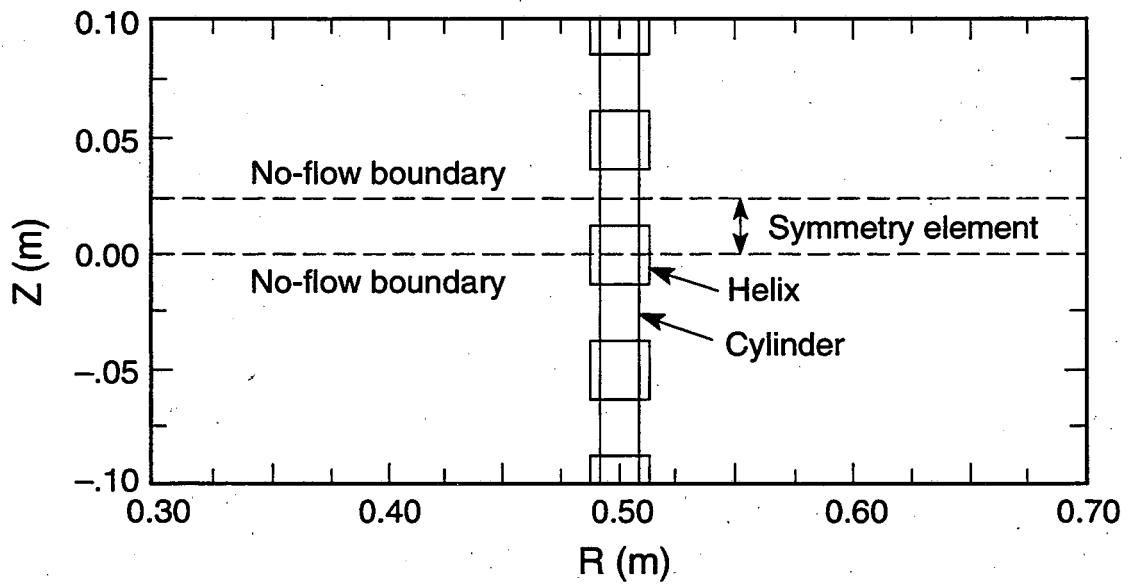
XBL 913-6703

Figure II.1 Computed average daily flow rate (\bar{Q}) and outlet temperature (T_{out}) for full-scale and reduced-scale infinite-radius models.



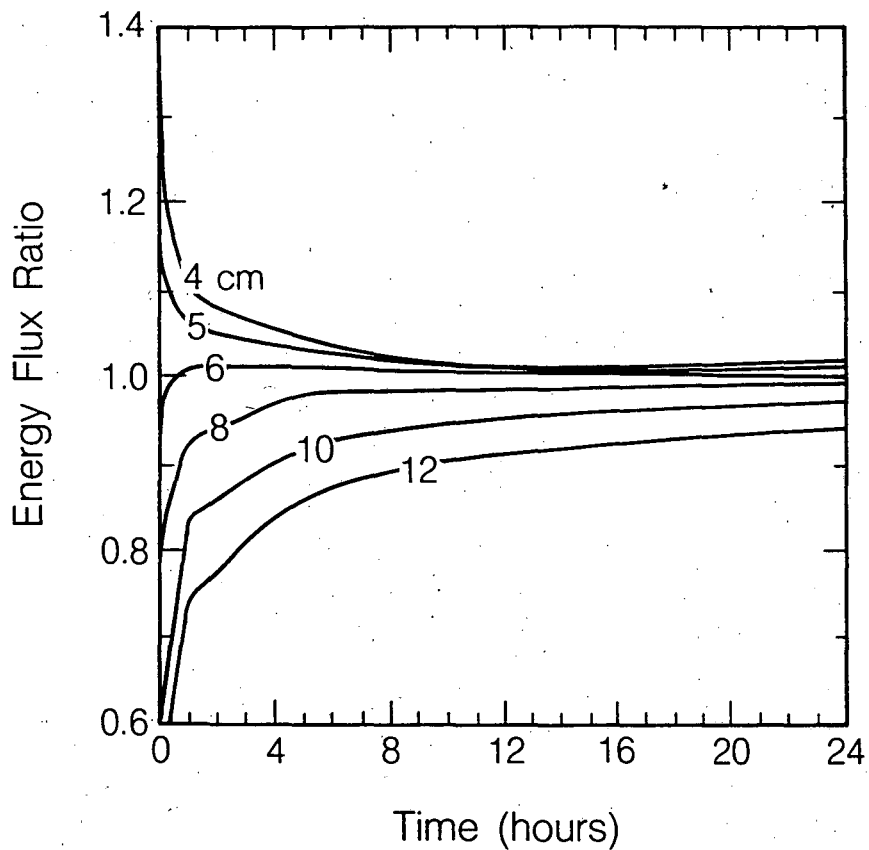
XBL 887-10351

Figure II.2 Temperature distributions (in °C) after 2 months of charge assuming thermal conductivity of 0.8 W/m K (A), 1.8 W/m K (B), and their difference, the delta model (C).



XBL 913-6699

Figure II.3 Schematic diagram showing the square-cross-section helix and cylindrical conduit models for the heat exchanger.



XBL 888-10371

Figure II.4 Energy flux ratio of the square-cross-section helix to the cylindrical conduit, for coil separation distance from 4 to 12 cm.

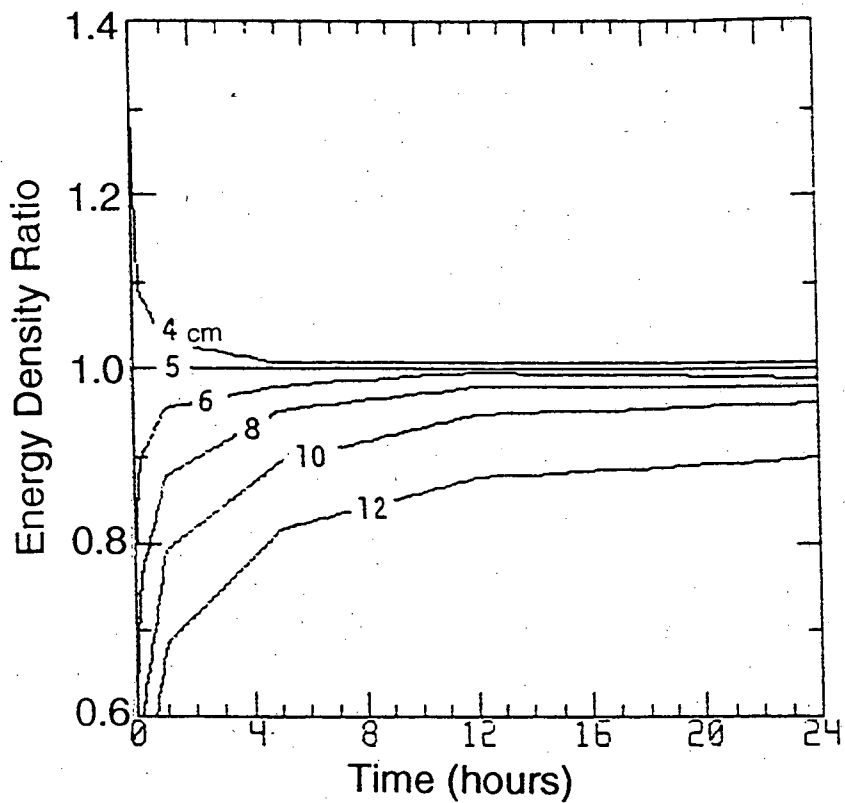
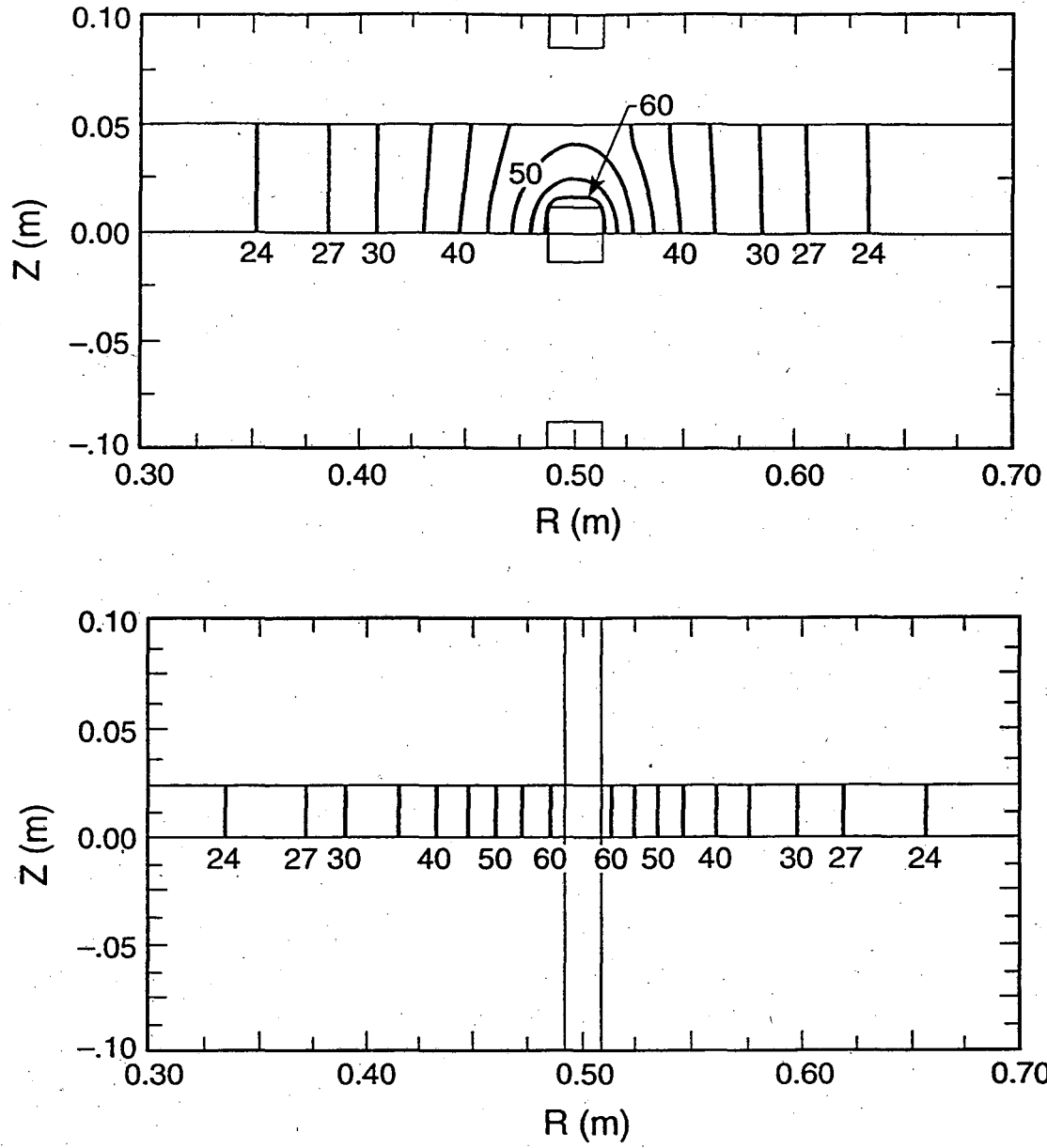


Figure II.5 Ratio of energy density deposited for various helix spacings to energy density deposited for 5 cm spacing.



XBL 913-6701

Figure II.6 Temperature distributions (in °C) after 1 hour of 'charge' for the helical and cylindrical heat-exchanger models.

PARTICLE SIZE DISTRIBUTION VS DEPTH

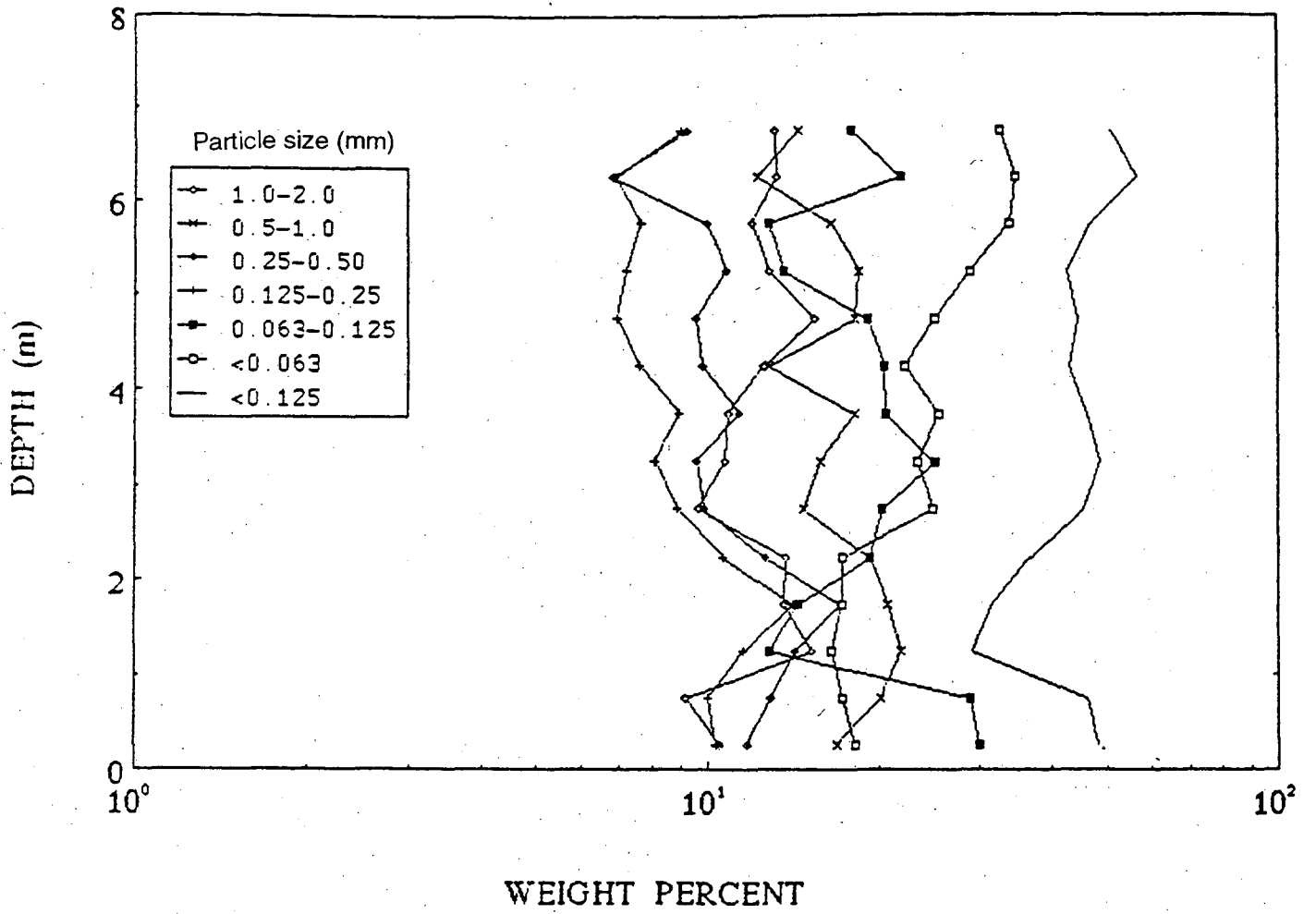


Figure II.7 Soil granulometric structure profile for observation well A.

EXCAVATED WELLS SOIL MOISTURE CONTENT

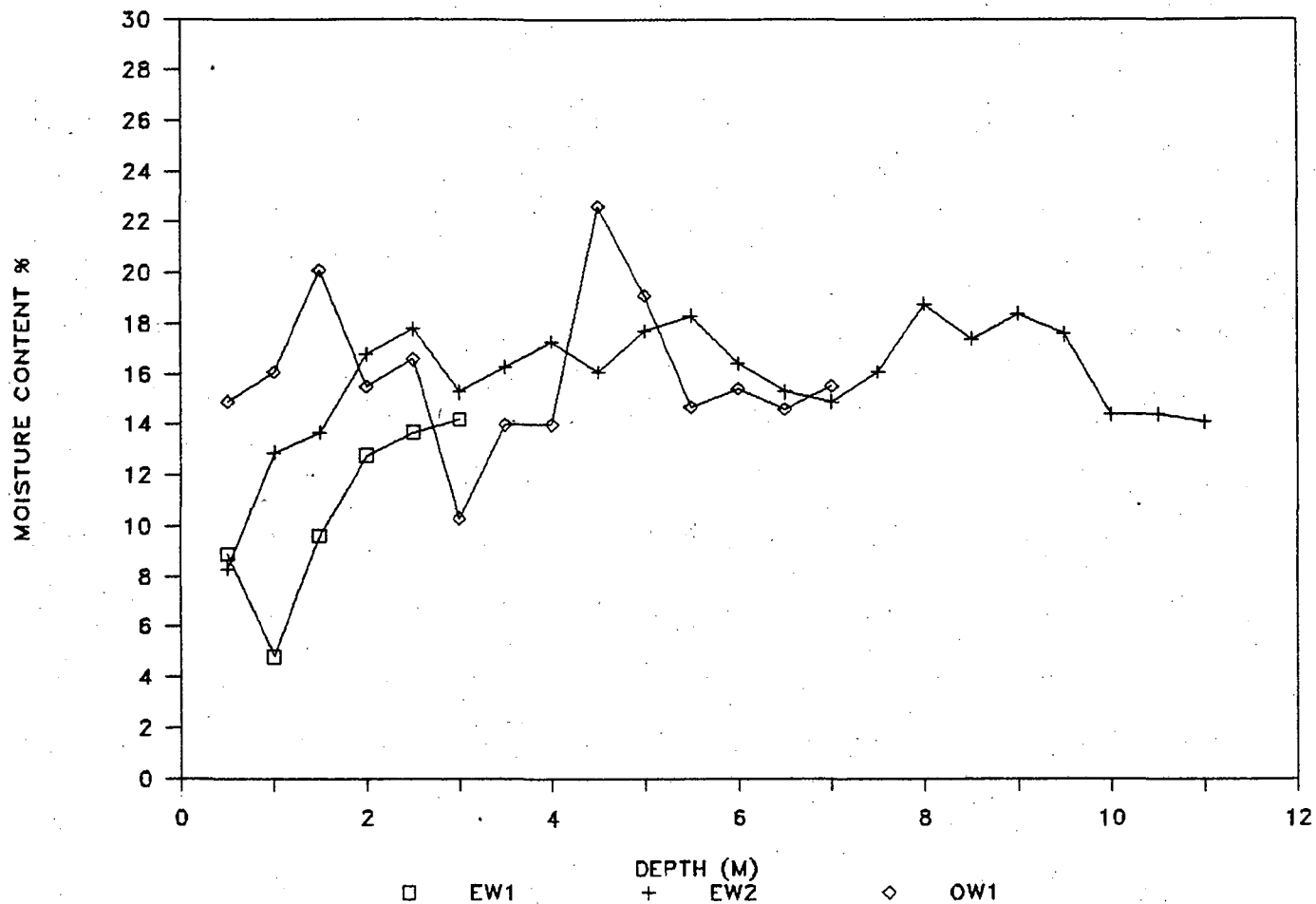
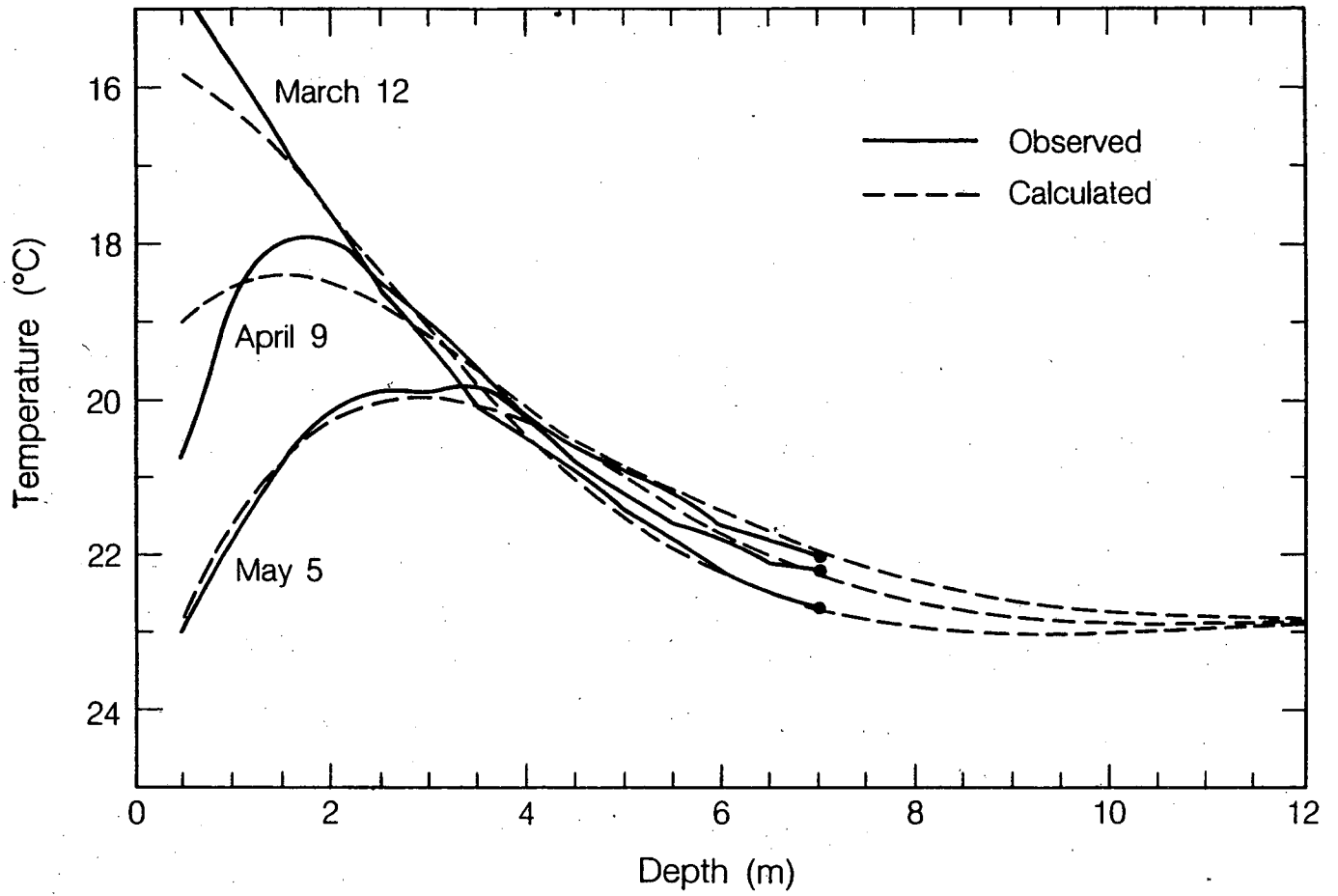


Figure II.8 Soil moisture content profile for three wells.



XBL 887-10354

Figure II.9 Observed and calculated soil temperature profiles.

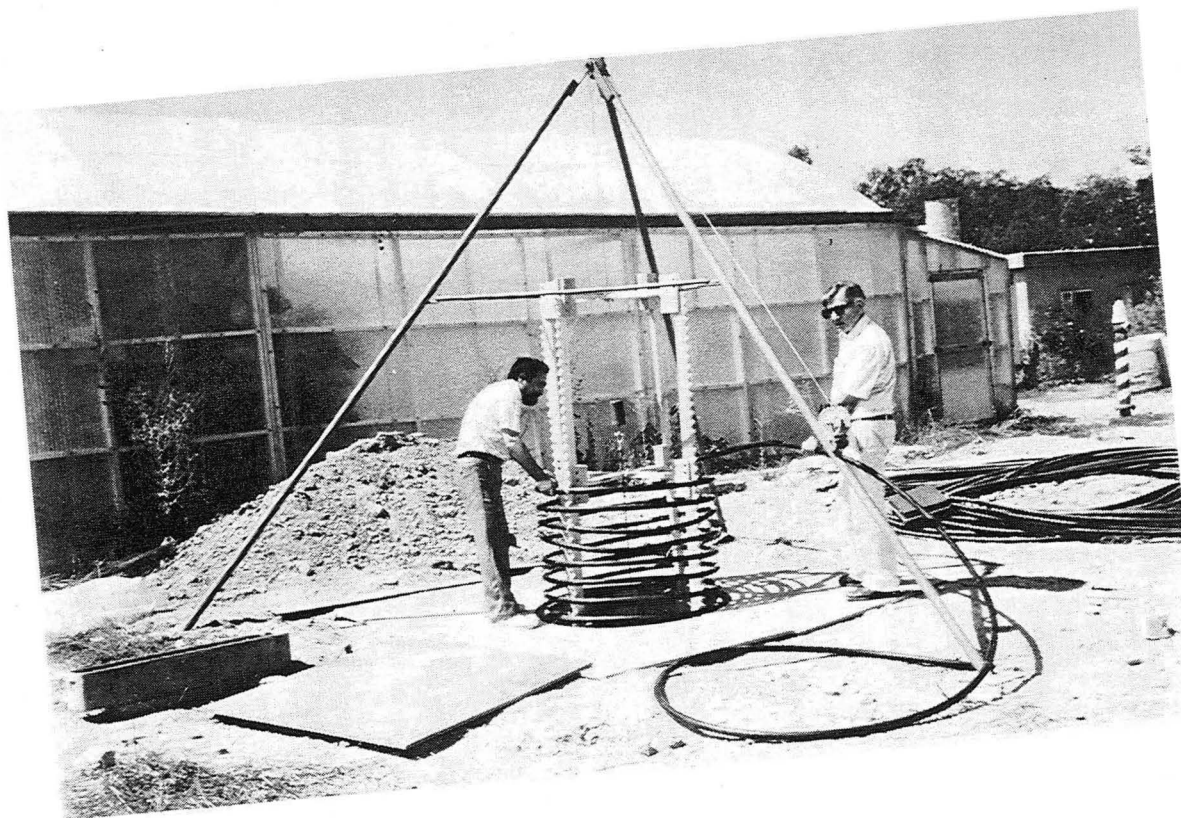


Figure II.10 Construction of the heat exchanger.

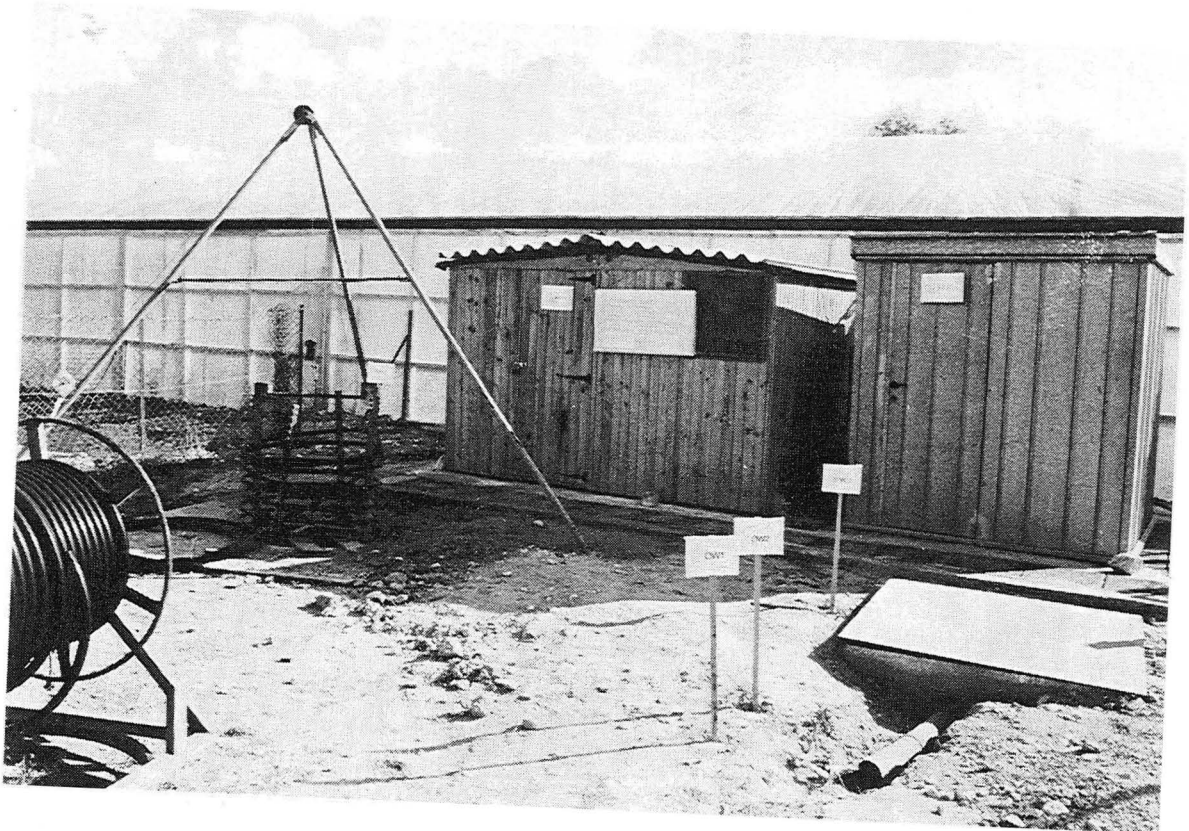


Figure II.11 Emplacement of the heat exchanger. The heat exchanger on the left has not yet been lowered into place. The heat exchanger on the right (labeled EW2) is in place and the hole has been backfilled with soil. The stakes labeled OW1 and OW2 identify observation well locations.

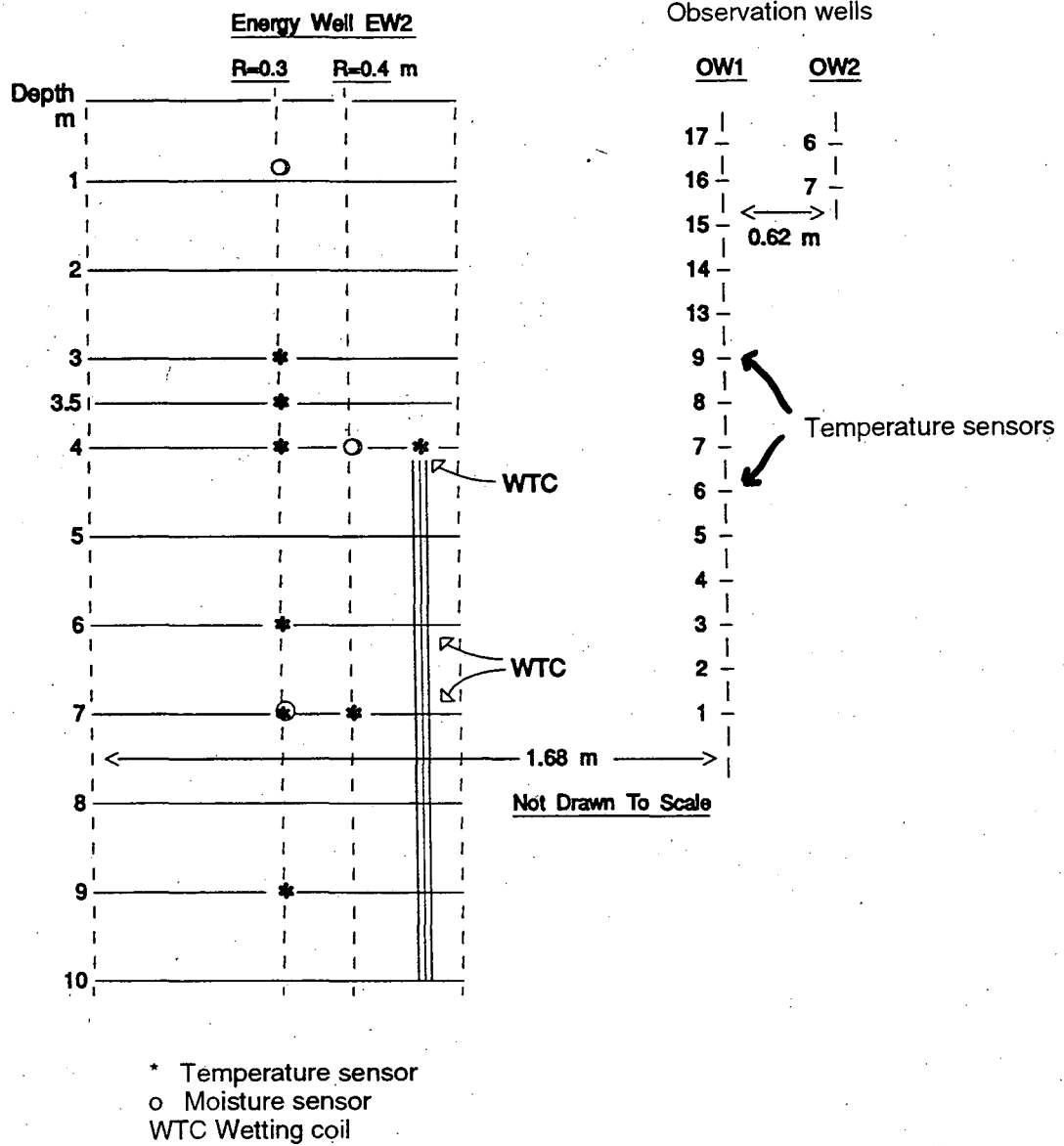


Figure II.12. Location of sensors in the storage volume.

UZIES-HEAT SUPPLY SYSTEM

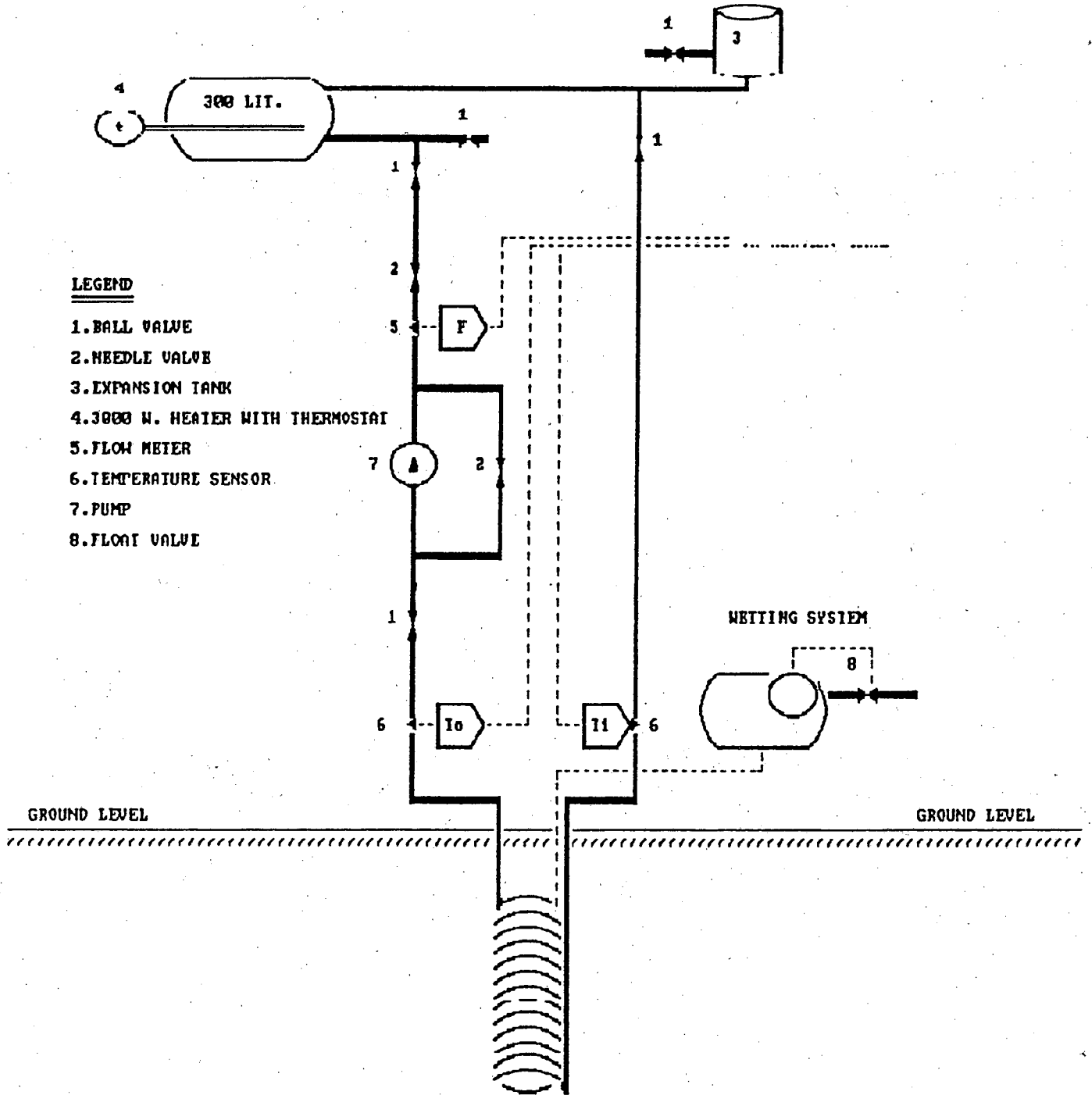
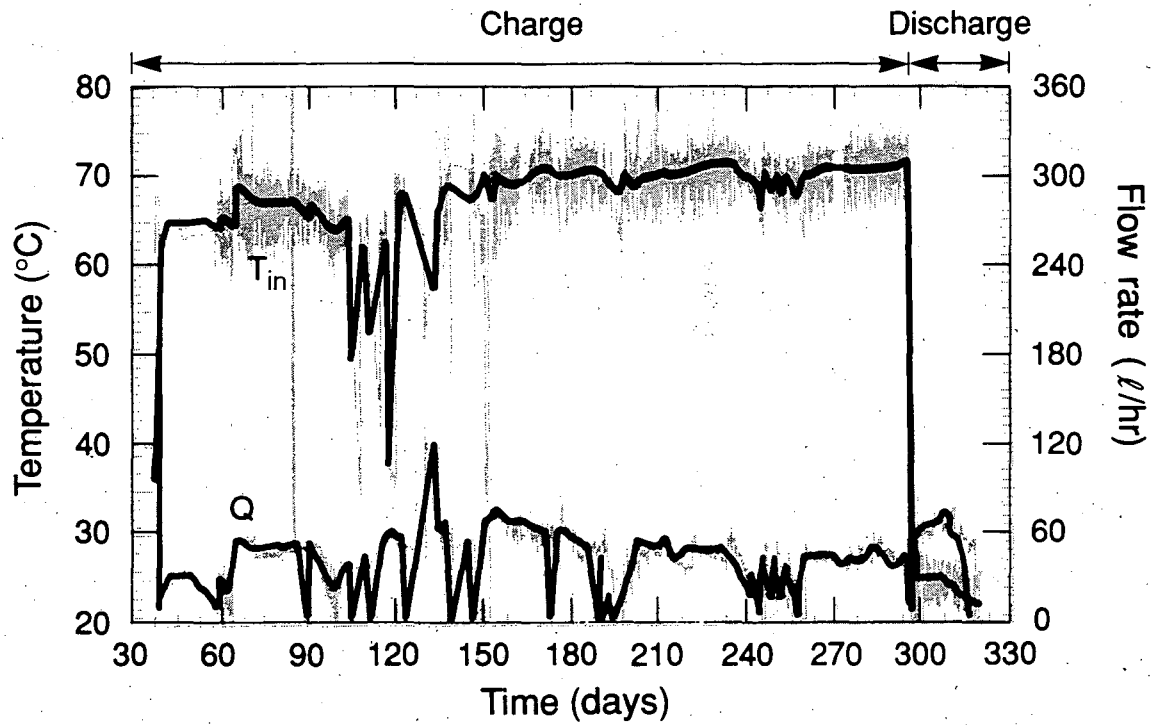


Figure II.13 Heat supply system.



XBL 901-6702

Figure III.1 Inlet temperature and flow rate for the 1989 run (gray lines), along with averaged values used in the numerical model (heavy black lines).

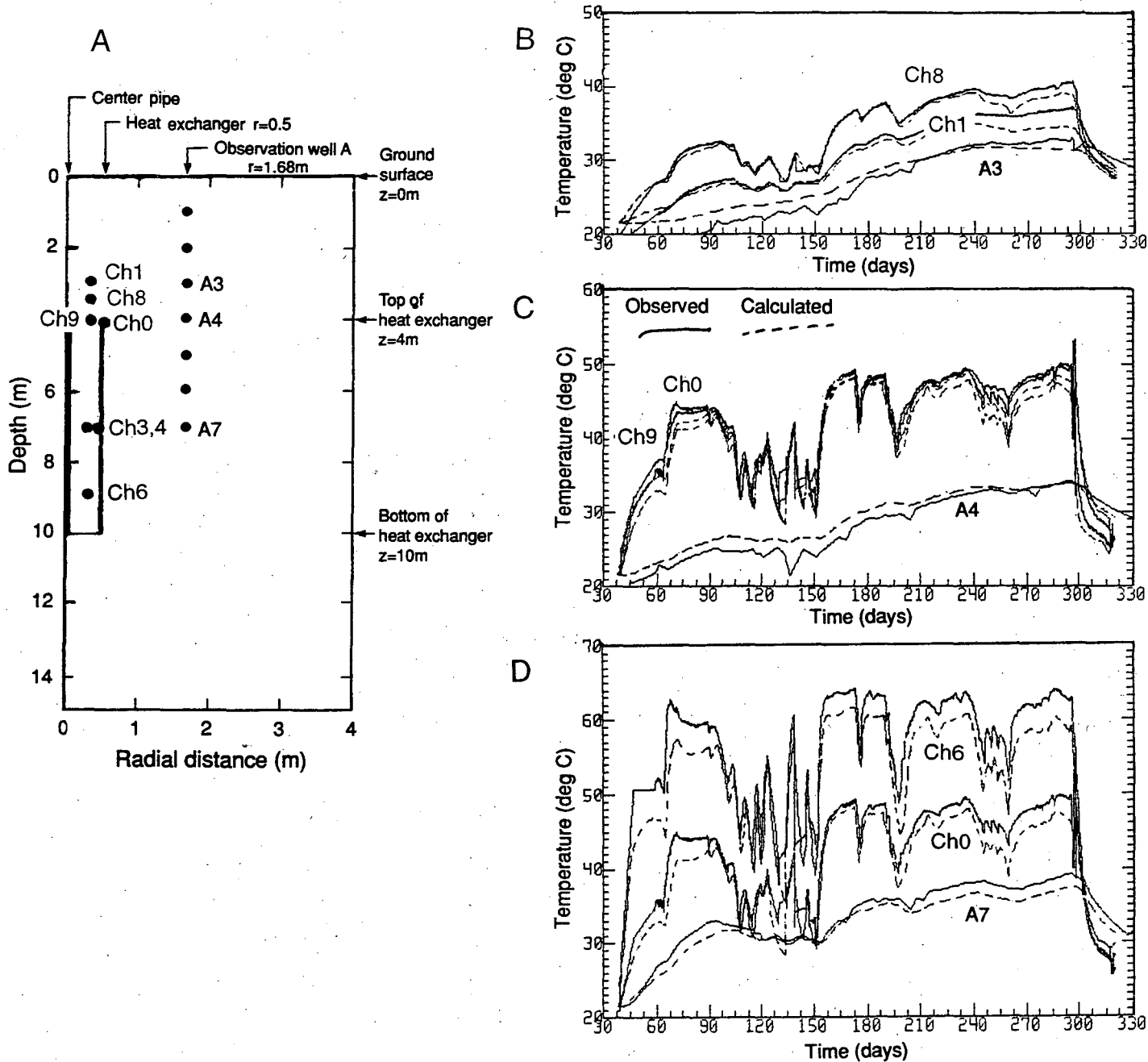
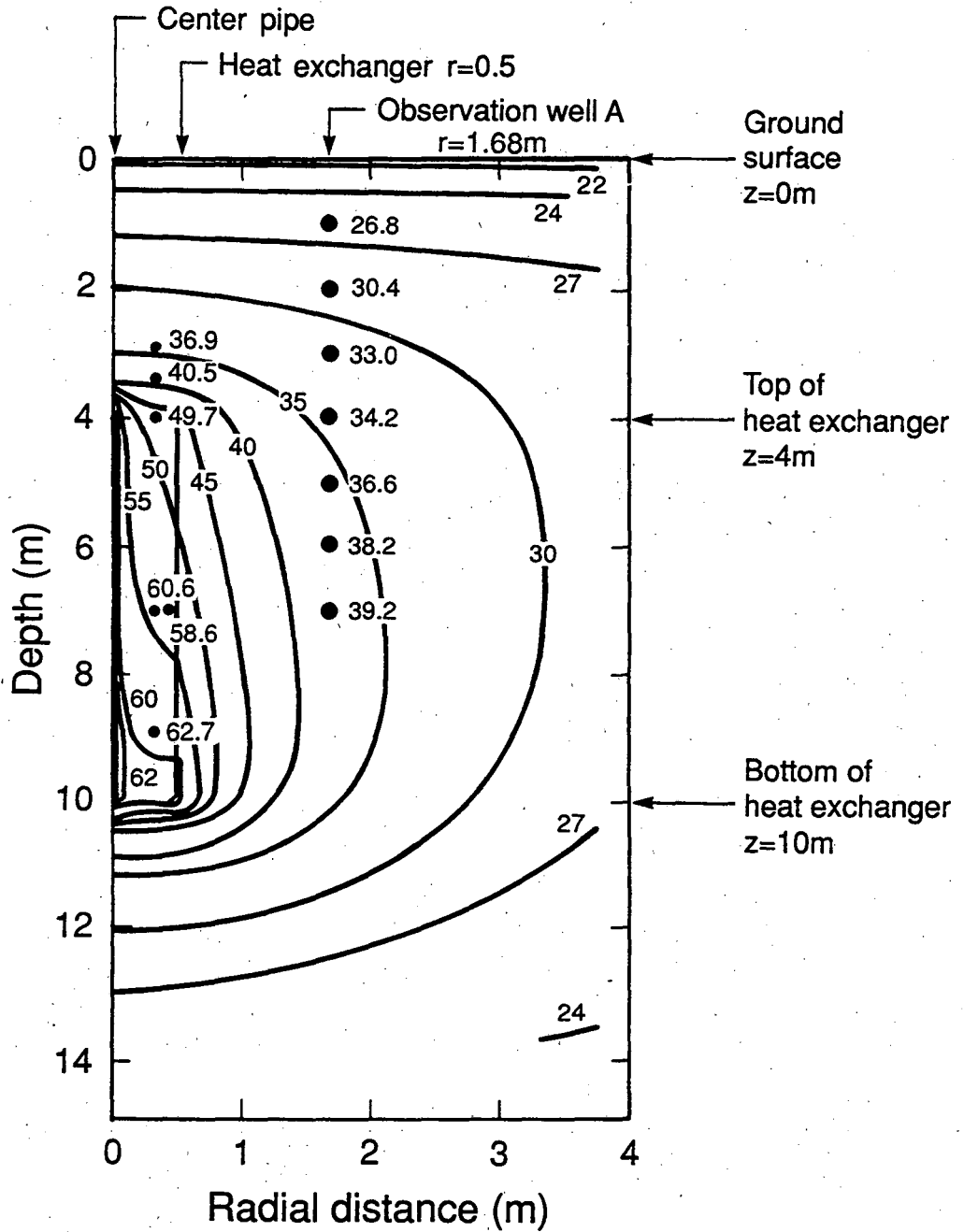


Figure III.2 Sensor locations (A) and observed and calculated temperatures (B, C, and D) for the 1989 run. The curve labeled Ch0 is the heat-exchanger outlet temperature, while the other curves show temperatures at sensor locations. Frame B shows temperatures at depths near 3 m, C at a 4 m depth. D at 7 and 9 m depths.



XBL 901-6703

Figure III.3 Calculated temperature distribution (in °C) at the end of the 1989 charge period (lines), and the observed temperatures at sensor locations (points).

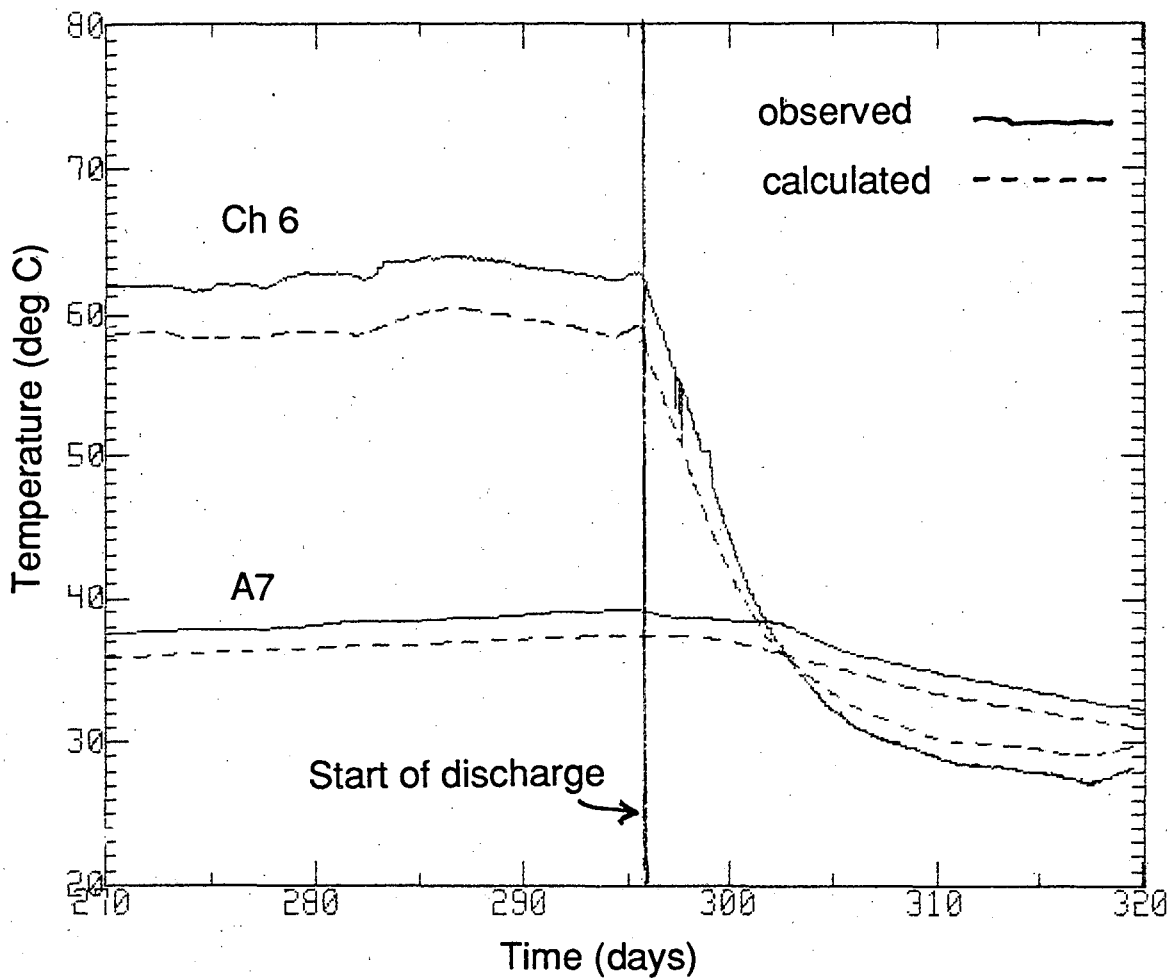


Figure III.4 Detailed view of calculated and observed temperatures at selected sensor locations for the discharge portion of the 1989 run.

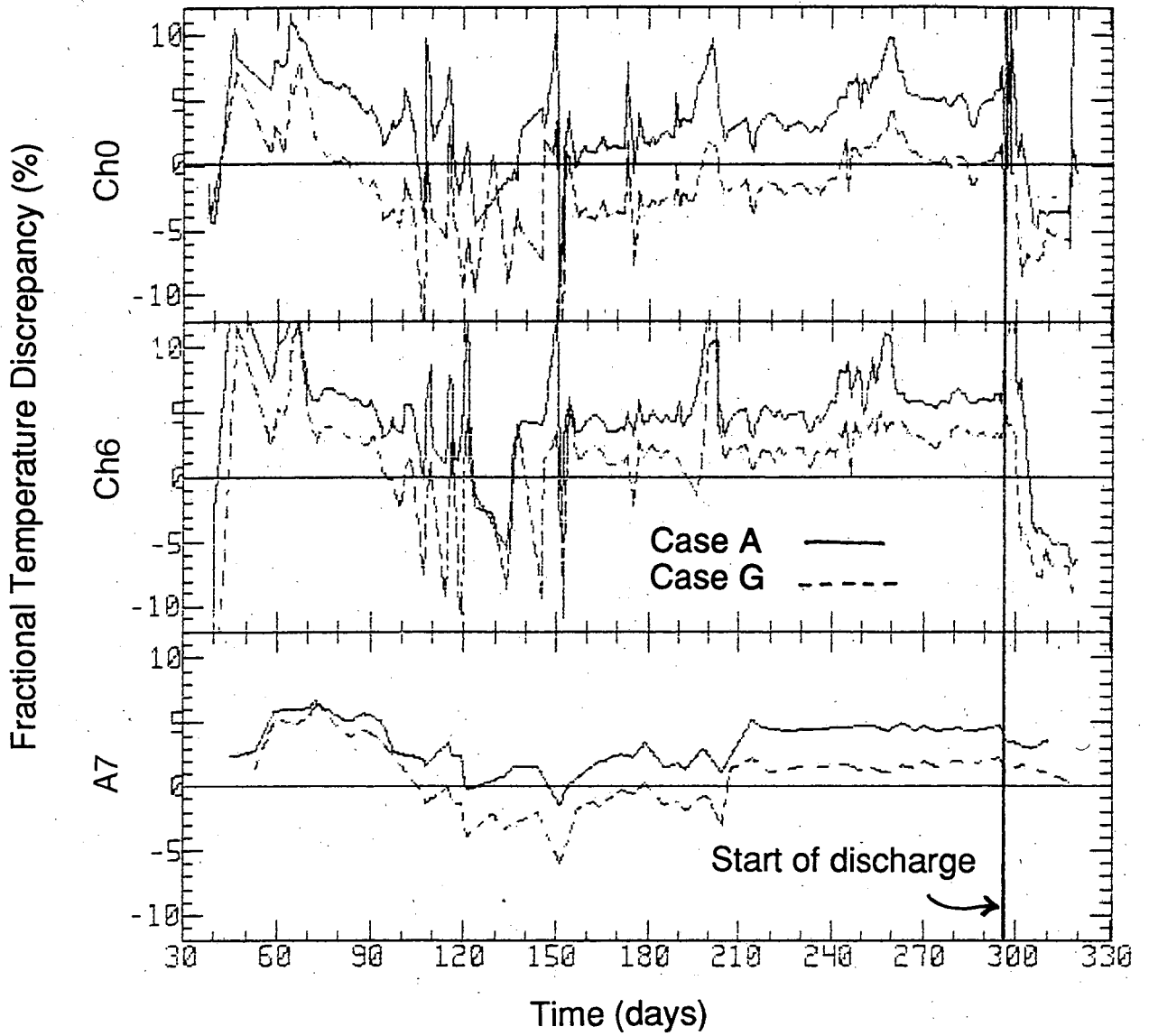


Figure III.5 Fractional discrepancy between observed and calculated temperatures, for the outlet temperature (Ch0) and at selected sensor locations, for the 1989 run.

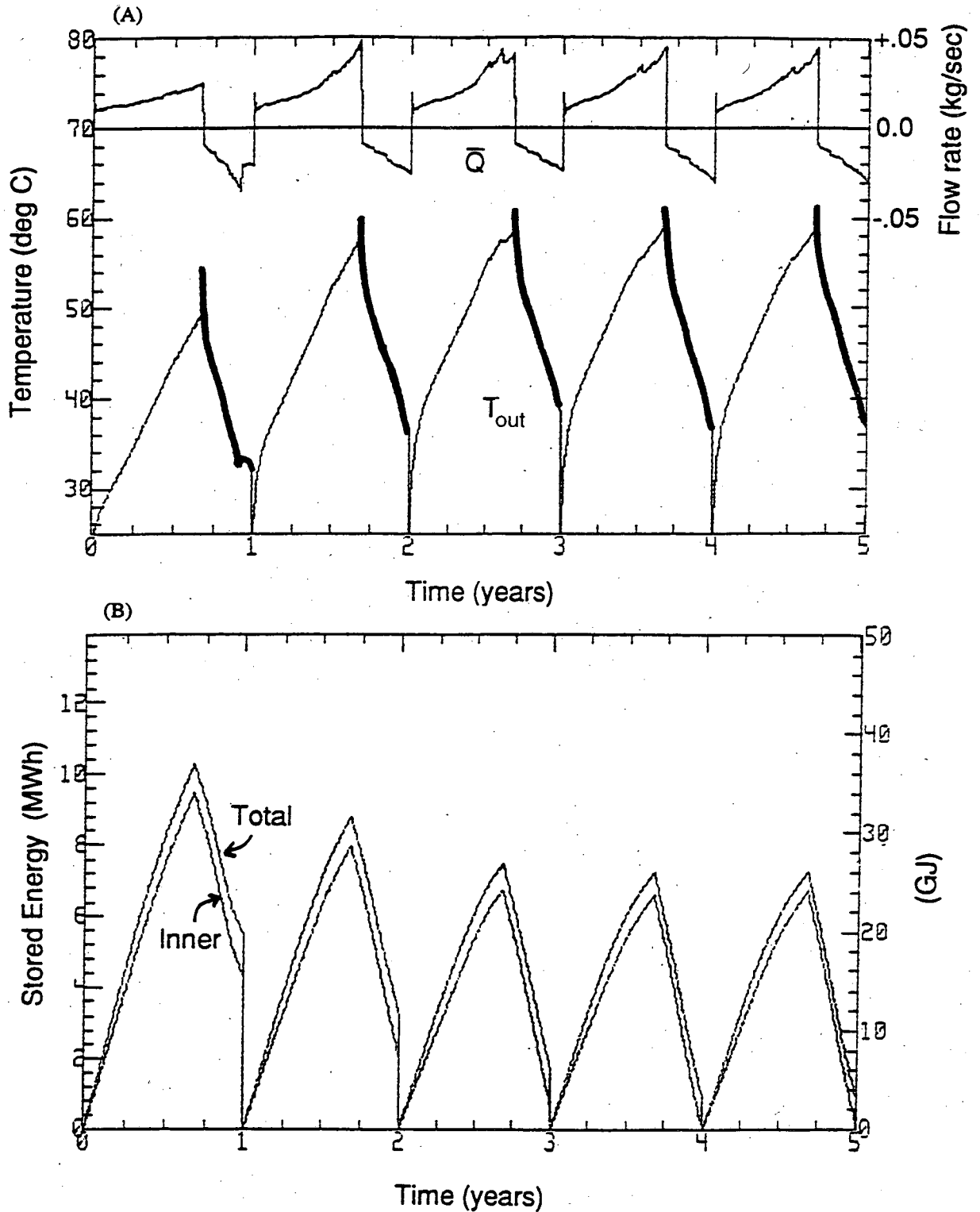


Figure III.6 Results of the five-year simulation for an operational well with a heat-exchanger inlet temperature of 65°C. A: Heat-exchanger outlet temperature (T_{out}) during charge and discharge (bold) periods, and water circulation rate (\bar{Q}). B: Stored energy in the soil; note the three-year transient.

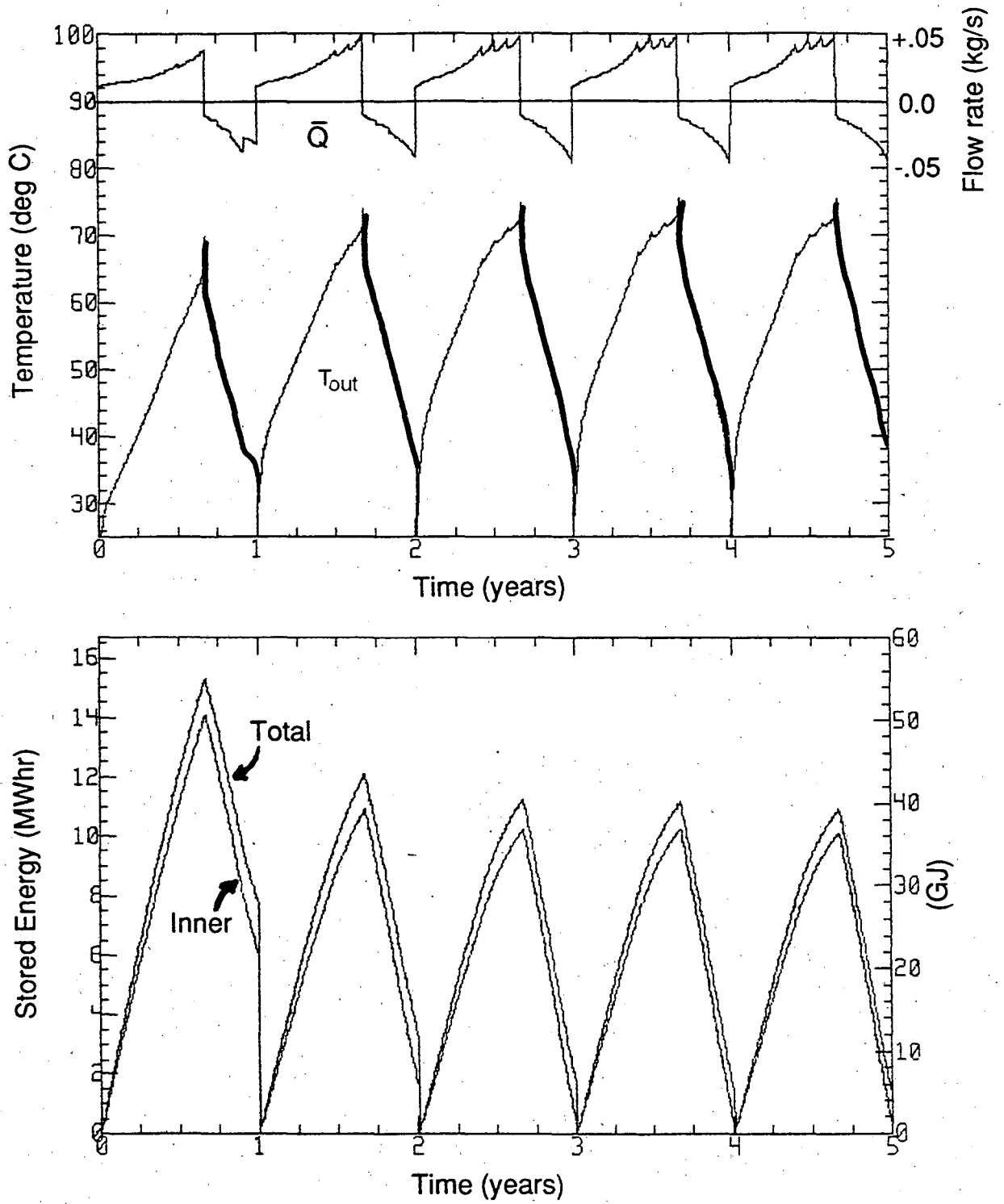
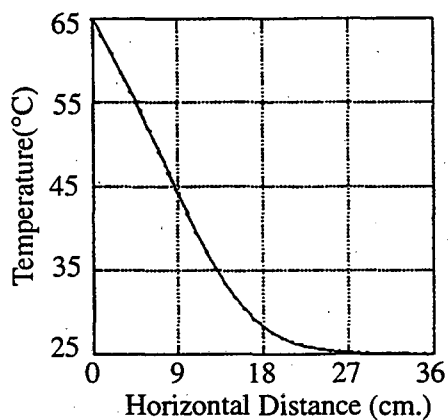
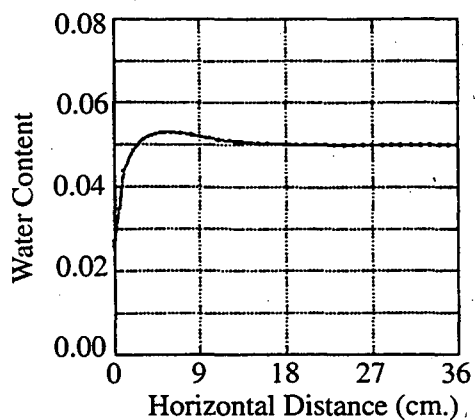
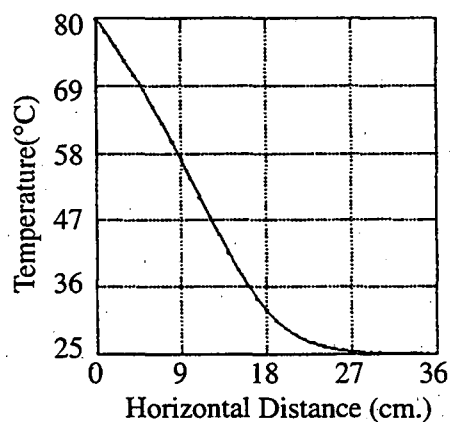
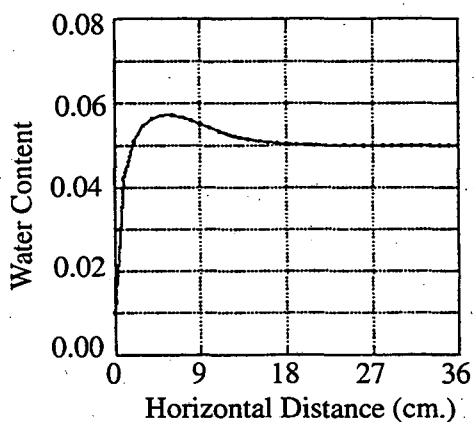


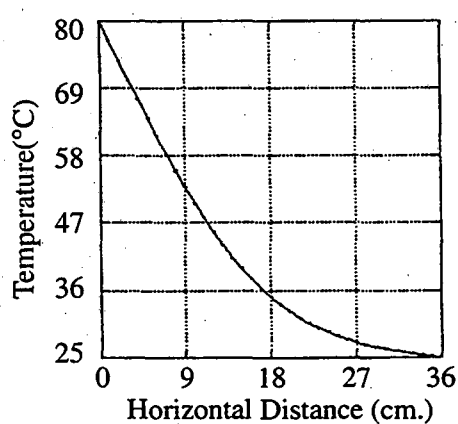
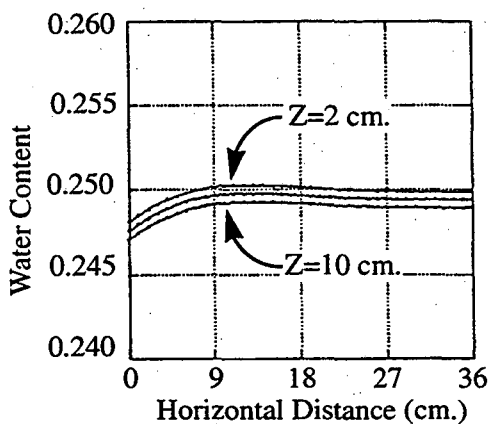
Figure III.7 Results of the five-year simulation for an operational well with a heat-exchanger inlet temperature of 80°C. See Figure III.6 for description of variables.



Sand $T_1 = 65^\circ\text{C}$
Transects $Z=2.0, 6.0, 10.0$ cm.



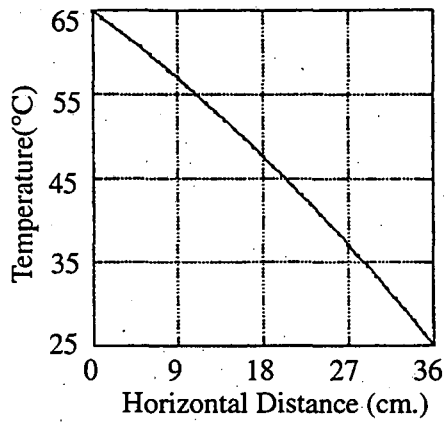
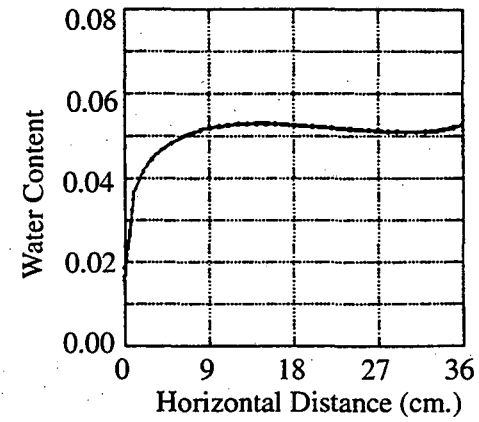
Sand $T_1 = 80^\circ\text{C}$
Transects $Z=2.0, 6.0, 10.0$ cm.



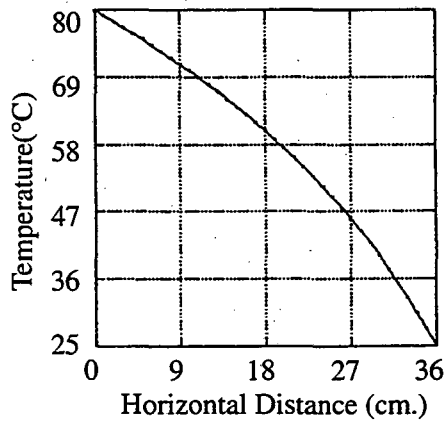
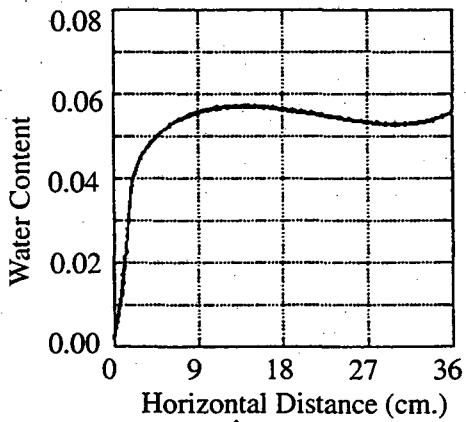
Silty clay $T_1 = 80^\circ\text{C}$
Transects $Z=2.0, 6.0, 10.0$ cm.

Simulation time = 4 hours

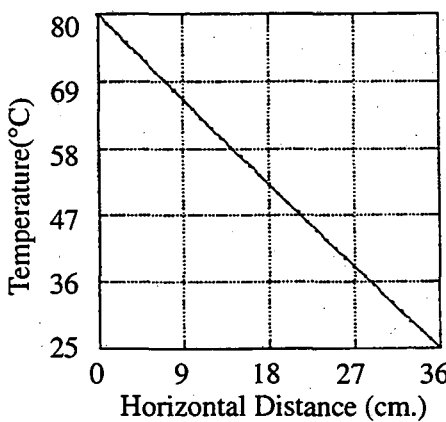
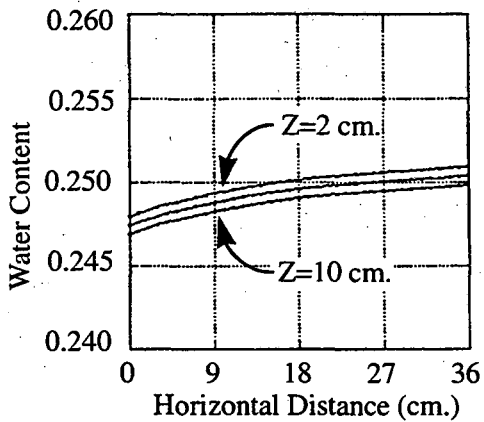
Figure IV.1 Simulated moisture-content and temperature ($^\circ\text{C}$) profiles after 4 hours.



Sand $T_1 = 65^\circ\text{C}$
Transects $Z=2.0, 6.0, 10.0$ cm.



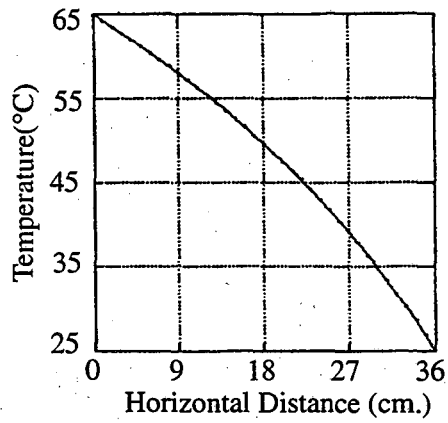
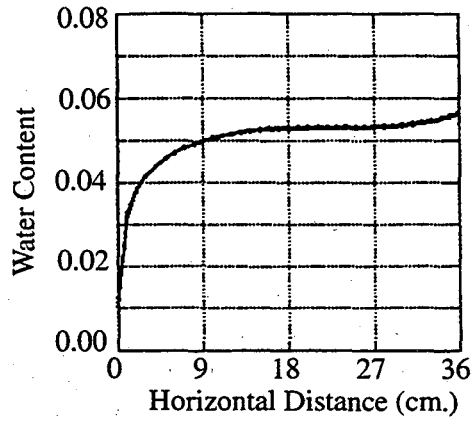
Sand $T_1 = 80^\circ\text{C}$
Transects $Z=2.0, 6.0, 10.0$ cm.



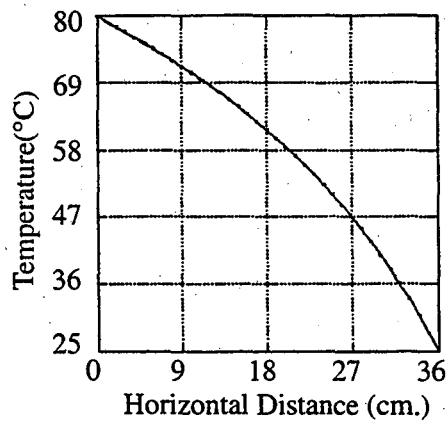
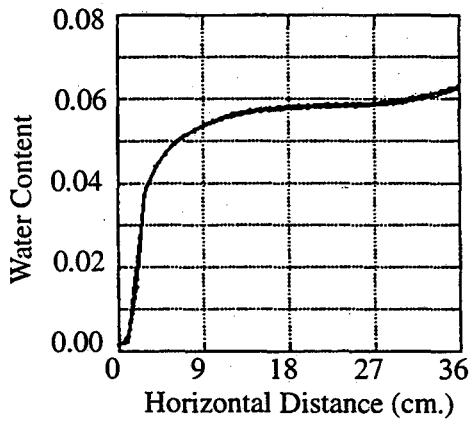
Silty clay $T_1 = 80^\circ\text{C}$
Transects $Z=2.0, 6.0, 10.0$ cm.

Simulation time = 24 hours

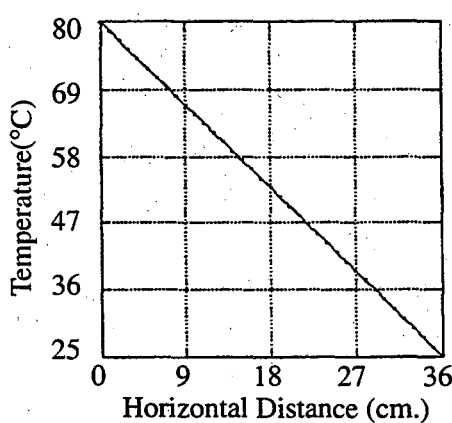
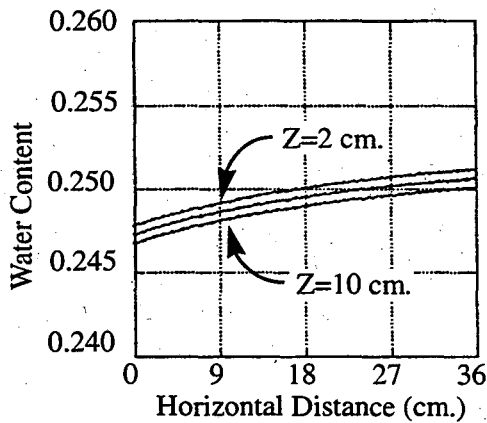
Figure IV.2 Simulated moisture-content and temperature ($^\circ\text{C}$) profiles after 24 hours.



Sand $T_1 = 65^\circ\text{C}$
Transects $Z=2.0, 6.0, 10.0$ cm.



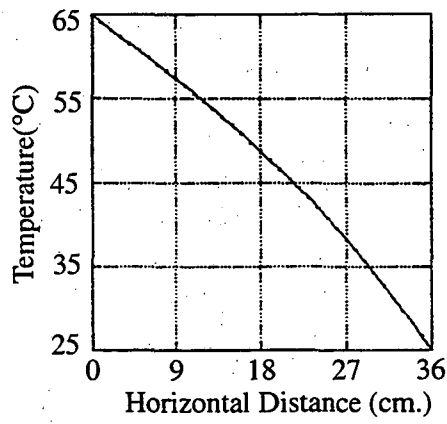
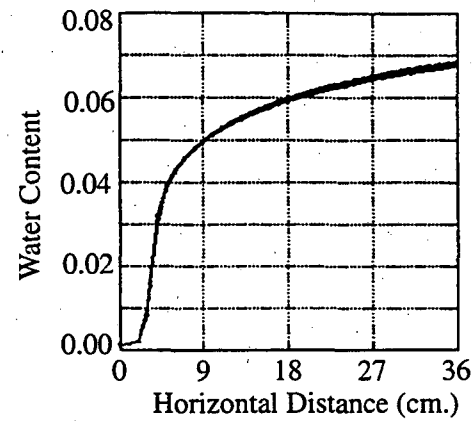
Sand $T_1 = 80^\circ\text{C}$
Transects $Z=2.0, 6.0, 10.0$ cm.



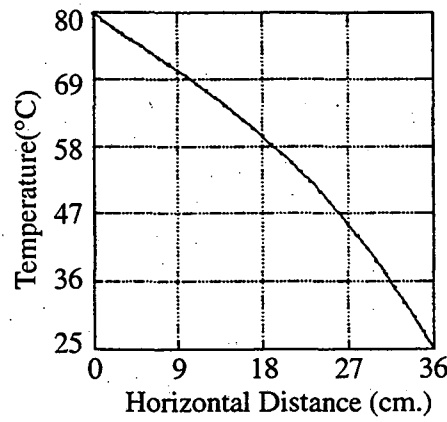
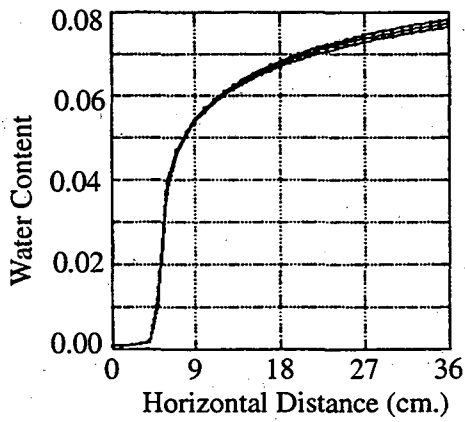
Silty clay $T_1 = 80^\circ\text{C}$
Transects $Z=2.0, 6.0, 10.0$ cm.

Simulation time = 48 hours

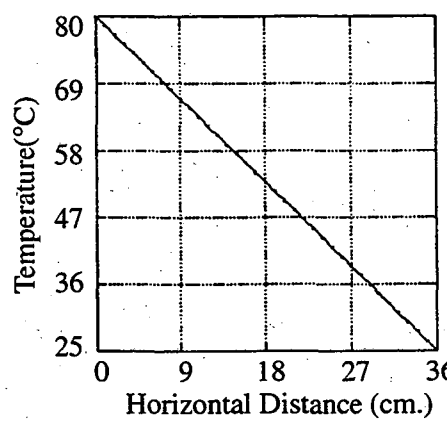
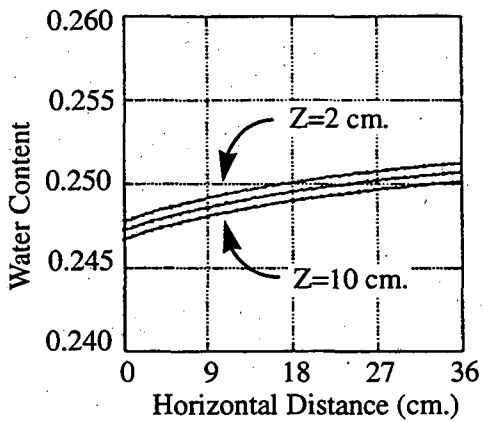
Figure IV.3 Simulated moisture-content and temperature ($^\circ\text{C}$) profiles after 48 hours.



Sand $T_1 = 65^\circ\text{C}$
Transects $Z=2.0, 6.0, 10.0$ cm.



Sand $T_1 = 80^\circ\text{C}$
Transects $Z=2.0, 6.0, 10.0$ cm.



Silty clay $T_1 = 80^\circ\text{C}$
Transects $Z=2.0, 6.0, 10.0$ cm.

Simulation time = Quasi steady state

Figure IV.4 Simulated moisture-content and temperature ($^\circ\text{C}$) profiles at quasi-steady state.

LAWRENCE BERKELEY LABORATORY
UNIVERSITY OF CALIFORNIA
TECHNICAL INFORMATION DEPARTMENT
BERKELEY, CALIFORNIA 94720